MULTIFUNCTIONAL POLYMER NANOCOMPOSITES THROUGH THE ADDITION OF GRAPHENE NANOPLATELETS AND THEIR USES IN AUTOMOTIVE FUEL TANKS

By

Keith T. Honaker

A DISSERTATION

Submitted to
Michigan State University
in partial fulfillment of the requirements
for the degree of

Chemical Engineering – Doctor of Philosophy

2017

ABSTRACT

MULTIFUNCTIONAL POLYMER NANOCOMPOSITES THROUGH THE ADDITION OF GRAPHENE NANOPLATELETS AND THEIR USES IN AUTOMOTIVE FUEL TANKS

By

Keith T. Honaker

Polymers offer a light-weighting alternative to many applications, especially in the automotive industry, but their properties are not always satisfactory. Combining a polymer with a nanofiller can allow for a composite with tunable properties, creating a multifunctional material. Current automotive fuel tanks are made from a layered structure, with the bulk being high density polyethylene (HDPE) sandwiched around a barrier polymer such as polyamide 610. The HDPE provides mechanical stability, while the barrier polymer prevents fuel from evaporating out of the system. Replacing this structure with a nanocomposite could offer a way to improve the efficiency of the system. Graphene nanoplatelets (GnP) are a few layered stack of graphene produced in a cost effective process They have excellent mechanical, thermal and electrical properties, and their platelet structure offers potential improvements to the barrier properties of a polymer This dissertation explores the addition of GnP to both HDPE and a barrier polymer.

GnP and HDPE were compounded through melt mixing and the properties of the composites were characterized over a large concentration range, 0-40 wt. percent GnP. It was found that the flexural modulus and strength of the materials increased with increasing GnP content. However, the impact resistance fell sharply. The thermal stability of the composites was improved, and the barrier properties to both oxygen and fuel were improved up to 20 wt. percent GnP, after which a plateau occurred. This was attributed to misalignment and dispersion issues of the GnP

Alternative processing techniques were explored to overcome the limits of melt mixing. Microlayer co-extrusion yielded highly aligned platelet, but the absolute value was not improved over melt mixing. Solution mixing yielded a better dispersion of the platelets, but that advantage was lost when re-processed through a melt mixing process. Cryo-milling the HDPE resulted in a small improvement to the dispersion of the GnP, resulting in improved barrier properties, but the mechanical properties were weakened. Coating the platelets with a low modulus, HDPE compatible material resulted in recovery of some lost impact resistance, but weakened the flexural improvements, and did not yield large improvements in barrier properties.

An alternative approach was to lay thin layers of GnP onto the surface of polymer using layer by layer deposition to control the completely control the alignment and dispersion of the GnP. This was done by both alternating the GnP with a cationic polymer, and by depositing monolayers of GnP successively onto the surface. Both methods resulted in 60% reductions in oxygen permeability with less than 1 wt. percent GnP

The final method explored was the melt mixing of GnP and a biobased polyamide. As with the HDPE composites, the flexural properties of the composite increased while the impact resistance was lessened. The thermal stability of the polymer was greatly improved. The barrier properties were also improved, and it was also found that increasing the mixing time in the melt extrusion process resulted in further enhancements. The electrical conductivity of the samples was unsatisfactory. To improve this, carbon nanotubes (CNT) and carbon nanofibers (CNF), one dimensional nanofillers, were added to the composites in small quantities. It was found that through the addition of these, the electrical conductivity was greatly improved by over an order of magnitude.

Copyright by
KEITH T. HONAKER
2017

Dedicated to my fiancée and my champ, Shannon Bowyer
& my parents, Maggie Honaker and Jason Schroeder

ACKNOWLEDGEMENTS

There are many people that have made earning my PhD possible. First most, I would like to thank my advisor Dr. Lawrence Drzal for accepting me into his group and giving me guidance along the way. His knowledge, support and encouragement were all essential for my growth and learning throughout the past five years.

I would also like to thank my committee members, Dr. R. Narayan, Dr. K. Jayaraman, and Dr. A. Loos for being on my committee to help test my knowledge and understanding.

All of the members of the CMSC, Brian Rook, Per Askeland, Mike Rich, and Ed Drown, are deeply thanked for their guidance and help in setting up experiments and understanding results.

Many thanks go out to Frederic Vautard for his collaboration in the lab work and analysis, and to both Hyundai USA and Ford Motor Company for sponsoring the research conducted in this dissertation.

All of my talented lab group members, who were always there to discuss interesting results and support each other's research: Markus, Nick, Dee, Yan, Zeyang, Mariana, and Mario. I hope all of you experience the successes you deserve.

A special thanks goes out to Dan and Markus, who were always there to keep things lighthearted, even when the situation was very stressful.

Last but not least, I want to thank my fiancée, Shannon Bowyer, for her love, support and patience while I pursued my PhD, and my parents, Maggie Honaker and Jason Schroeder, for their encouragement, care and guidance throughout my life.

TABLE OF CONTENTS

LIST OF TABLES

LIST OF FIGURES

CHAPTER 1 - INTRODUCTION AND LITERATURE REVIEW

1.1 Introduction

Polymer composites are a growing area of interest in many manufacturing industries. Over 300 tons of polymers are produced each year [1]. Polymers are known for their ease of processing compared to metals, and polymer composites offer property enhancement over the base polymer in many areas, such as mechanical, barrier, electrical and thermal properties [2]. There are many types of fillers than can be added to a polymer matrix to tailor their properties, but nanomaterials have picked up interest for their great composite property enhancements at lower loadings than micron scale materials [3]. There tends to be a larger relative improvement when using nanoscale instead of microscale materials due to the larger aspect ratio and surface area of the nanoscale fillers [4]. The ability to tailor a polymer's properties would provide versatility for many industries in meeting set standards while making their products more efficient.

One industry that has had a significant increase in polymer composite research is the automotive industry. Automotive manufacturers are facing government issued fuel economy and emission regulations and have to consider that consumers desire more fuel efficient vehicles due to higher gasoline prices. Vehicle weight greatly effects fuel economy, resulting in manufacturers investigating any opportunities that could aid in light weighting. The fuel tank and line systems in a vehicle are a potential area for light weighting and also must be improved from their current state to meet government emissions standards set to take effect in 2018. Currently fuel tanks are made with a layered structure, as illustrated in Figure 1.1: a barrier polymer, such as ethylene vinyl alcohol (EVOH) or a polyamide, is sandwiched between two layers of high density

polyethylene (HDPE) and regrind (recycled polymer), with an adhesive bonding the three together [5]. It is necessary to incorporate EVOH or polyamides into the structure because oxygen and fuel can permeate through HDPE easily. With the 6 layer structure, there is 150 times less permeation through the walls compared to the neat polymer alone [6]. Ideally the barrier polymer could be eliminated in the future as currently used ones are typically costly, synthesized from non-renewable sources and its properties tend to degrade under high humidity conditions [7], [8]. Components of a fuel tank and line system need to be mechanically sound to ensure it doesn't break, thermally and chemically stable to withstand the harsh operating conditions of automotive vehicles, exhibit superior barrier properties to ensure there are no emissions via permeation through the walls of the tank, and electrically conductive to dissipate static charges to decrease the risk of fires. A nanocomposite could offer the potential to eliminate the layered structure, simplifying the manufacturing process and removing the barrier polymer, while still meeting or exceeding the required properties of a fuel tank. Alternatively, the barrier polymer could be replaced with a biobased polymer composite that would meet the necessary standards and regulations, while potentially decreasing the long term cost in both a money aspect and environmental impact aspect.

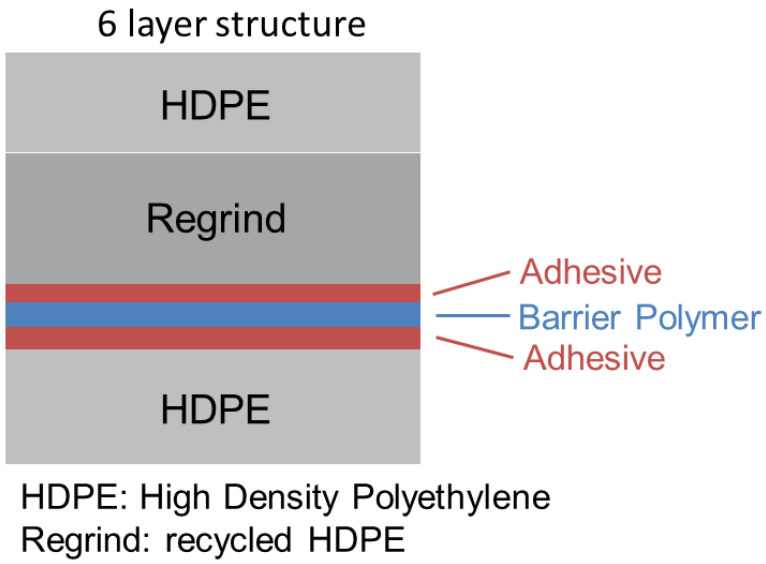

Figure 1.1. Layered structure of a polymer fuel tank.

1.2 Properties of Polymers and Polymer Nanocomposites

1.2.1 Crystallinity

The crystallinity of a polymer defines how ordered the structure is. If a polymer is amorphous, the chains of polymer are disordered and tangled resulting in a softer, more ductile material, while in a crystalline structure the chains are highly ordered and straight yielding a more rigid, brittle material [9]. Many polymers, including HDPE and the barrier polymers in fuel tanks, are semi-crystalline. The degree of crystallinity can greatly influence the properties of a polymer, and can be changed depending on the processing conditions [10]. It has also been documented that the presence of a nanofiller like GnP can result in a change of crystallinity, which would further alter the properties of the composite [11]. Crystallinity can typically be estimated by

calculating the enthalpy of melting and comparing it to the theoretical melting enthalpy of a 100% crystalline polymer [11].

1.2.2 Mechanical Properties

Mechanical properties of polymers and their composites are important to ensure there are no unexpected failures when used in applications. Some of the major defining properties are tensile strength, tensile modulus, flexural strength, flexural modulus, and impact strength. Standard sample preparation and testing procedures have been established for these tests by the American Society for Testing Methods (ASTM). For the tensile properties, the polymer is put into tension, and then the stress is increased until the sample breaks, while the elongation of the sample is monitored [12]. The flexural properties are typically measured by supporting a beam across two points, and then applying a steadily increasing load to the center point, monitoring elongation of the sample [13]. While tensile and flexural test yield information about how a polymer performs under a slowly applied force, impact resistance give information about how it performs when a load is applied nearly instantaneously. Typically this property is measured by notching a specimen to dictate where the crack will form, and then swinging a hammer pendulum into the sample, monitoring how far the pendulum swings after hitting the sample compared to when it freely swings [14].

1.2.3 Electrical Properties

The conductivity of a material is important in many applications, such as the need to dissipate a static charge in a fuel tank and line system. Many polymers will be insulating in their neat state, however, the electrical conductivity can drastically improve when the electrical percolation threshold is reached [15]. The percolation threshold is the point at which there is an interconnected network of filler within the polymer [16]. Conductivity can be measured in-plane and through-plane by forcing a current through the material and measuring the voltage drop to determine the resistance of the material.

1.2.4 Barrier Properties

Barrier properties characterize a polymer's ability to resist the flow of a fluid through it. Typically the gas permeation can be measured by mounting a known exposed area of a film of material into an enclosed environment, purging the system with a clear gas, such as hydrogen and nitrogen, and then pressurizing one side with a desired gas. A sensor on the other side measures how much of that gas permeates through the film, and once steady state has occurred, the permeation is known [17]. Fuel permeation, important if the material would be used in vehicle fuel systems, can be measured through a weight loss method, where the area the fuel is free to permeate out is known. A container of the material is made, and a known weight of fuel is added. The weight of the container is then monitored over time until a steady rate of change is achieved to determine fuel permeation [18].

1.3 Types of Nanocomposites

1.3.1 Layered Silicate Nanocomposites

In the 1990s, the Toyota Motor Company reported that mechanical properties of a Nylon-6 polymer had been greatly improved through the addition of a small amount of montmorillonite, a nanoclay that is made of layered silicates [19]. Silicates are platelet in structure and commonly consist of a layer of aluminum or magnesium atoms with tetrahedron silicate molecules, a silicon ion surrounded by four oxygen ions, bonded to the surface [20]. The surface of the silicate layer will be slightly negatively charged, and are weakly attracted to other layers via alkali or alkaline earth ions that are found within the gallery, the space between the silicate layers. Due to the weak attraction forces, it is relatively easy to fill the gallery with a polymer, and exfoliate the platelets apart to create a uniform polymer-nanoclay composite [21]. Three types of composites can result of mixing layered silicates with a polymer, as seen in Figure 1.2.

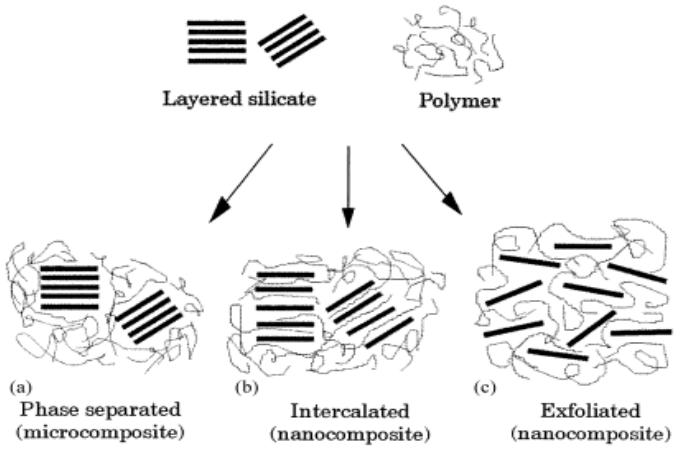

Figure 1.2. Types of nanocomposites yielded with a platelet structured nanofiller [21]. Copied with permission

In order to achieve the best property enhancement, it is necessary to have a structure that has been exfoliated, as shown in part c. This would take the most advantage of the high aspect ratio of the nanoclays. In general the structure formed will be dependent on the mixing process and how well the nanoclay and polymer interact with one another.

Nanoclays as a filler in a polymer matrix have been studied extensively to this date. The addition of a nanoclay to the thermoset combination of polymethylmethacrylate (PMMA) and epoxy matrices resulted in an increase in tensile modulus, tensile strength and impact strength up to a critical weight percent of nanoclays [22]. Similar results for the increase in tensile and toughness properties were reported for poly(vinyldiene fluoride) (PVDF) [23]. In a thermoplastic environment, Chen et al. reported an increase in the tensile modulus and strength for a montmorillonite and polypropylene (PP) composite [24]. Another system of PP and montmorillonite demonstrated an increase in impact strength with 4 weight percent nanoclay [25]. However, it has also been observed that nanoclay additions can have a negative effect on the impact strength, suggesting composite impact strength is greatly dependent on the interaction between the polymer and nanoclay [26]. Flexural strength and modulus also tend to be enhanced with the addition of nanoclays to polymers [27].

In addition to the mechanical property enhancement, permeation resistance to water and gases has been shown to increase with increasing nanoclay concentration in multiple polymeric systems [27]–[30]. The reasoning for the improvement to the barrier properties is that the platelet structure and large aspect ratio of platelet diameter to thickness creates a diffusion path that is more tortuous than the neat polymer due to the impermeability of the nanoclays [21], [31], [32]. This can be represented by Figure 1.3. With a 15% wt. montmorillonite in HDPE composite, there was a 30% reduction in oxygen barrier properties [33]. While the increase in mechanical

and barrier properties would be promising for use in fuel tanks, the nanoclays do not impart electrical conductivity to the polymer matrix when added. In this sense, nanoclay composites are inferior to one containing carbon based nanofillers derived from graphite [34].

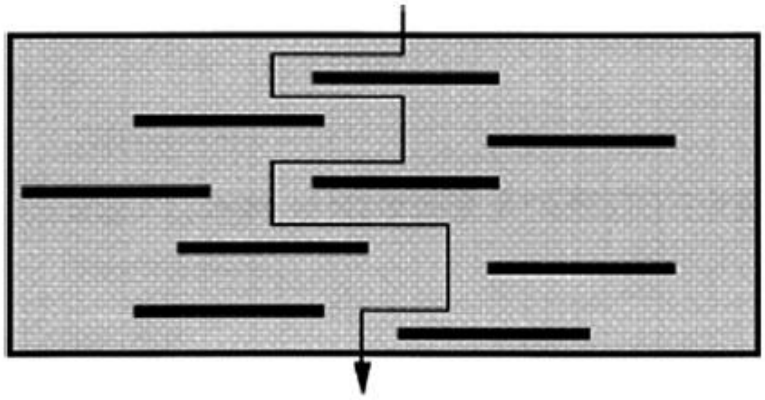

Figure 1.3. Tortuous diffusion path through a nano-platelet filled composite [31]. Copied with permission

1.3.2 Carbon Based Nanofiller Composites

Pristine graphene is a sheet of sp^2 hybridized carbon, with high mechanical, electrical, and thermal properties, but it is difficult to cost effectively produce in large amounts [3]. Graphene is essentially the building block other carbon-based nanofillers, as illustrated in Figure 1.4. If the graphene is wrapped into a ball, it forms bukeyballs, first discovered by Kroto et al. in 1985 [35]. If graphene is rolled up into a tube, a carbon nanotube (CNT) is formed. Stacks of graphene are what forms graphite, a common material used in many applications. All types of carbon nanomaterials are of heavy interest in research. In addition to the graphene based derivative, carbon black is widely researched for its ability to improve thermal and electrical conductivity

[36]. Carbon fiber, a cost effective micron-scale filler, is considered for many applications where mechanical property reinforcement is valued most [37].

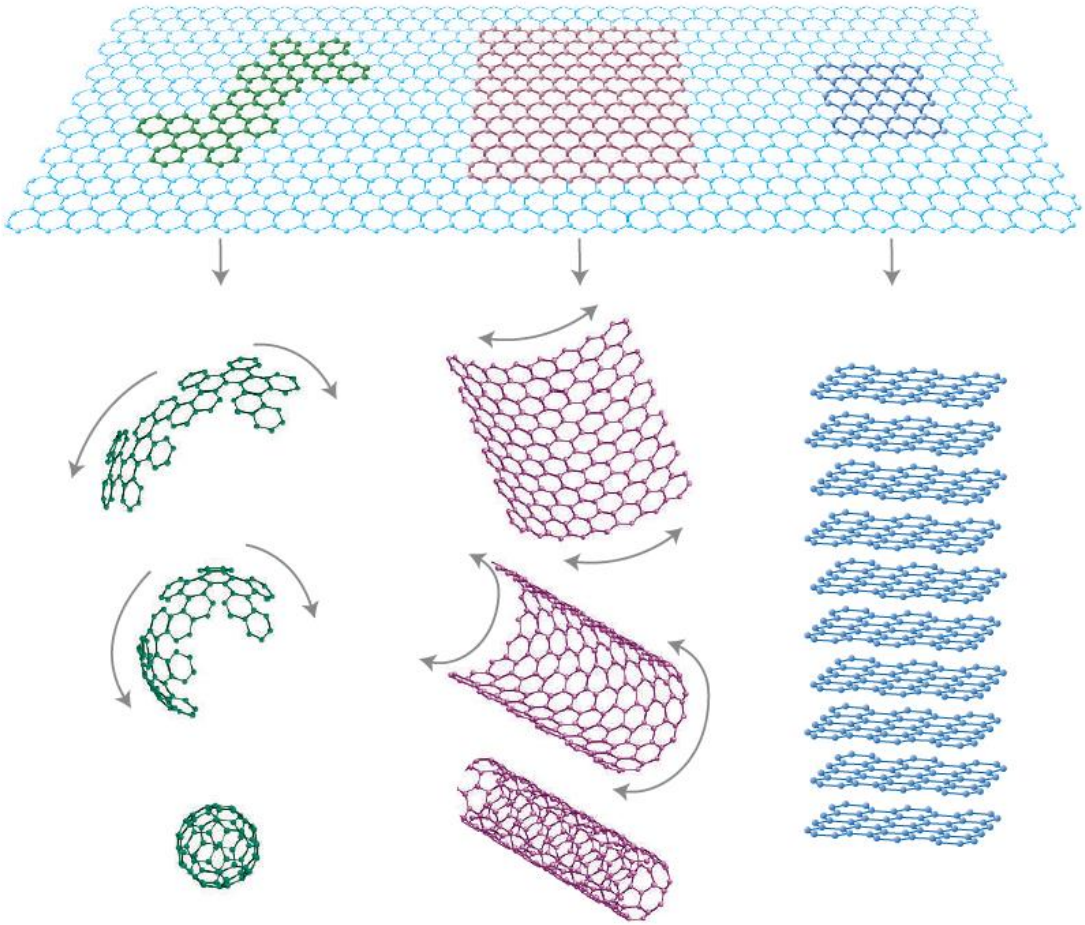

Figure 1.4. Illustration of how 2D graphene can be wrapped into 0D buckyballs, rolled into 1D nanotubes, or stacked into 3D graphite [38]. Copied with permission.

CNTs are of interest because of their extremely high mechanical properties, with a modulus of a CNT reaching over a terapascal [39]. There can be both single-walled nanotubes (SWNTs) or multi-walled nanotubes (MWNTs), which are essentially just multiple CNT layered inside of each other. SWNTs are much more costly to produce, though they tend to exhibit better overall properties. Even the MWCNTs are very costly relative to most other carbon derived nanoparticles [3], [4], [40]. Despite this, their impact on polymer composite properties has spurred a lot of research into optimizing the use of CNTs in nanocomposites. Many experiments have shown that the tensile modulus and strength of various polymer matrices increase when CNTs are added [41]–[44]. However, it has also been shown that the addition of CNTs resulted in a decrease of flexural modulus and strength of an epoxy system, but this was attributed to the fact that there was weak adhesion between the CNT and the polymer matrix [45]. Moniruzzaman et al. showed that the addition of CNT to a thermoset epoxy matrix would actually increase the flexural strength and modulus when there was a good dispersion and good bonding with the matrix [46]. Additionally, in an epoxy system, the impact strength has been shown to decrease when CNTs are present [47]. In an HDPE matrix, the impact strength actually increased up to a critical percentage, which could be attributed to the fact that the properties of the composite are highly dependent on the nanotube orientation and concentration [42], [44].

For electrical properties, adding CNTs to a polymer matrix has been shown the capability to increase the conductivity compared to the neat polymer by multiple orders of magnitude, with concentrations as low as 0.1 weight percent [43]. Others have reported the percolation threshold, the point where there is a conductive pathway of particles in the matrix, to be around 3.0 weight percent [40]. It has been thoroughly demonstrated that the more aligned the nanotubes, the less the conductivity enhancement in the opposite direction of alignment [48], [49]. This is easily

explained by the fact that when the tubes are aligned, they do not touch each other as often as when the order is random. Although CNT composites tend to have greatly improved mechanical and electrical properties, the barrier properties remain largely unaffected. The 1D structure will not create a tortuous path of diffusion, so there will not be any additional permeation resistance to oxygen and water as expected with the nanoclay fillers [3]. This greatly reduces their usefulness in fuel tank and line systems, where barrier properties are highly valued. In the same vein, carbon black and carbon fibers also tend to improve mechanical and electrical properties, but do not have a large impact on barrier properties [32].

While pristine graphene is very difficult to synthesize in a cost effective manner, graphene oxide can be made from bulk graphite and exhibits interesting properties when incorporated into polymers. The synthesis of graphene oxide is typically performed by oxidizing bulk graphite with a strong oxidizing agent, like nitric acid or potassium permanganate, and then exfoliating it in a solvent via sonication or mechanical stirring, resulting in nano and microscale materials [50]. From here, graphene oxides can either be functionalized by replacing the groups bonded to the surface to improve adhesion to a polymer matrix, or the surface can be reduced, removing some of the oxygen present, and resembling a structure that is closer to that of pristine graphene [3], [50], [51]. While graphene oxide is not conductive, when reduced, the conductivity can be restored [50], [51]. One issue with graphene oxide is that due to many carbon atoms in the sp^3 conformation, the structure can be much more wave like rather than platelet like, which would not be as ideal for barrier property enhancement, and can also adversely affect mechanical and thermal properties as well. [52].

An alternative, carbon based material has been developed recently that exhibits mechanical properties and electrical properties similar to CNTs, while still being platelet in structure like

nanoclays, which would benefit barrier properties. Graphene nanoplatelets (GnP) are stacks of a few layers of graphene with a thickness of 6 nm and a diameter on the microscale. The surface is all sp^2 hybridized carbon, while the edge groups are generally functionalized as depicted in Figure 1.5.

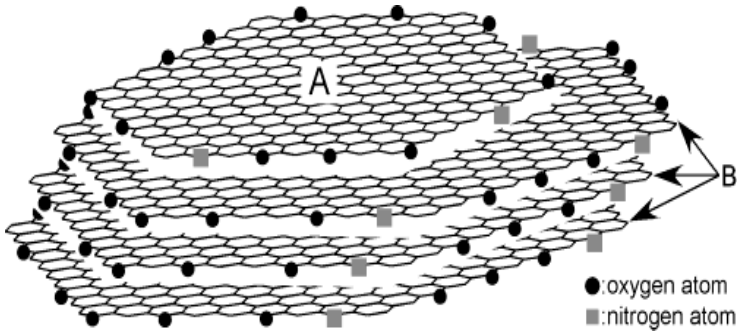

Figure 1.5. Theoretical illustration of graphene nanoplatelets. [53] Copied with permission.

This material is available commercially, and produced in an industrial robust process by rapidly heating acid intercalated graphite to yield expanded graphite worms, which are then mechanically or ultrasonically ground into the desired platelet size [54]. Figure 1.6 shows scanning electron microscopy images of the stages of GnP production. With excellent mechanical and electrical properties, previous research on this material has focused on the incorporation into PP, HDPE and epoxy systems. Additions of GnP to these polymers have been shown in increase the tensile modulus and strength [3], [55], [56]. Further investigations have shown similar improvements to the flexural properties [55], [57]. The impact resistance has not been studied as extensively, but it has been reported that the addition of GnP results in a decrease in impact resistance, like other nanofillers tend to do [55]. The conductivity of a polymer

composite with GnP has also been shown to greatly improve, particularly in the in-plane direction [58], [59]. However, the percolation threshold has been reported as high as 10 volume percent with unmodified GnP, likely due to aggregation of the platelets and poor dispersion [60].

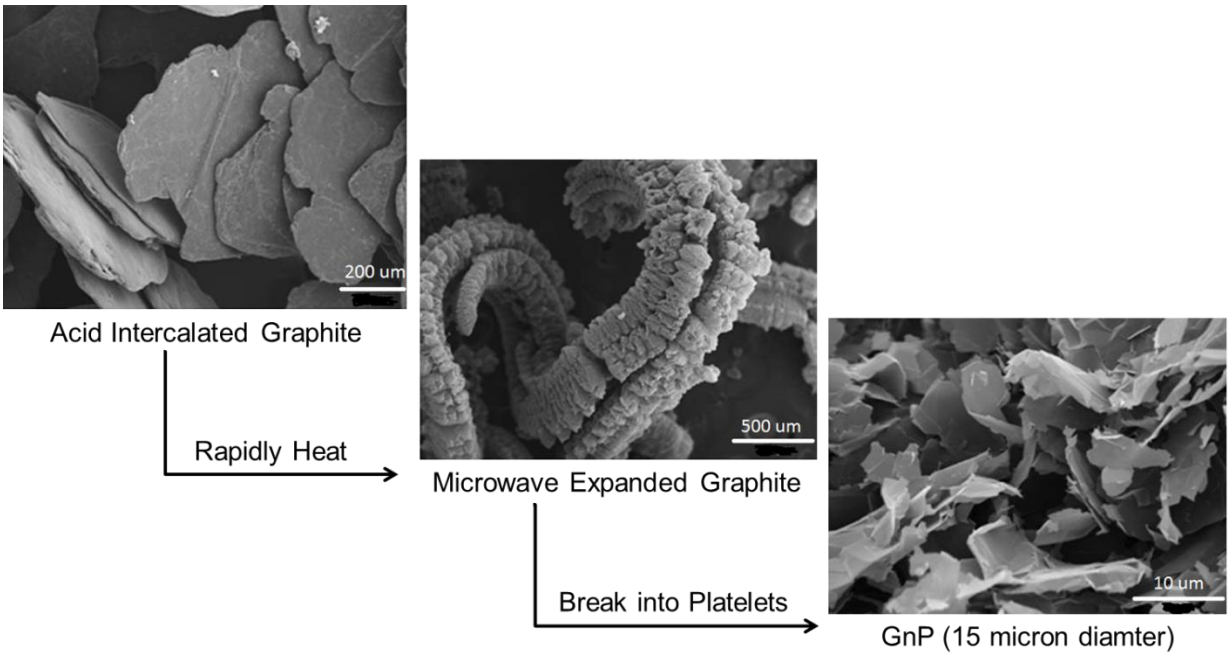

Figure 1.6. Synthesis of graphene nanoplatelets. [54] Copied with permission.

Another promising aspect of GnP is the effect on permeation resistance. It has been demonstrated that the barrier properties of a polymer improve to the same degree, if not better than when nanoclays are used [32], [61]. Like with the nanoclays, this is explained by the tortuous path created by the platelets, as depicted in Figure 1.3.

1.4 Theory of Barrier Properties of Nanocomposites with a Platelet Nanofiller

For a neat polymer, the crystallinity of the polymer greatly influences the barrier properties. The free volume of a polymer characterizes the amount of space in a polymer matrix that is not occupied by the constituent atoms of the polymer [62]. Permeation of gaseous molecules requires sufficient free volume into which the molecules can move. Once a platelet nanofiller is added, the permeation properties will be altered, as shown with Figure 1.3. Theoretical modelling of this tortuous path phenomenon has been presented by Bharadwaj, shown in the two following equations [63]:

$$\frac{P_s}{P_p} = \frac{1 - \phi_s}{1 + \frac{L}{2W}\phi_s\left(\frac{2}{3}\right)\left(S + \frac{1}{2}\right)} \qquad \text{(Eqn 1)}$$

$$S = \frac{1}{2}\langle 3\cos^2\theta - 1\rangle \qquad \text{(Eqn 2)}$$

where P_s is the composite permeability, P_p is the neat polymer permeability, Φ_s is the volume fraction of the filler, L is the diameter of the filler, and W is the thickness of the filler. The values of S and W are depicted in Figure 1.7 [63].

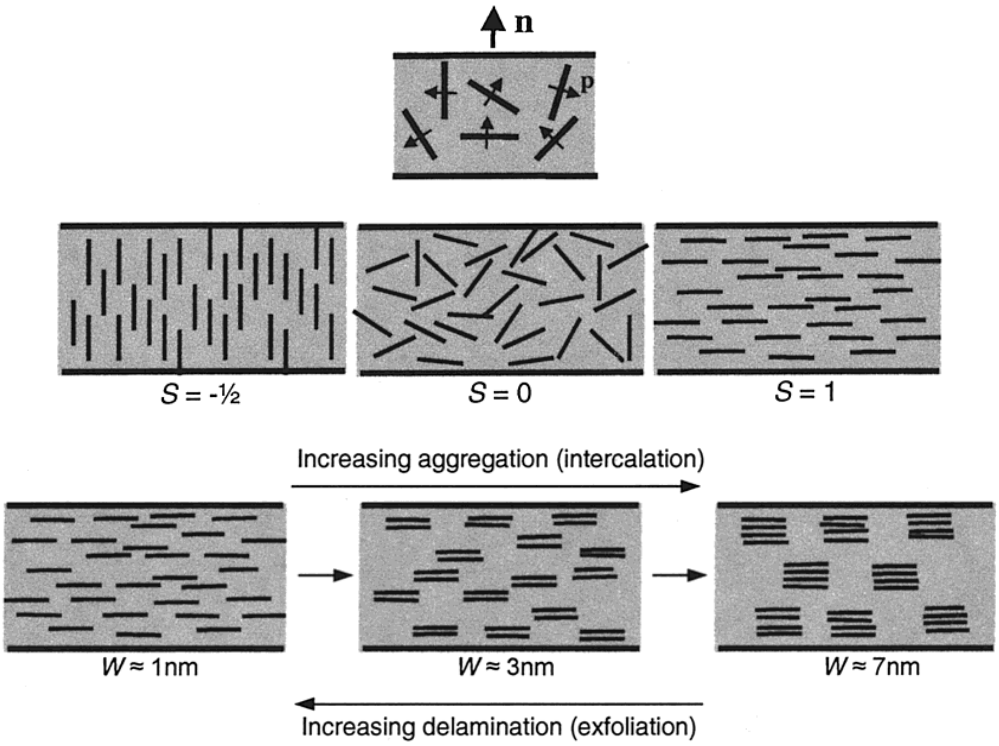

Figure 1.7. Illustration of important variables for barrier property modelling [63]. Copied with permission.

For a platelet nanofiller, like GnP, it is clear that the two major factors that would impact barrier properties of the composite are the alignment of the particles (S) and the dispersion of the particles (W). If GnP with a 15 micron diameter and a thickness of 6 nm is perfectly dispersed and aligned into a polymeric system, there should be a reduction in gas permeability by 98%. This highlights the potential of GnP to be used as an additive to improve the barrier properties of a polymer composite.

1.5 Processing Polymer Nanocomposites

One of the most cost effective and commonly used methods to synthesize nanocomposites is via melt mixing [28], [64]. Typically, melt mixing heats the nanofiller and the polymer up to its melting point, and rapidly spinning screws exert mechanical shear forces on the polymer and exfoliates the nanoparticles into the matrix to achieve a good dispersion. However, good dispersions can be difficult to achieve with carbon based nanoparticles, partially due to the viscous environment during melt mixing [65]. An extension of melt mixing that has shown promise in creating uniformly aligned nanoparticles, a key factor in the impact of the nanofiller on the barrier properties, is microlayer coextrusion [66], [67]. In this process, a melt mixed composite is fed into a multi-layer die, and in the die the stream of polymer is cut in half vertically and then the two created streams are compressed back together, forming multiple "layers" in one film. If this method was used on a nanocomposite, the repeated forces of compression should force the particles to align.

Alternatively, solution mixing is also an effective way to compound the polymer and the nanofiller, providing a less viscous mixing environment compared to melt mixing. The lower viscosity tends to make it easier to achieve a uniform dispersion of nanoparticle, though would be more costly to implement on an industrial scale [59], [68]. Once the material has been solution dispersed, it could be directly molded into a composite sample, or re-processed through melt mixing to mold samples.

Another approach on improving barrier properties that is an extension of the solution based approach is layer by layer deposition of nanoparticles. This process takes advantage of ionic charges of a polymer (typically positively charges) and nanofiller (typically negatively charged):

a substrate is dipped in a solution containing a cationic polymer, dried, and then dipped into a solution containing an anionic nanoparticle. By alternating numerous times, a uniform layer by layer structure is formed. This process is well documented with nanoclays, greatly improving the barrier properties, but nanoclays do not provide electrical conductivity for the thin film [69]–[72]. This method has been briefly investigated with GnP, but barrier properties were not examined in the study [73]. There are also other methods of depositing a thin layer of GnP on a surface, such as taking advantage of self-assemble of GnP at a chloroform-water interface [74].

1.6 Modification of Nanofillers

Modifying a nanofiller prior to incorporation into a polymer has the potential to yield a better dispersion and thus further property enhancement. There are two methods to achieve this: covalent and non-covalent. It has been shown in previous research that bonding polymer compatible groups covalently to the nanofiller yields good results [50], [75]–[77]. GnP has functional groups at the edges, as shown in Figure 1.5, which could be used for functionalization. Alternatively, it has also been demonstrated that a non-covalent coating can result in improved dispersion as well. Jiang and Drzal previously showed that coating GnP with a low molecular weight paraffin wax prior to incorporation into HDPE yielded improved dispersion [2]. Similarly, a wax coating has also been shown to improve the dispersion of CNT in HDPE [44]. Nanofiller modification may be necessary to achieve optimal nanocomposite properties.

1.7 Significant Research Proposal

Automotive manufacturers are facing stricter emissions and fuel economy regulations that require light weighting and material optimization to achieve. Current vehicle fuel tank and line structures are made with a layered structure, illustrated in Figure 1.1. A nanocomposite with GnP offers a potential alternative that could offers an impermeable, conductive composite that would meet the strict regulations governing fuel tanks. The focus of the research hereafter presented is as follows:

(1) Establish a melt mixing baseline of GnP in an HDPE grade that is currently used in automotive fuel tanks. Melt mixing is the most cost effect, industrial applicable process for nanocomposite synthesis, and mixing GnP and HDPE has the potential to eliminate the layered structure with a single layer of composite material. In order to do so, the mechanical properties (flexural and impact resistance) must remain sound, while the barrier properties must be improved to the level of the barrier property. Ideally, the percolation threshold should also be met so that the composite can dissipate a potential static charge.

(2) Once a baseline is established, investigate alternative processing techniques to optimize the barrier properties of the HDPE/GnP composite. These include microlayer co-extrusion to force alignment of the platelets, solution mixing to investigate the dispersion of the platelets in a non-viscous environment, and coating the platelets with a compatible wax to improve the surface interaction between GnP and HDPE

(3) Utilize thin film deposition techniques, like layer by layer or self-assembly, to apply a thin coating of GnP to a polymer substrate and investigate the barrier property improvements.

(4) Investigate the effects of GnP on the barrier polymer. Using a melt mixing and other approaches like with HDPE, the barrier polymer may be optimized with GnP to reduce the thickness necessary in the fuel tank. The mechanical properties would still need to remain sound, while improving the barrier properties and electrical conductivity.

(5) Examine the synergistic effects of other nanofillers with GnP to achieve electrical conductivity. If GnP is aligned in the polymer matrix for barrier property enhancement, this may negatively affect the through-plane conductivity of the polymer composite. Adding small amounts of another nanofiller that does not tend to orient with flow, such as CNT, may result in great improvement in conductivity.

REFERENCES

REFERENCES

[1] I. Vlassiouk, M. Regmi, P. Fulvio, S. Dai, P. Datskos, G. Eres, and S. Smirnov, "Role of hydrogen in chemical vapor deposition growth of large single-crystal graphene," *ACS Nano*, vol. 5, no. 7, pp. 6069–6076, 2011.

[2] X. Jiang and L. T. Drzal, "Improving electrical conductivity and mechanical properties of high density polyethylene through incorporation of paraffin wax coated exfoliated graphene nanoplatelets and multi-wall carbon nano-tubes," *Compos. Part A Appl. Sci. Manuf.*, vol. 42, no. 11, pp. 1840–1849, 2011.

[3] J. R. Potts, D. R. Dreyer, C. W. Bielawski, and R. S. Ruoff, "Graphene-based polymer nanocomposites," *Polymer (Guildf).*, vol. 52, no. 1, pp. 5–25, 2011.

[4] F. Hussain, "Review article: Polymer-matrix Nanocomposites, Processing, Manufacturing, and Application: An Overview," *J. Compos. Mater.*, vol. 40, no. 17, pp. 1511–1575, 2006.

[5] N. Hata and T. Negi, "Fuel Tank," US Patent 6,033,749, 2000..

[6] Schutz, "Basics on permeation and EVOH Basics on permeation and EVOH." [Online]. Available: http://www.ipacksystems.com/downloads/Schutz_EVOH.pdf. [Accessed: 20-Feb-2017].

[7] H. Kwon, D. Kim, and J. Seo, "Thermal and barrier properties of EVOH/EFG nanocomposite films for packaging applications: Effect of the mixing method," *Polym. Compos.*, vol. 16, no. 2, pp. 1–10, Dec. 2014.

[8] K. K. Mokwena and J. Tang, "Ethylene Vinyl Alcohol: A Review of Barrier Properties for Packaging Shelf Stable Foods," *Crit. Rev. Food Sci. Nutr.*, vol. 52, no. 7, pp. 640–650, 2012.

[9] A. Rudin, *Elements of Polymer Science and Engineering*. 1999.

[10] D. G. M. Wright, R. Dunk, D. Bouvart, and M. Autran, "The effect of crystallinity on the properties of injection moulded polypropylene and polyacetal," *Polymer (Guildf).*, vol. 29, pp. 793–796, 1988.

[11] K. Kalaitzidou, H. Fukushima, P. Askeland, and L. T. Drzal, "The nucleating effect of exfoliated graphite nanoplatelets and their influence on the crystal structure and electrical conductivity of polypropylene nanocomposites," *J. Mater. Sci.*, vol. 43, no. 8, pp. 2895–2907, 2008.

[12] "ASTM D638, Standard test method for tensile properties of plastics," no. C, pp. 1–16, 2013.

[13] "ASTM D790 Standard Test Methods for Flexural Properties of Unreinforced and Reinforced Plastics and Electrical Insulating Materials," *Annu. B. ASTM Stand.*, no. C, pp. 1–11, 2011.

[14] "ASTM D256-10 Standard Test Methods for Determining the Izod Pendulum Impact Resistance of Plastics," vol. i, pp. 1–20, 2010.

[15] S. Stankovich, D. A. Dikin, G. H. B. Dommett, K. M. Kohlhaas, E. J. Zimney, E. A. Stach, R. D. Piner, S. T. Nguyen, and R. S. Ruoff, "Graphene-based composite materials," *Nature*, vol. 442, no. 7100, pp. 282–286, 2006.

[16] V. K. S. Shante and S. Kirkpatrick, *Advances in Physics An introduction to percolation theory*, no. October 2012. 2006.

[17] D. J. Sekelik, E. V. Stepanov, S. Nazarenko, D. Schiraldi, a. Hiltner, and E. Baer, "Oxygen barrier properties of crystallized and talc-filled poly(ethylene terephthalate)," *J. Polym. Sci. Part B Polym. Phys.*, vol. 37, no. 8, pp. 847–857, 1999.

[18] J. Yeh, S. Huang, and W. Yao, "Gasoline Permeation Resistance of Containers of Polyethylene , Polyethylene / Modified Polyamide and Polyethylene / Blends of Modified Polyamide and Ethylene Vinyl Alcohol," pp. 532–538, 2002.

[19] A. Usuki, Y. Kojima, M. Kawasumi, A. Okada, Y. Fukushima, T. Kurauchi, and O. Kamigaito, "Synthesis of nylon 6-clay hybrid," *J. Mater. Res.*, vol. 8, no. 5, pp. 1179–1184, May 1993.

[20] E. P. Giannelis, R. Krishnamoorti, and E. Manias, "Polymer-Silicate Nanocomposites : Model Systems for Confined Polymers and Polymer Brushes," *Polymer (Guildf).*, vol. 138, pp. 107–147, 1999.

[21] M. Alexandre and P. Dubois, "Polymer-layered silicate nanocomposites: Preparation, properties and uses of a new class of materials," *Mater. Sci. Eng. R Reports*, vol. 28, no. 1, pp. 1–63, 2000.

[22] J. H. Park and S. C. Jana, "Mechanism of exfoliation of nanoclay particles in epoxy-clay nanocomposites," *Macromolecules*, vol. 36, no. 8, pp. 2758–2768, 2003.

[23] D. Shah, P. Maiti, E. Gunn, D. F. Schmidt, D. D. Jiang, C. A. Batt, and E. P. Giannelis, "Dramatic Enhancements in Toughness of Polyvinylidene Fluoride Nanocomposites via Nanoclay-Directed Crystal Structure and Morphology," *Adv. Mater.*, vol. 16, no. 14, pp. 1173–1177, 2004.

[24] L. Chen, S. C. Wong, and S. Pisharath, "Fracture properties of nanoclay-filled polypropylene," *J. Appl. Polym. Sci. J. Appl. Polym. Sci.*, vol. 88, no. 14, pp. 3298–3305, 2003.

[25] Q. Yuan and R. D. K. Misra, "Impact fracture behavior of clay-reinforced polypropylene nanocomposites," *Polymer (Guildf).*, vol. 47, pp. 4421–4433, 2006.

[26] T. D. Fornes, P. J. Yoon, H. Keskkula, and D. R. Paul, "Nylon 6 nanocomposites: the effect of matrix molecular weight," *Polymer (Guildf).*, vol. 42, no. 25, pp. 09929–09940, 2001.

[27] S. S. Ray and M. Bousmina, "Biodegradable polymers and their layered silicate nanocomposites: In greening the 21st century materials world," *Prog. Mater. Sci.*, vol. 50, no. 8, pp. 962–1079, 2005.

[28] D. R. Paul and L. M. Robeson, "Polymer nanotechnology: Nanocomposites," *Polymer (Guildf).*, vol. 49, no. 15, pp. 3187–3204, 2008.

[29] T. Tanaka, "Dielectric nanocomposites with insulating properties," *IEEE Trans. Dielectr. Electr. Insul.*, vol. 12, no. 5, pp. 914–928, 2005.

[30] P. B. Messersmith and E. P. Giannelis, "Synthesis and barrier properties of poly(ε-caprolactone)-layered silicate nanocomposites," *J. Polym. Sci. Part A Polym. Chem.*, vol. 33, no. 7, pp. 1047–1057, 1995.

[31] a. a. Azeez, K. Y. Rhee, S. J. Park, and D. Hui, "Epoxy clay nanocomposites – processing, properties and applications: A review," *Compos. Part B Eng.*, vol. 45, pp. 308–320, 2013.

[32] K. Kalaitzidou, H. Fukushima, and L. T. Drzal, "Multifunctional polypropylene composites produced by incorporation of exfoliated graphite nanoplatelets," *Carbon N. Y.*, vol. 45, no. 7, pp. 1446–1452, 2007.

[33] M. F. Horst, L. M. Quinzani, and M. D. Failla, "Rheological and barrier properties of nanocomposites of HDPE and exfoliated montmorillonite," *J. Thermoplast. Compos. Mater.*, pp. 106–125, 2012.

[34] W. Zheng and S. C. Wong, "Electrical conductivity and dielectric properties of PMMA/expanded graphite composites," *Compos. Sci. Technol.*, vol. 63, no. 2, pp. 225–235, 2003.

[35] H. W. Kroto, J. R. Heath, S. C. O'Brien, R. F. Curl, and R. E. Smalley, "C 60: buckminsterfullerene," *Nature*, vol. 318, p. 162, 1985.

[36] F. El-Tantawy, K. Kamada, and H. Ohnabe, "In situ network structure, electrical and thermal properties of conductive epoxy resin-carbon black composites for electrical heater applications," *Mater. Lett.*, vol. 56, no. 1–2, pp. 112–126, 2002.

[37] J. J. Lesko, A. Machida, S. H. Rizkalla, F. Asce, T. C. Triantafillou, and M. Asce, "Fiber-Reinforced Polymer Composites for Construction — State-of-the-Art Review," vol. 6, no.

May, pp. 73–87, 2002.

[38] A. K. Geim and K. S. Novoselov, “The rise of graphene,” *Nat. Mater.*, vol. 6, no. 3, pp. 183–191, 2007.

[39] K. Lau, C. Gu, and D. Hui, “A critical review on nanotube and nanotube/nanoclay related polymer composite materials,” *Compos. Part B Eng.*, vol. 37, no. 6, pp. 425–436, 2006.

[40] Y. Li, J. Zhu, S. Wei, J. Ryu, Q. Wang, L. Sun, and Z. Guo, “Poly(propylene) Nanocomposites Containing Various Carbon Nanostructures,” *Macromol. Chem. Phys.*, vol. 212, no. 22, pp. 2429–2438, 2011.

[41] J. N. Coleman, U. Khan, and Y. K. Gun’ko, “Mechanical Reinforcement of Polymers Using Carbon Nanotubes,” *Adv. Mater.*, vol. 18, no. 6, pp. 689–706, 2006.

[42] J. N. Coleman, U. Khan, W. J. Blau, and Y. K. Gun’ko, “Small but strong: A review of the mechanical properties of carbon nanotube–polymer composites,” *Carbon N. Y.*, vol. 44, no. 9, pp. 1624–1652, 2006.

[43] M. Moniruzzaman and K. I. Winey, “Polymer nanocomposites containing carbon nanotubes,” *Macromolecules*, vol. 39, no. 16, pp. 5194–5205, 2006.

[44] Y. Zou, Y. Feng, L. Wang, and X. Liu, “Processing and properties of MWNT/HDPE composites,” *Carbon N. Y.*, vol. 42, no. 2, pp. 271–277, 2004.

[45] K. Lau, S. Shi, L. Zhou, and H. Cheng, “Journal of Composite Materials,” *Composites*, vol. 37, no. 4, pp. 365–376, 2003.

[46] M. Moniruzzaman, F. Du, N. Romero, and K. I. Winey, “Increased flexural modulus and strength in SWNT/epoxy composites by a new fabrication method,” *Polymer (Guildf).*, vol. 47, no. 1, pp. 293–298, 2006.

[47] H. Miyagawa and L. T. Drzal, “Thermo-physical and impact properties of epoxy nanocomposites reinforced by single-wall carbon nanotubes,” *Polymer (Guildf).*, vol. 45, no. 15, pp. 5163–5170, 2004.

[48] R. Haggenmueller, H. H. Gommans, a. G. Rinzler, J. E. Fischer, and K. I. Winey, “Aligned single-wall carbon nanotubes in composites by melt processing methods,” *Chem. Phys. Lett.*, vol. 330, no. 3–4, pp. 219–225, 2000.

[49] W. a D. Heer, W. S. Bacsa, a Chatelain, and T. Gerfin, “Aligned Carbon Nanotube Films : Production and Optical and Electronic Properties,” *Science (80-.).*, vol. 268, no. 5212, p. 845, 1995.

[50] D. R. Dreyer, S. Park, C. W. Bielawski, and R. S. Ruoff, “The chemistry of graphene oxide,” *Chem. Soc. Rev.*, vol. 39, no. 1, pp. 228–240, 2010.

[51] H. Kim, A. A. Abdala, and C. W. Macosko, "Graphene/Polymer Nanocomposites," *Macromolecules*, vol. 43, no. 16, pp. 6515–6530, 2010.

[52] X. Shen, X. Lin, N. Yousefi, J. Jia, and J. K. Kim, "Wrinkling in graphene sheets and graphene oxide papers," *Carbon N. Y.*, vol. 66, pp. 84–92, 2014.

[53] L. T. Drzal, "A Multi-functional Nanomaterial Additive for Polymers and Composites," *www.xgsciences.com*, 2012.

[54] S. Kim, I. Do, and L. T. Drzal, "Thermal stability and dynamic mechanical behavior of exfoliated graphite nanoplatelets-LLDPE nanocomposites," *Polym. Compos.*, vol. 31, no. 5, pp. 755–761, Jan. 2009.

[55] X. Jiang and L. T. Drzal, "Multifunctional high density polyethylene nanocomposites produced by incorporation of exfoliated graphite nanoplatelets 1: Morphology and mechanical properties," *Polym. Compos.*, vol. 16, no. 2, p. NA-NA, 2009.

[56] D. Lahiri, R. Dua, C. Zhang, I. De Socarraz-Novoa, A. Bhat, S. Ramaswamy, and A. Agarwal, "Graphene nanoplatelet-induced strengthening of ultrahigh molecular weight polyethylene and biocompatibility in vitro," *ACS Appl. Mater. Interfaces*, vol. 4, no. 4, pp. 2234–2241, 2012.

[57] S. Chatterjee, J. W. Wang, W. S. Kuo, N. H. Tai, C. Salzmann, W. L. Li, R. Hollertz, F. A. Nüesch, and B. T. T. Chu, "Mechanical reinforcement and thermal conductivity in expanded graphene nanoplatelets reinforced epoxy composites," *Chem. Phys. Lett.*, vol. 531, pp. 6–10, 2012.

[58] X. Jiang and L. T. Drzal, "Multifunctional high-density polyethylene nanocomposites produced by incorporation of exfoliated graphene nanoplatelets 2: Crystallization, thermal and electrical properties," *Polym. Compos.*, vol. 33, no. 4, pp. 636–642, Apr. 2012.

[59] K. Kalaitzidou, H. Fukushima, and L. T. Drzal, "A route for polymer nanocomposites with engineered electrical conductivity and percolation threshold," *Materials (Basel).*, vol. 3, no. 2, pp. 1089–1103, 2010.

[60] X. Jiang and L. T. Drzal, "Reduction in percolation threshold of injection molded high-density polyethylene/exfoliated graphene nanoplatelets composites by solid state ball milling and solid state shear pulverization," *J. Appl. Polym. Sci.*, vol. 124, no. 1, pp. 525–535, Apr. 2012.

[61] Y. Cui, S. I. Kundalwal, and S. Kumar, "Gas barrier performance of graphene/polymer nanocomposites," *Carbon N. Y.*, vol. 98, pp. 313–333, 2016.

[62] B. Freeman and A. Hill, "Free volume and transport properties of barrier and membrane polymers," *ACS Symp. Ser.*, vol. 710, pp. 306–325, 1998.

[63] R. K. Bharadwaj, "Modeling the barrier properties of polymer-layered silicate nanocomposites," *Macromolecules*, vol. 34, no. 26, pp. 9189–9192, 2001.

[64] Z. Spitalsky, D. Tasis, K. Papagelis, and C. Galiotis, "Carbon nanotube-polymer composites: Chemistry, processing, mechanical and electrical properties," *Prog. Polym. Sci.*, vol. 35, no. 3, pp. 357–401, 2010.

[65] W. Ming-Wen, H. Tze-Chi, and Z. Jie-Ren, "Sintering Process and Mechanical Property of MWCNTs/HDPE Bulk Composite," *Polym. Technol. Eng.*, vol. 48, no. 8, pp. 821–826, 2009.

[66] C. D. Mueller, S. Nazarenko, T. Ebeling, T. L. Schuman, A. Hiltner, and E. Baer, "Novel structures by microlayer coextrusion?talc-filled PP, PC/SAN, and HDPE/LLDPE," *Polym. Eng. Sci.*, vol. 37, no. 2, pp. 355–362, 1997.

[67] D. Jarus, "Barrier properties of polypropylene/polyamide blends produced by microlayer coextrusion," *Polymer (Guildf).*, vol. 43, no. 8, pp. 2401–2408, 2002.

[68] G. Hu, C. Zhao, S. Zhang, M. Yang, and Z. Wang, "Low percolation thresholds of electrical conductivity and rheology in poly(ethylene terephthalate) through the networks of multi-walled carbon nanotubes," *Polymer (Guildf).*, vol. 47, no. 1, pp. 480–488, 2006.

[69] M. A. Priolo, D. Gamboa, K. M. Holder, and J. C. Grunlan, "Super gas barrier of transparent polymer-clay multilayer ultrathin films," *Nano Lett.*, vol. 10, no. 12, pp. 4970–4974, 2010.

[70] M. A. Priolo, D. Gamboa, and J. C. Grunlan, "Transparent clay-polymer nano brick wall assemblies with tailorable oxygen barrier," *ACS Appl. Mater. Interfaces*, vol. 2, no. 1, pp. 312–320, 2010.

[71] M. A. Priolo, K. M. Holder, D. Gamboa, and J. C. Grunlan, "Influence of clay concentration on the gas barrier of clay-polymer nanobrick wall thin film assemblies," *Langmuir*, vol. 27, no. 19, pp. 12106–12114, 2011.

[72] M. A. Priolo, K. M. Holder, S. M. Greenlee, B. E. Stevens, and J. C. Grunlan, "Precisely tuning the clay spacing in nanobrick wall gas barrier thin films," *Chem. Mater.*, vol. 25, no. 9, pp. 1649–1655, 2013.

[73] J. Lu, I. Do, H. Fukushima, I. Lee, and L. T. Drzal, "Stable Aqueous Suspension and Self-Assembly of Graphite Nanoplatelets Coated with Various Polyelectrolytes," *J. Nanomater.*, vol. 2010, pp. 1–11, 2010.

[74] S. Biswas and L. T. Drzal, "A novel approach to create a highly ordered monolayer film of graphene nanosheets at the liquid-liquid interface," *Nano Lett.*, vol. 9, no. 1, pp. 167–172, 2009.

[75] A. Hirsch, “Functionalization of single-walled carbon nanotubes,” *Angew. Chemie - Int. Ed.*, vol. 41, no. 11, pp. 1853–1859, 2002.

[76] X. Hu, E. Su, B. Zhu, J. Jia, P. Yao, and Y. Bai, “Preparation of silanized graphene/poly(methyl methacrylate) nanocomposites in situ copolymerization and its mechanical properties,” *Compos. Sci. Technol.*, vol. 97, no. September, pp. 6–11, 2014.

[77] M. A. Downey, “TOUGHENING OF CARBON FIBER-REINFORCED EPOXY POLYMER COMPOSITES VIA COPOLYMERS AND GRAPHENE NANO-PLATELETS,” Michigan State University, 2016.

CHAPTER 2 - INVESTIGATING THE MECHANICAL AND BARRIER PROPERTIES TO OXYGEN AND FUEL OF HIGH DENSITY POLYETHYLENE – GRAPHENE NANOPLATELET COMPOSITES

2.1 Introduction

Polymer composites are a growing area of interest, especially for the auto industry, for light weighting and fuel efficiency purposes. In particular, some thermoplastics like polyethylene or polypropylene offer low cost and ease of processing (via injection molding or extrusion), and adding fillers can improve their thermo-mechanical properties, thermal or electrical conductivity, or generate better barrier properties [1]. The properties of a composite material tend to not only depend on the properties of its constituents (matrix and filler) but also on the properties of the interface/interphase between them [2]. This is particularly true for nano-composites, as the surface area of the interface increases with a size reduction of the filler (at iso-volume concentration). Recently, the development of particles with an anisotropic shape (like rods, tubes, platelets, or even stars) has triggered a high level of interest because of the possibility to generate anisotropic properties, usually at low concentration [3].

Auto manufacturers are constantly looking for an improvement in vehicle fuel economy. This can be done by light weighting, but also by reducing the fuel evaporative emissions (hydrocarbon vapors that escape from a vehicle fuel system), which requires the use of light materials with optimal barrier properties for the manufacture of fuel lines and fuel tanks. Currently, fuel tanks have a layered structure made of a film with high barrier properties, such as polyamide 6 (PA 6) or ethylene vinyl alcohol (EVOH), sandwiched between layers of a semi-crystalline thermoplastic such as high density polyethylene (HDPE). An adhesive layer of maleic

anhydride grafted polypropylene insures good adhesion between them. Producing a fuel tank with a layered structure is not straightforward at the industrial scale, and EVOH is a relatively expensive thermoplastic that is sensitive to the ambient humidity level, as moisture greatly affects its barrier properties [4]. Moreover, while EVOH is an excellent barrier against diffusion of pure hydrocarbon based fuel, the barrier properties are reduced with fuel blends containing ethanol which are slated for increases. Standards set by the California Air Resources Board for low emission vehicles (LEV) state that no more than 2 grams of hydrocarbons can be emitted during 24 hours per car. However, future regulations for LEV II decrease that amount to 0.5g, and even stricter partial zero emissions reduce the value to 0.054 g. Fuel tank designs will need to be modified to reach these standards.

The advent of platelet shaped nanoparticles offers a promising new alternative to the multilayer approach. Because of their impenetrable nature and their platelet morphology, the addition of platelet shaped nanoparticles forces gases that penetrate the polymer to follow a tortuous path, which slows down their diffusivity, as shown in Figure 2.1. For example, nanoclay based polymer composites have been extensively investigated, with a large focus on montmorillonite composites. Nanoclays are layered silicates with Van Der Waals attraction forces between the layers, which can be overcome relatively easily in order to intercalate the polymer matrix between the layers [5]–[7]. Sharp improvements of the toughness of polypropylene have been reported with the addition of nanoclays [8], [9], as well as an improvement of the barrier properties of the hosting polymer matrix [10], [11].

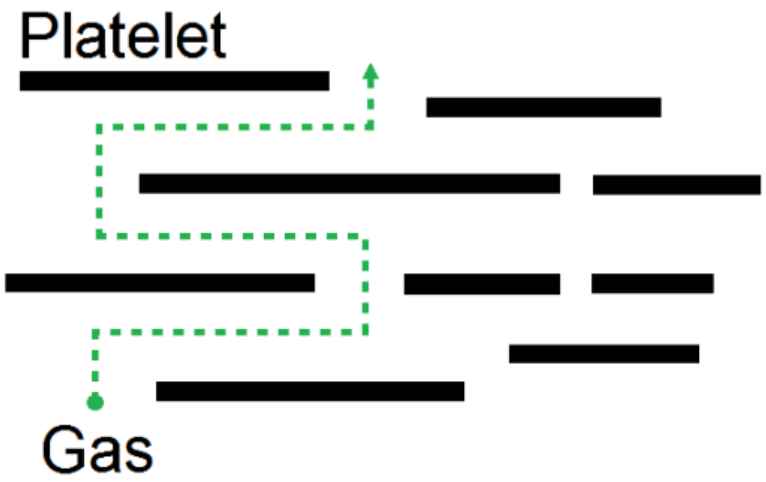

Figure 2.1. Tortuous path created by platelet shaped nanoparticles in a polymer matrix.

Like layered silicates, graphene possesses a platelet-like structure, which induces the same mechanism regarding barrier properties. Additionally, graphene has high electrical and thermal conductivities, whereas layered silicates do not. This means that graphene-based nanocomposites could offer more versatility if the concentration, dispersion and orientation of the graphene platelets are such that they lead to the generation of a percolated network [12]. While manufacturing pristine, highly crystalline, single layer graphene can be accomplished in a bottom-up approach via chemical vapor deposition [13], this process is not applicable for the production of industrial quantities at a cost effective price. Graphene nanoplatelets (GnP), made of a few stacked layers of graphene, can be produced in a cost effective, industrially robust process using a top down approach by intercalating bulk graphite with sulfuric acid, rapidly heating to induce expansion and then mechanically or ultrasonically reducing the GnP size [14]. GnP produced by this method contains oxygen functional groups at the edges of the platelets,

with relatively few defects on the surface. The GnP thickness is less than 10 nm, and their diameter can be controlled between several hundred of nanometers up to 80 microns.

Previous investigations with this material has focused on its combination with thermoplastics like polypropylene [15], low [16] and high [17] density polyethylene, and thermosets such as epoxy [18] or vinyl ester resins [19], but the main focus of was mechanical reinforcement and electrical and thermal conductivity. The barrier properties of similar systems, especially regarding fuel, have not been investigated extensively. Literature has shown that at the same loadings of GnP and nanoclays, the GnP composites will exhibit better permeation resistance to oxygen [20]. Recent studies have shown that incorporating graphene materials at extremely low concentrations of less than 1 wt. % has actually resulted in an increase in permeation due to voids at the interface of the filler and the polymer, however higher concentrations would be expected to result in enhanced barrier properties [21].

Assessing the barrier and the mechanical properties of HDPE-GnP composites as an alternative material for fuel tanks is the focus of this investigation.

2.2 Materials and Methods

2.2.1 Materials

High density polyethylene (HDPE) was supplied by INEOS Olefins and Polymers USA under the trade name K46-06-185 and was used as received. It has a density of 0.946 g.cm-3 (ASTM D4883) and a melt index (190 ºC/21.600 g) of 4.2 g/10 min (ASTM D1238). Three grades of

graphene nanoplatelets (GnP-M-15, GnP-M-5 and GnP-C-750) were obtained from XG Sciences (Lansing, Michigan, USA). Grades GnP-M-15 and GnP-M-5 have a surface area of 120-150 $m^2.g^{-1}$, an average thickness of 6 nm, and an average diameter of 15 μm and 5 μm, respectively. Grade GnP-C-750 has a surface area of 750 $m^2.g^{-1}$, an average thickness of 6 nm, and a diameter comprised between 300 nm and 1 μm. All samples were heated for 1 hour at 450 °C in an air circulating oven to remove any trace volatile compounds remaining from the manufacturing process.

2.2.2 Nanocomposite Processing

A co-rotating, twin-screw, DSM 15 cc extruder was used to process all of the nanocomposites. The DSM and injection molder can be seen in Figure 2.2. The melt temperature was set to 210 ºC and the twin-screws were rotating at 40-50 rpm, maintaining a constant shear force of approximately 6000 N. HDPE and GnP, in the dry state at room temperature, were manually mixed by hand and then transferred to the extruder and allowed to mix for 5 minutes. The composite was then transferred to a Daca Micro-injector. The temperature holding barrel for the injector was set to 210 ºC, the mold was set to 110 ºC and the pressure for the injection molding was 150 psi (1.0 MPa). Different molds were used to manufacture the tensile, flexural and Izod impact resistance test specimens. Neat HDPE and HDPE-GnP composites were processed under the same conditions. The range of GnP concentration was varied from 0.2 wt. % up to 30 or 40 wt. %, depending on the viscosity of the melt. Film samples for oxygen permeation testing were made by compressing two flexural specimens together between two mirror-finished platens, heated to 180 ºC and maintained at 180 °C for 5 minutes in a heated Carver press. A pressure of

550 psi was applied. The whole assembly was contained within a vacuum bag made with a polyamide film during pressing to avoid the generation of bubbles in the HDPE-GnP film. This resulted in films with thicknesses from 150 to 200 microns. The same procedure was used to make films for fuel permeation testing, by compressing two Izod test specimens under vacuum. The thickness of those films was typically higher, between 0.5 and 1.0 mm.

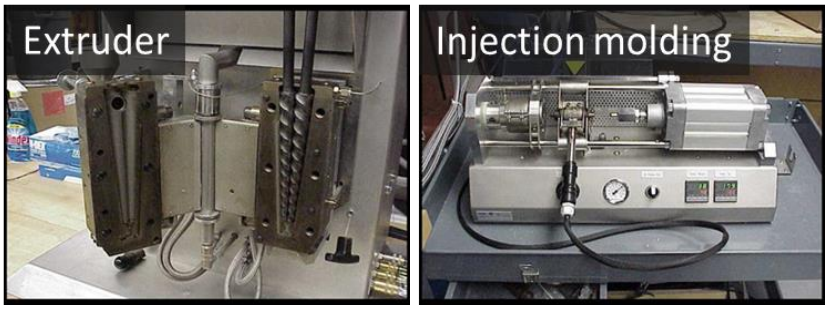

Figure 2.2. DSM micro-extruder and injection molder.

2.2.3 Testing Procedures

A UTS SFM-20 testing machine was used to measure the flexural properties of the composites according to ASTM D790 using a 100 lb load cell and a displacement speed of 0.05 $in.min^{-1}$. The thickness to span ratio was 1/16. 10 specimens were tested for each composite system.

Izod impact specimens were notched with a motorized tooth notcher 24 hours prior to testing, and then tested with a TMI impact apparatus and a 1 lb hammer, following ASTM D256. 10 specimens were tested for each composite system.

The crystallinity level was measured by Differential Scanning Calorimetry (DSC) with a TA Instruments Q2000 differential scanning calorimeter. Samples were first heated with a rate of 20 ºC.min^{-1} to 160 ºC, and held at 160 °C for 5 minutes before being cooled down to 40 ºC with a rate of 20 ºC.min^{-1}. This erased any thermal history of the specimens before assessing the influence of the GnP particles on the crystallinity of HDPE. The samples were then reheated to 160 ºC with a rate of 20 ºC.min^{-1}. The crystallinity of the HDPE matrix can be calculated according to Equation 1:

$$\boldsymbol{x}\% = \frac{\mathbf{1}}{\mathbf{1}-\boldsymbol{wt}.\%}\frac{\boldsymbol{\delta H_m}}{\boldsymbol{\delta H_m^0}} \quad \textbf{(}\text{Equation 1)}$$

where x% is the crystallinity, δH_m is the melting enthalpy of the sample, and δH^0_m is the theoretical melting enthalpy of pure crystalline HDPE, which is estimated by Mirabella et al. to be 288 J/g [22]. Three specimens were tested for each composite system.

The thermal stability of the composites was investigated via thermogravimetric analysis (TGA) using a Q500 machine from TA Instruments. In this process, the samples were heated in air to 600 °C at a rate of 10 ºC.min^{-1} and the amount of sample lost over time was monitored.

Permeation to oxygen was measured using a Mocon OX-TRAN 2/20 ML. Films were conditioned for 6 hours prior to testing. The resulting oxygen transmission rate was normalized with respect to film thickness.

Fuel permeation was performed using CARB phase II fuel (provided by the Haltermann Solutions Company) following the SAE International J2665 cup weight loss procedure with the 68-3014 vapometer system from the Thwing-Albert Instrument Company. Essentially, cups containing the fuel were sealed with the film to be tested and the mass loss of the assembly due to gas diffusion was monitored every 24 hours. The cups containing the fuel were kept in an explosion-proofed oven at 60 ºC and a flow of nitrogen through the oven was maintained during the entire time of the experiment to flush the flammable vapors out. The resulting fuel transmission rate was normalized with respect to film thickness.

A Zeiss EVO LS25 scanning electron microscope was used to examine the cross-section of flexural specimens. The acceleration voltage was 4 kV. In order to reveal the distribution and the orientation of the GnP platelets, some of the flexural test specimens were cut in half in the width direction and the generated surface was etched in a 50-50 oxygen/nitrogen plasma environment for 14 minutes with a power of 375W. The specimens were then coated with a 3 nm film of tungsten using a Leica EM MED020 sputter-coater.

2.3 Results and Discussion

2.3.1 SEM Characterization of the GnP Dispersion in HDPE

Optimal barrier and mechanical properties can only be achieved with a good dispersion of the GnP particles in the HDPE matrix. Oxygen plasma etching revealed the quality of the GnP dispersion in HDPE, and is shown in Figure 2.3 with SEM images.

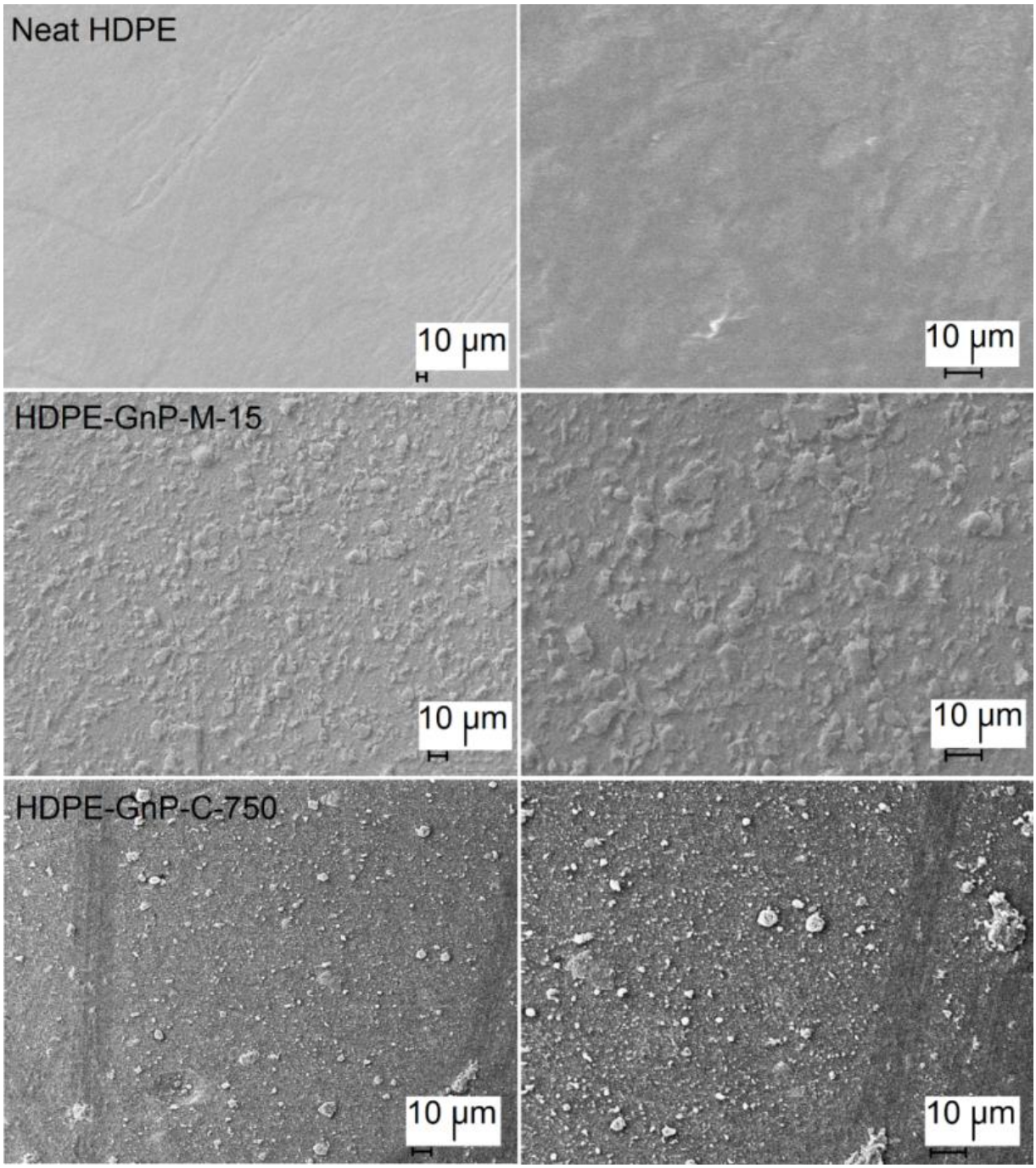

Figure 2.3. SEM images neat HDPE and HDPE composites with 5 wt. % of GnP-M-15 and GnP-C-750.

It is clear that the level of dispersion is directly related to the GnP particle size and associated surface area. In term of the quality of dispersion, the SEM pictures of the HDPE-GnP-M-5 pictures look very similar to the ones corresponding to the HDPE-GnP-M-15 composites and were not included. Both M grade GnPs had a similar surface area (120-150 m^2/g). The level of π-π interactions between the graphene sheets was similar as well, so an identical level of shear forces applied to the GnP particles led to a similar level of dispersion. On the contrary, a striking difference was observed with GnP-C-750 particles. Those particles are the smallest of the three references but their surface area is much higher ($750m^2/g$), which generate a higher level of π-π interactions. The dispersion of these particles was much worse, as large aggregates of several microns can be seen. When considering the images of the HDPE-GnP-M-15 composite, there are many small particles surrounding the 10-15 micron platelets, showing that there is size reduction occurring during the melt mixing process. This resulted in the generation of a significant quantity of 5-15 micron platelets. Regarding GnP-M-5 particles, not much particle size reduction was noticed, suggesting there is a threshold in size leading to size reduction during mixing.

2.3.2 Crystallinity of HDPE-GnP Composites

The typical DSC curve corresponding to a neat HDPE or a HDPE-GnP system is displayed in Figure 2.4. The value of the enthalpy of fusion was considered to be the area of the peak located between 70 °C and 140 °C. The crystallinity of the HDPE matrix (calculated according to Equation 1) as a function of GnP concentration is presented in Figure 2.5 for all three grades of GnP. It has been previously demonstrated that the addition of GnP to a semi-crystalline polymer can result in an increase in crystallinity due a nucleation effect of the GnP surface [23]. At low

concentrations of GnP (from 0.2 wt. % to 2 wt. %), there is a significant increase in the crystallinity of HDPE in comparison to the neat polymer, up to 8%. However, as the concentration of GnP increased, the crystallinity of the matrix did not increase any further. With a higher density of platelets in the matrix, there are more nucleation sites, but the mobility and diffusion of the HDPE chains is also reduced, limiting the growth of the HDPE crystallites [23]. It is hypothesized that these two mechanisms counteract each other at a concentration of 5 wt. %. At higher concentrations, the agglomeration of the platelets prevents a steady increase of the crystallinity as function of the GnP concentration. At very high concentration in GnP-M-15 (above 20 wt. %), the crystallinity of HDPE is actually lower compared to neat HDPE. Since the crystallinity for all of the composites above a 2 wt. % concentration of GnP is within 5% of the neat polymer crystallinity, it is expected that the small changes in crystallinity would not have a large effect on the mechanical or barrier properties.

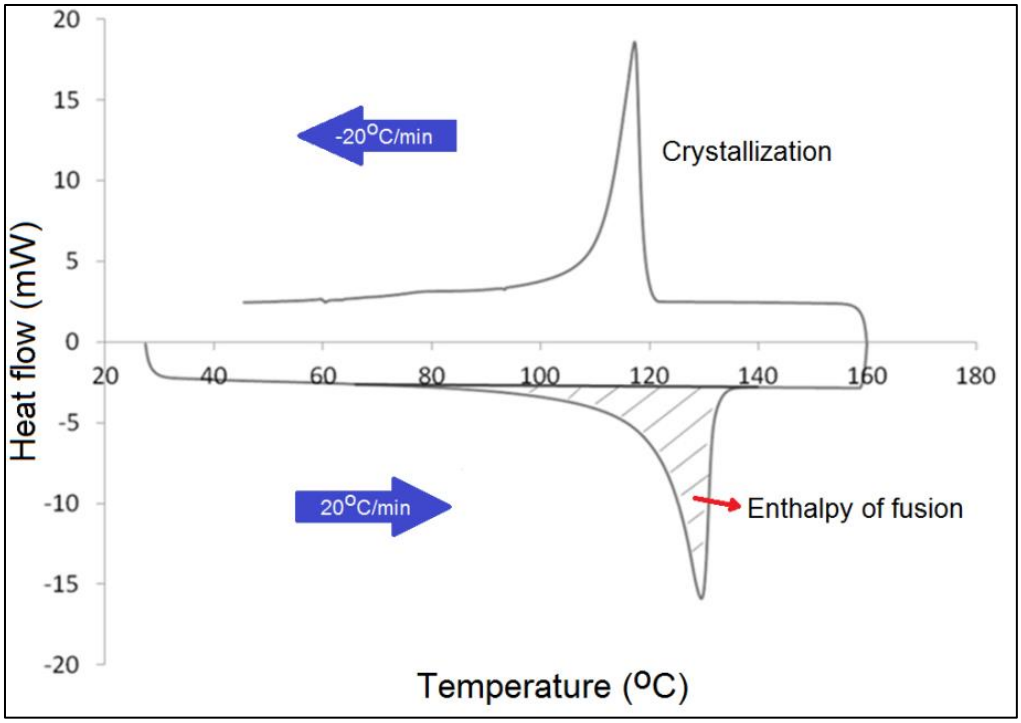

Figure 2.4. DSC curve of a HDPE-GnP composite.

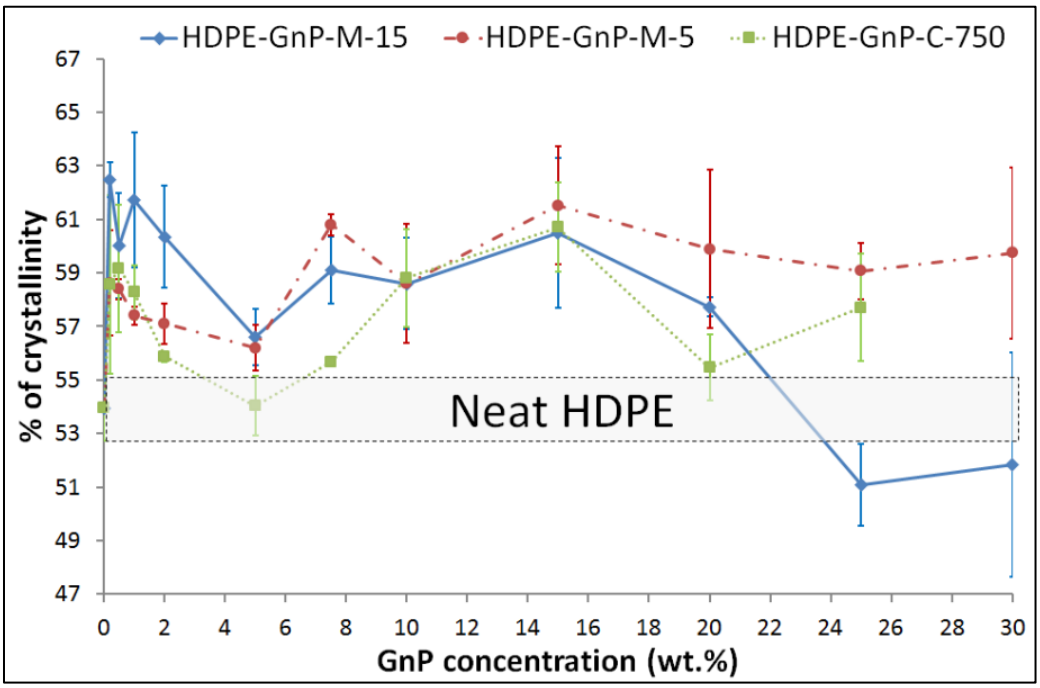

Figure 2.5. Crystallinity of HDPE-GnP composites from 0 to 30 wt. % GnP.

2.3.3 Thermal Stability of HDPE-GnP Composites

GnP is known to be a very good heat conductor. This effect is shown in the results of TGA in Figure 2.6. With both GnP-M-15 and GnP-C-750, the thermal stability of the HDPE is improved. As the concentration of the GnP increases, the degradation of the HDPE is delayed further. Another potential reason for the improvement in the thermal stability is because the addition of the GnP restricts the diffusion of oxygen, as will be shown, which may slow combustion. The thermal curves for GnP-M-5 yielded similar results to those obtained with GnP-M-15.

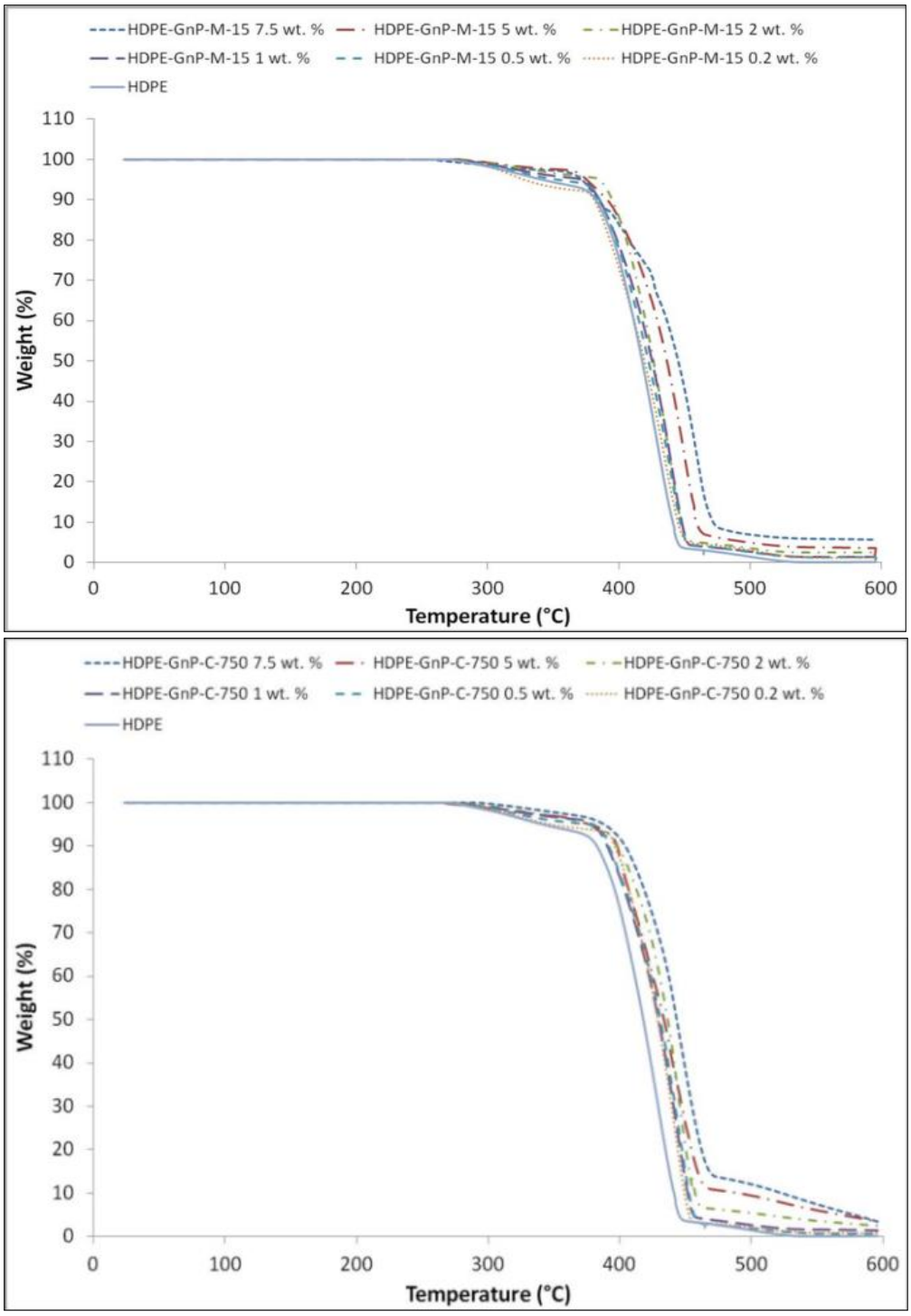

Figure 2.6. TGA analysis of HDPE-GnP composites.

2.3.4 Flexural Properties of HDPE-GnP Composites

Both flexural modulus and strength at yield of the HDPE-GnP composites are shown in Figure 2.7. As mentioned previously, melt viscosity limited the production of samples with the extruder, so concentrations of GnP above 25 wt. % and 30 wt. % for GnP-C-750 and GnP-M-5 respectively, could not be processed. For all three grades of GnP, the flexural modulus and strength tend to increase with increasing GnP content. For concentrations under 2 wt. %, there was no significant difference for either the modulus or the yield strength between the three GnP grades. The M grade GnPs resulted in a higher increase in stiffness than the C-750 grade at lower concentrations, probably due to agglomeration issues that were identified earlier in Figure 2. At concentrations of 7.5% wt. and higher, GnP-M-5 yielded higher increases in both modulus and strength than GnP-M-15 due to its smaller platelet size. Larger platelets can result in higher local stresses, which increase the chance of failure. At lower concentrations, the difference between GnP-M-15 and GnP-M-5 is most likely not evident due to the size reduction of GnP-M-15 during extrusion. After 7.5% wt., the C-750 composites also begin to exhibit strength that is greater than that of the equivalent M-grade composites. This could be due to the fact that the M-grade materials begin to agglomerate at higher concentrations like the C-750 material does even at low concentrations. This would result in even higher local stress concentrations in the M-grade composites due to the increased size of the agglomerates. At 10% wt. concentration in GnP-M-5 there is a 100% increase in modulus and a 40% increase in flexural strength in comparison to neat HDPE.

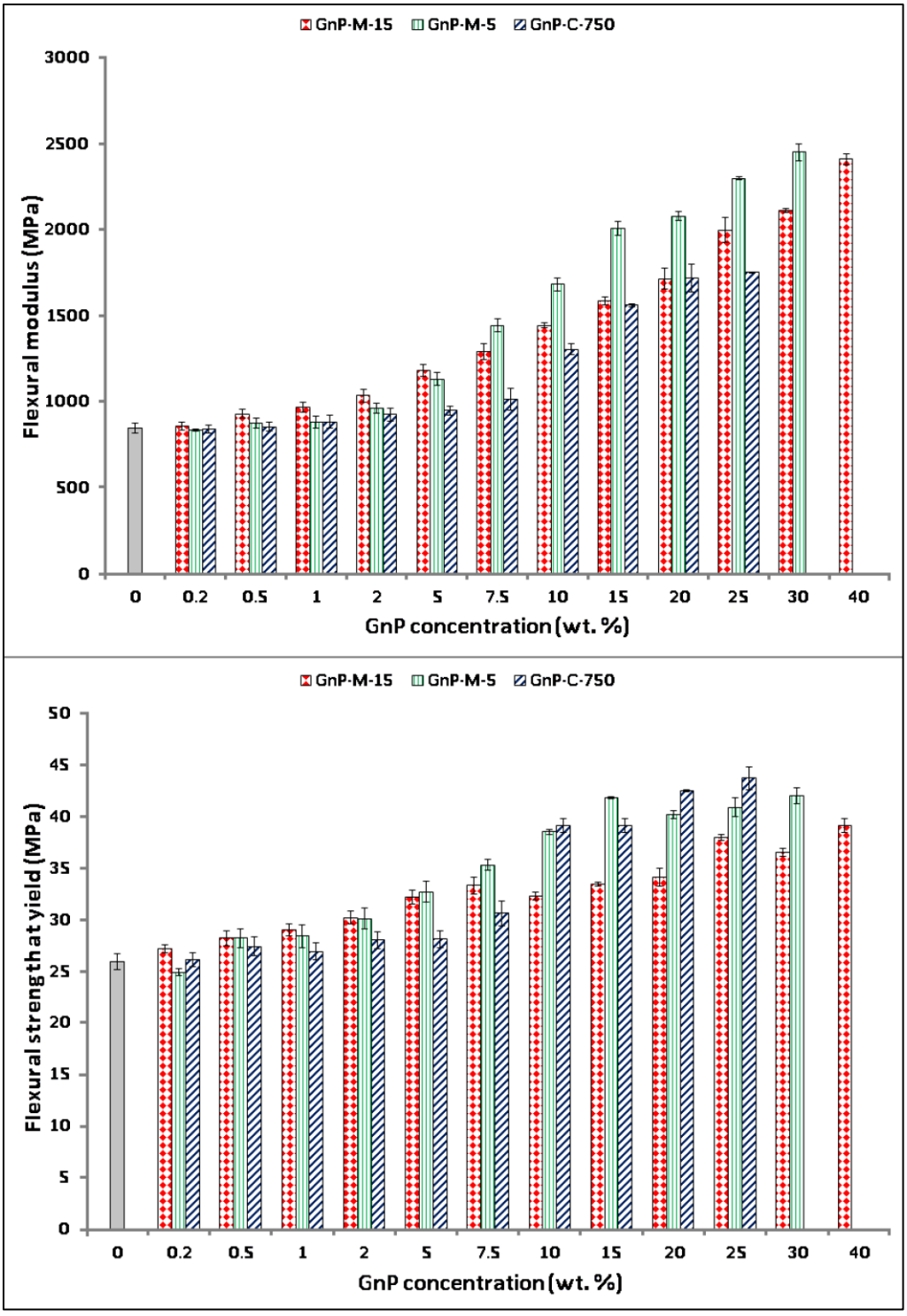

Figure 2.7. Evolution of the flexural modulus and strength at yield as a function of the GnP weight concentration.

2.3.5 Izod Impact Resistance of HDPE-GnP Composites

The addition of GnP to the HDPE matrix results in a large decrease in impact resistance for all grades, as seen in Figure 2.8. Even with a small addition of 0.2 wt. % of the M grade, a 46% decrease in impact resistance is observed. Increasing GnP concentration results in a further decrease. The smaller platelet size of the GnP-C-750 resulted in a lesser effect on the impact properties than the M grade materials, despite the agglomeration issues. If a better dispersion of the GnP-C-750 had been achieved, it could be expected that there would be an even smaller reduction in impact resistance.

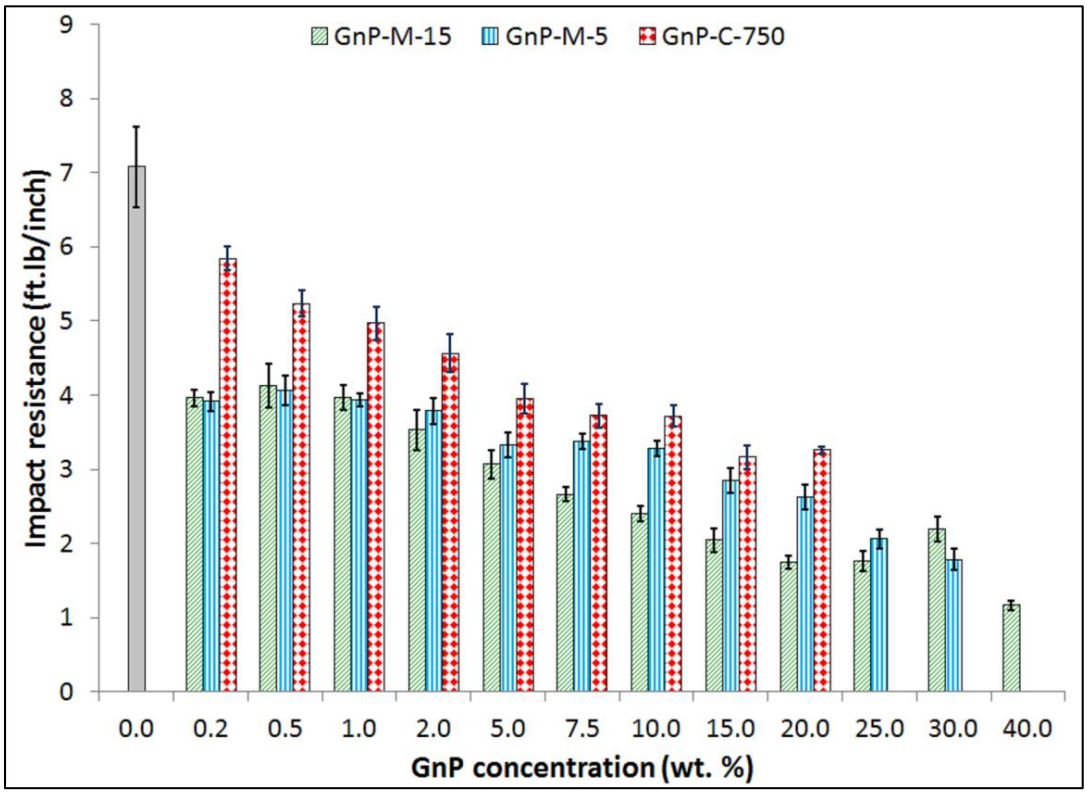

Figure 2.8. Evolution of the Izod impact resistance as a function of the GnP weight concentration.

The SEM images of the Izod impact fractures in Figure 2.9 help to explain these results. The profile of the neat HDPE break is relatively smooth near the notch and then wavy as the crack propagated. When GnP is added to composite, the fracture generated a cellular like structure with a GnP platelet at the center of each cell. The stress concentration around each particle weakens the overall impact resistance. In the GnP-C-750 corresponding samples, agglomerates of the platelets made the particles appear more like a ball rather than a platelet, but the overall cell-like structure is still apparent. The cellular structure could be explained by a more crystalline polymer around the GnP, as reported by the DSC analysis, with the platelets being a nucleation site and amorphous polymer surrounding the "cells." It is also clear at high magnification that there is poor interfacial adhesion between the GnP and the HDPE matrix, as evidenced by the lack of polymer present on the GnP surface, which is expected to have negative effects on the mechanical properties.

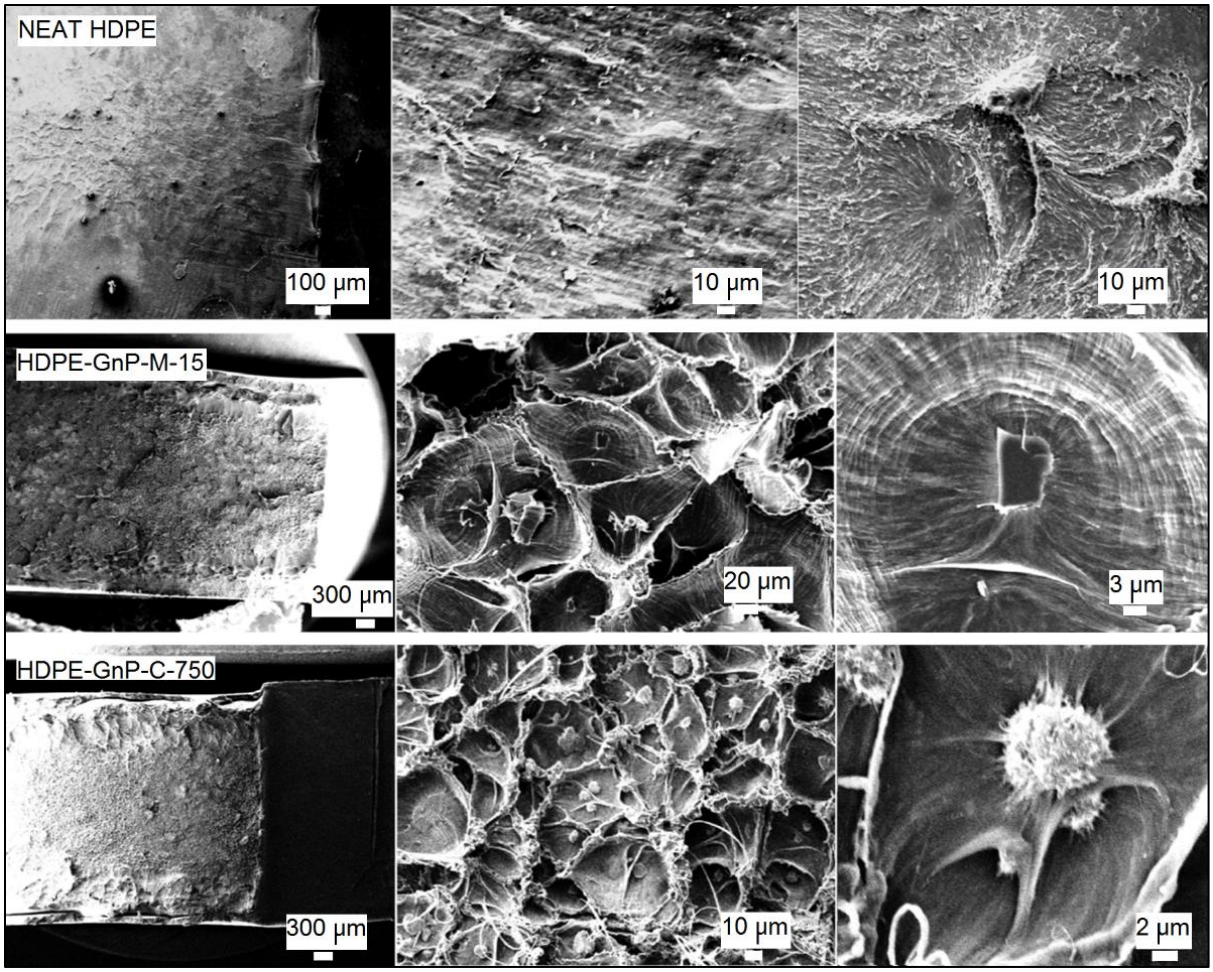

Figure 2.9. SEM images of the fracture surface of Izod test specimens with increasing magnification from left to right.

2.3.6 Oxygen Permeation Barrier Properties of HDPE-GnP Composites

As expected, adding GnP to the HDPE matrix decreases the steady state permeation to oxygen, as shown in Figure 2.10. The best results are obtained using the platelets with the highest aspect ratio, GnP-M-15. As expected, the smallest aspect ratio platelets, GnP-C-750, had the least effect on barrier properties, but the large amount of agglomeration also had an obvious negative impact. For Gnp-M-15 and GnP-M-5, increasing the GnP content resulted in additional decrease

in the oxygen permeation until a concentration of 20% wt. was reached. The GnP-M-15 composites produced a 77% reduction in oxygen permeation at this concentration. These results follow similar reductions that were found in melt mixing of polymers and graphenic materials presented in a review article by Cui et. al. [24]. A higher concentration did not result in further improvement, suggesting the effect of the tortuous path is limited by the dispersion of the GnP in the polymer matrix. At the high concentrations, the GnP was so agglomerated, that the tortuous path was mostly likely shortened overall, leading to a higher permeation rate above 20% wt. While this is a significant reduction in oxygen permeation, theoretical models suggest that there should be a 98% reduction in permeation with GnP-M-15 platelets assuming perfect dispersion and orientation [25]. Cross-sections of the films were plasma treated to expose the platelets, and examined with an SEM. There was a general alignment of the platelets with the flow direction of injection molding, which has been previously reported with GnP [26]. However, there were still misaligned platelets and agglomerations present even with the M grade materials, as seen in Figure 2.11. Compared to EVOH, which yields a value of 0.5 mL.mm/(m^2.day), the best HDPE-GnP composite was still an order of magnitude higher in oxygen permeation. Clearly there is still room for improvement in the GnP, especially through a better dispersion of GnP in the polymer matrix.

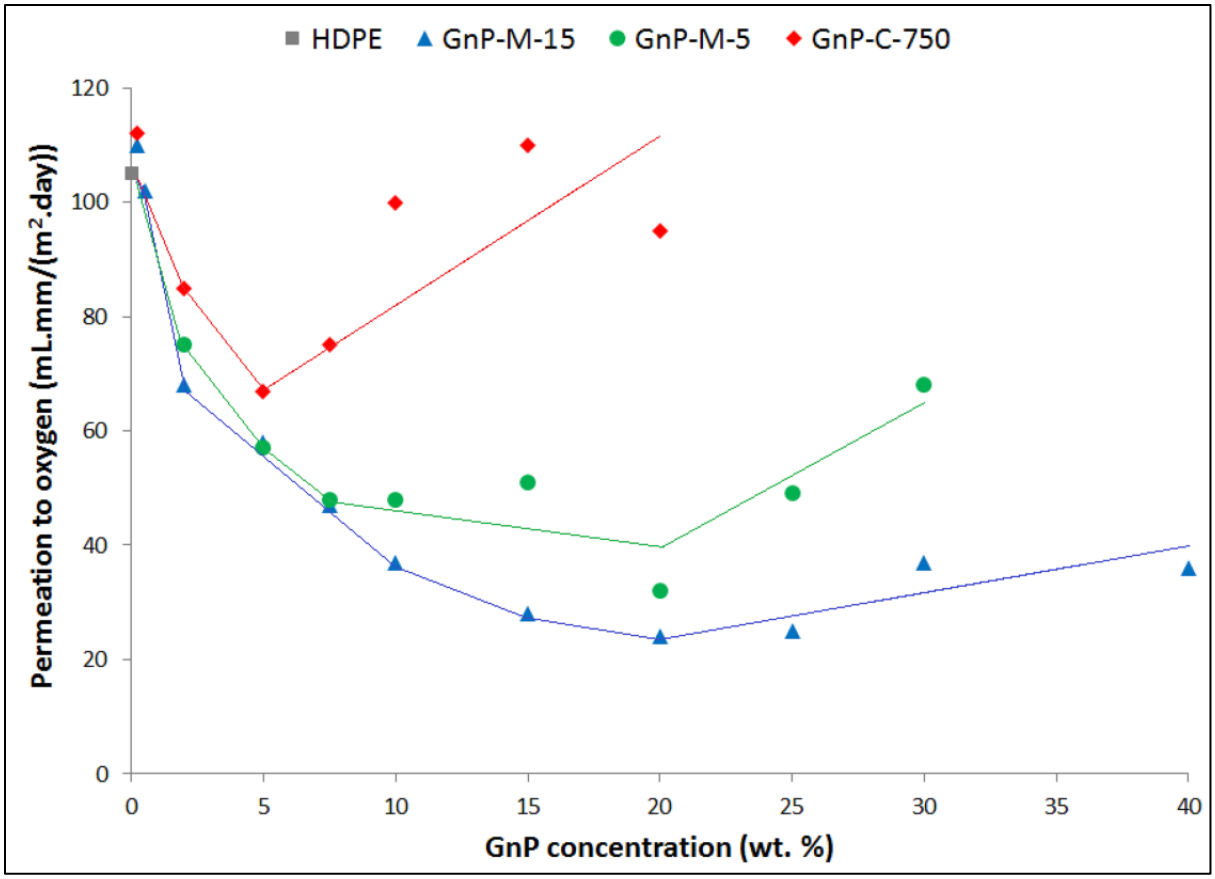

Figure 2.10. Permeation to oxygen as a function of GnP weight concentration.

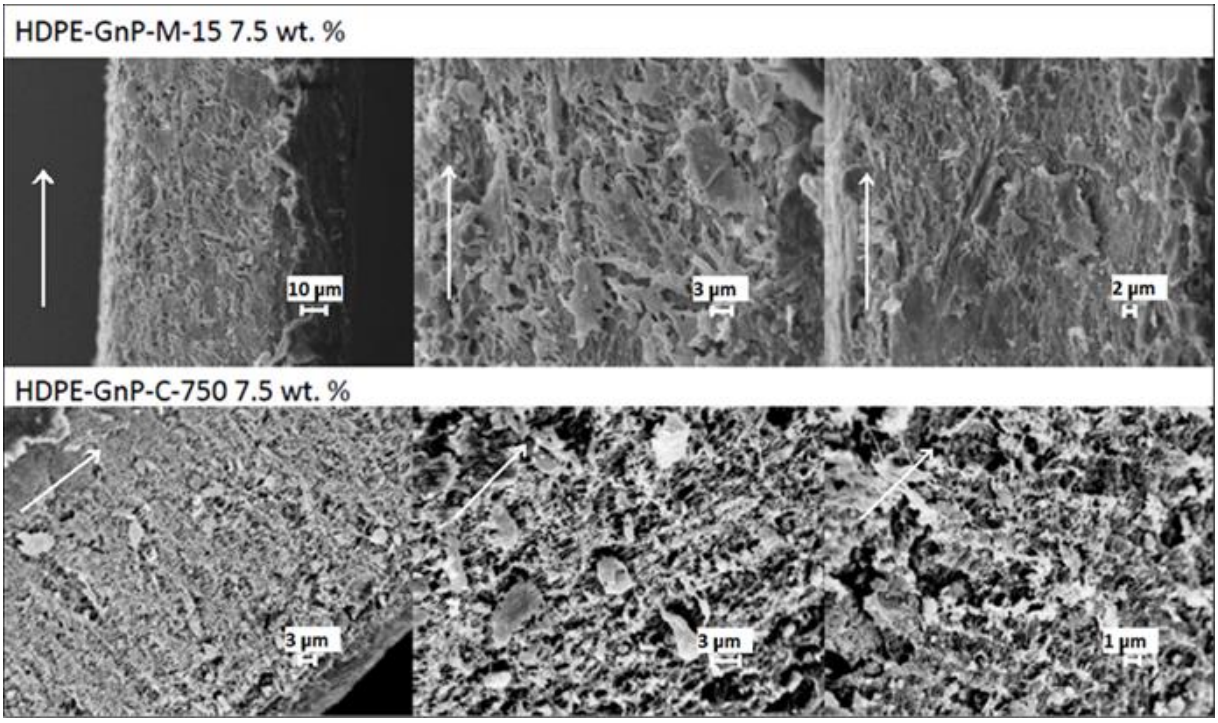

Figure 2.11. SEM of plasma treated film cross-section for 7.5 wt. % GnP-M-15 and GnP-C-750 composites.

2.3.7 Fuel Permeation Barrier Properties of HDPE-GnP Composites

The fuel permeation of pure HDPE was measured to be 270 g.mm/(m2.day), which is close to the value of 310 g.mm/(m2.day) reported by Nulman et al. [27]. The fuel permeation results of the HDPE-GnP composites are shown in Figure 2.12, and follow very similar trends to the oxygen permeation. GnP-C-750 again had the smallest effect, due to both aspect ratio and agglomeration issues. For both M grade GnP composites, there is a steep drop in fuel permeation up to a weight concentration of 7.5 wt. %. After this concentration, the improvement tapers off. GnP-M-15 yielded the best results at lower concentration, but at higher concentrations, there is a similar impact between the GnP-M-15 and GnP-M-5. For the GnP-M-15 composites, there is a 64% reduction in fuel permeation at a 7.5 wt. % concentration and a 74% reduction at 15 wt. %,

compared to a 55% and 73% reduction in oxygen permeation for the same concentrations respectively.

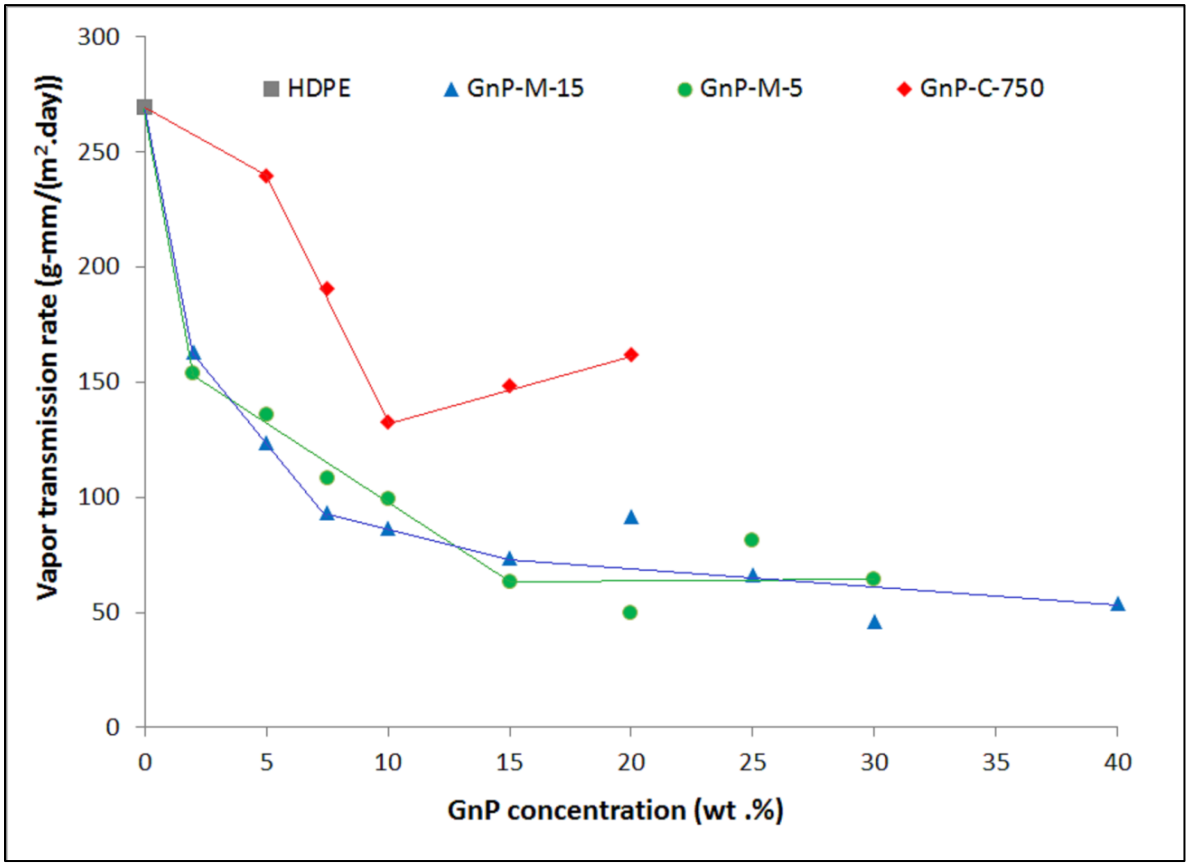

Figure 2.12. Permeation to fuel as a function of GnP weight concentration.

If only GnP-M-15 and GnP-M-5 composites are considered for the concentrations less than 25wt. % GnP (due to increased agglomeration issues at higher concentrations), a direct correlation between the oxygen and fuel permeation was found. This correlation is presented in Figure 2.13. The oxygen permeation test is much simpler and time efficient to conduct than the fuel permeation test. The strong correlation between the results of the two tests means the oxygen test can be used as an efficient screening tool prior to testing materials for fuel permeation.

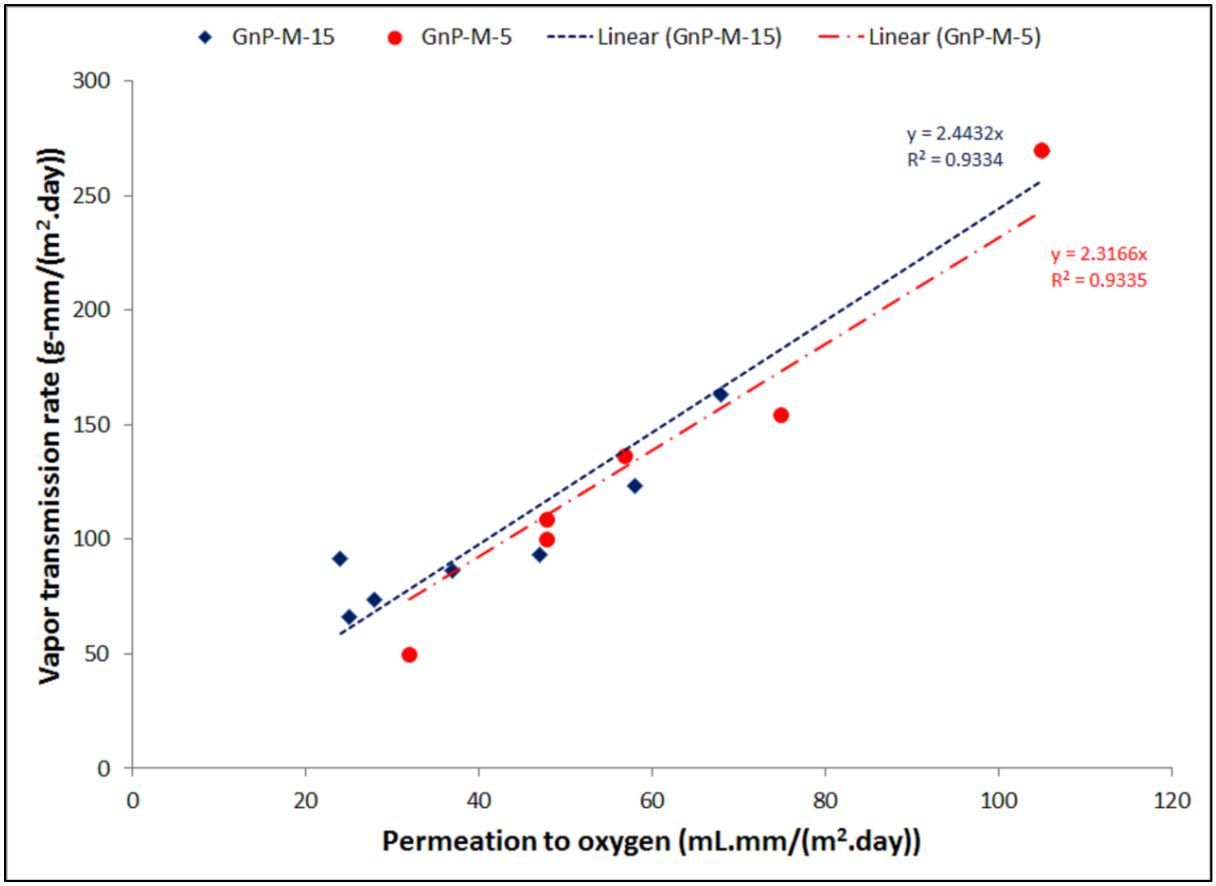

Figure 2.13. Correlation between permeation to oxygen and permeation to fuel of HDPE-GnP composites.

2.4 Conclusions

Melt mixing of HDPE and GnP was investigated as a cost effective method to manufacture HDPE composites for use in fuel lines and fuel tanks. A clear reduction in oxygen permeation with respect to neat HDPE was measured, highlighting the barrier properties generated by the GnP nanoparticles. A 20 wt. % GnP-M-15 composite yielded a 77% reduction in oxygen permeation. The largest platelets yielded the highest reduction in oxygen transmission. The smallest platelets, GnP-C-750, were poorly dispersed and did not lead to acceptable barrier properties. Similar trends were observed with fuel permeation as a 15 wt. % GnP-M-15 composite yielded a 74% reduction in fuel permeation (compared to a 73% reduction in oxygen permeation at the same loading). Adding GnP to HDPE also affected the mechanical properties. In general, there was an increase in flexural modulus and flexural strength with an increase in GnP concentration. Smaller platelets induced better strength due to lower local stresses. However, when significant agglomeration occurred this effect was nullified, as evidenced by the GnP-C-750 composite results. While the flexural modulus and strength were improved, a large, 46% decrease in impact resistance was observed even with only 0.2 wt. % GnP added to HDPE. Increasing the GnP content resulted in a further reduction of impact resistance. The addition of GnP also enhanced the thermal stability of the composites. It is clear that further enhancement could be obtained with a modification and optimization of the surface of the GnP particles and perhaps the use of alternative mixing methods. Tailoring the surface properties could potentially lead to better interfacial adhesion with the matrix, which could improve the impact properties. The level of dispersion could be optimized as well, leading to further improvement of the mechanical properties and also of the barrier properties. Better control of the orientation of the GnP could also be a parameter to consider for supplemental decrease of oxygen and fuel

permeation. Alternative methods for surface modification, mixing, particle dispersion and orientation control, and composite manufacturing are currently being investigated to address those issues.

REFERENCES

REFERENCES

[1] L. C. Tang, Y. J. Wan, D. Yan, Y. B. Pei, L. Zhao, Y. B. Li, L. Bin Wu, J. X. Jiang, and G. Q. Lai, "The effect of graphene dispersion on the mechanical properties of graphene/epoxy composites," *Carbon N. Y.*, vol. 60, pp. 16–27, 2013.

[2] F. Vautard, P. Fioux, L. Vidal, J. Schultz, M. Nardin, and B. Defoort, "Influence of the carbon fiber surface properties on interfacial adhesion in carbon fiber-acrylate composites cured by electron beam," *Compos. Part A Appl. Sci. Manuf.*, vol. 42, no. 7, pp. 859–867, 2011.

[3] J. R. Potts, D. R. Dreyer, C. W. Bielawski, and R. S. Ruoff, "Graphene-based polymer nanocomposites," *Polymer (Guildf).*, vol. 52, no. 1, pp. 5–25, 2011.

[4] H. Kwon, D. Kim, and J. Seo, "Thermal and barrier properties of EVOH/EFG nanocomposite films for packaging applications: Effect of the mixing method," *Polym. Compos.*, vol. 16, no. 2, pp. 1–10, Dec. 2014.

[5] E. P. Giannelis, R. Krishnamoorti, and E. Manias, "Polymer-Silicate Nanocomposites : Model Systems for Confined Polymers and Polymer Brushes," *Polymer (Guildf).*, vol. 138, pp. 107–147, 1999.

[6] M. Alexandre and P. Dubois, "Polymer-layered silicate nanocomposites: Preparation, properties and uses of a new class of materials," *Mater. Sci. Eng. R Reports*, vol. 28, no. 1, pp. 1–63, 2000.

[7] J. H. Park and S. C. Jana, "Mechanism of exfoliation of nanoclay particles in epoxy-clay nanocomposites," *Macromolecules*, vol. 36, no. 8, pp. 2758–2768, 2003.

[8] L. Chen, S. C. Wong, and S. Pisharath, "Fracture properties of nanoclay-filled polypropylene," *J. Appl. Polym. Sci. J. Appl. Polym. Sci.*, vol. 88, no. 14, pp. 3298–3305, 2003.

[9] Q. Yuan and R. D. K. Misra, "Impact fracture behavior of clay-reinforced polypropylene nanocomposites," *Polymer (Guildf).*, vol. 47, pp. 4421–4433, 2006.

[10] a. a. Azeez, K. Y. Rhee, S. J. Park, and D. Hui, "Epoxy clay nanocomposites – processing, properties and applications: A review," *Compos. Part B Eng.*, vol. 45, pp. 308–320, 2013.

[11] S. S. Ray and M. Bousmina, "Biodegradable polymers and their layered silicate nanocomposites: In greening the 21st century materials world," *Prog. Mater. Sci.*, vol. 50, no. 8, pp. 962–1079, 2005.

[12] W. Liu, I.-H. Do, H. Fukushima, and L. T. Drzal, "Influence of Processing on Morphology, Electrical Conductivity and Flexural Properties of Exfoliated Graphite Nanoplatelets-Polyamide Nanocomposites," *Carbon Lett.*, vol. 11, no. 4, pp. 279–284,

2010.

[13] I. Vlassiouk, M. Regmi, P. Fulvio, S. Dai, P. Datskos, G. Eres, and S. Smirnov, “Role of hydrogen in chemical vapor deposition growth of large single-crystal graphene,” *ACS Nano*, vol. 5, no. 7, pp. 6069–6076, 2011.

[14] L. Drzal and H. Fukushima, “Expanded graphite and products produced therefrom,” US Patent 7550529 B2, 2009.

[15] K. Kalaitzidou, H. Fukushima, and L. T. Drzal, “Mechanical properties and morphological characterization of exfoliated graphite-polypropylene nanocomposites,” *Compos. Part A Appl. Sci. Manuf.*, vol. 38, no. 7, pp. 1675–1682, 2007.

[16] S. Kim, I. Do, and L. T. Drzal, “Thermal stability and dynamic mechanical behavior of exfoliated graphite nanoplatelets-LLDPE nanocomposites,” *Polym. Compos.*, vol. 31, no. 5, pp. 755–761, Jan. 2009.

[17] X. Jiang and L. T. Drzal, “Multifunctional high-density polyethylene nanocomposites produced by incorporation of exfoliated graphene nanoplatelets 2: Crystallization, thermal and electrical properties,” *Polym. Compos.*, vol. 33, no. 4, pp. 636–642, Apr. 2012.

[18] S. Chatterjee, J. W. Wang, W. S. Kuo, N. H. Tai, C. Salzmann, W. L. Li, R. Hollertz, F. A. Nüesch, and B. T. T. Chu, “Mechanical reinforcement and thermal conductivity in expanded graphene nanoplatelets reinforced epoxy composites,” *Chem. Phys. Lett.*, vol. 531, pp. 6–10, 2012.

[19] W. Liu, I. Do, H. Fukushima, and L. T. Drzal, “Exfoliated Graphite Nanoplatelet-Vinyl Ester Nanocomposites,” in *7th Annual Automotive Composites Conference and Exhibition*, 2007.

[20] K. Kalaitzidou, H. Fukushima, and L. T. Drzal, “Multifunctional polypropylene composites produced by incorporation of exfoliated graphite nanoplatelets,” *Carbon N. Y.*, vol. 45, no. 7, pp. 1446–1452, 2007.

[21] K. J. Berean, J. Z. Ou, M. Nour, M. R. Field, M. M. Y. A. Alsaif, Y. Wang, R. Ramanathan, V. Bansal, S. Kentish, C. M. Doherty, A. J. Hill, C. McSweeney, R. B. Kaner, and K. Kalantar-Zadeh, “Enhanced gas permeation through graphene nanocomposites,” *J. Phys. Chem. C*, vol. 119, no. 24, pp. 13700–13712, 2015.

[22] F. M. Mirabella and A. Bafna, “Determination of the crystallinity of polyethylene/??-olefin copolymers by thermal analysis: Relationship of the heat of fusion of 100% polyethylene crystal and the density,” *J. Polym. Sci. Part B Polym. Phys.*, vol. 40, pp. 1637–1643, 2002.

[23] K. Kalaitzidou, H. Fukushima, P. Askeland, and L. T. Drzal, “The nucleating effect of exfoliated graphite nanoplatelets and their influence on the crystal structure and electrical conductivity of polypropylene nanocomposites,” *J. Mater. Sci.*, vol. 43, no. 8, pp. 2895–2907, 2008.

[24] Y. Cui, S. I. Kundalwal, and S. Kumar, “Gas barrier performance of graphene/polymer nanocomposites,” *Carbon N. Y.*, vol. 98, pp. 313–333, 2016.

[25] R. K. Bharadwaj, “Modeling the barrier properties of polymer-layered silicate nanocomposites,” *Macromolecules*, vol. 34, no. 26, pp. 9189–9192, 2001.

[26] K. Kalaitzidou, H. Fukushima, and L. T. Drzal, “A route for polymer nanocomposites with engineered electrical conductivity and percolation threshold,” *Materials (Basel).*, vol. 3, no. 2, pp. 1089–1103, 2010.

[27] M. Nulman, A. Olejnik, M. Samus, E. Fead, and G. Rossi, “Fuel Permeation Performance of Polymeric Materials,” *SAE Tech. Pap.*, vol. 2001–01–19, no. 724, 2001.

CHAPTER 3 - ADDITIONAL PROCESSING METHODS OF HDPE-GNP NANOCOMPOSITES AND THEIR MECHANICAL AND BARRIER PROPERTIES

3.1 Introduction

In previous research, melt mixing of graphene nanoplatelets (GnP) and high density polyethylene (HDPE) was investigated. This research seeks to expand on the results of the previous and use additional processing techniques for the composites to optimize the properties.

There are many ways to process thermoplastic polymer nanocomposites. Melt mixing followed by injection molding is typically the most straight-forward and cost effective way, but does not always yield optimal results for mechanical and barrier properties [1], [2]. Particle dispersion and alignment are two key factors that play a role in the effect of nanoparticles on the properties of the composites, especially mechanical and barrier properties. The mechanical properties would be negatively affected if there are large agglomerations of particle in the nanocomposites due to increased stress concentration sites. With poor dispersion and alignment, the barrier properties would also not be optimal. The effects of dispersion an alignment can be estimated using Equation 1 and Equation 2 from Bharadwaj [3]:

$$\frac{P_s}{P_p} = \frac{1-\phi_s}{1+\frac{L}{2W}\phi_s\left(\frac{2}{3}\right)\left(S+\frac{1}{2}\right)} \qquad \text{(Equation 1)}$$

$$S = \frac{1}{2}\langle 3\cos^2\theta - 1\rangle$$

(Equation 2)

where P_s is the composite permeability, P_p is the neat polymer permeability, Φ_s is the volume fraction of the filler, L is the diameter of the filler, and W is the thickness of the filler. The values of S and W are depicted in Figure 3.1 [3].

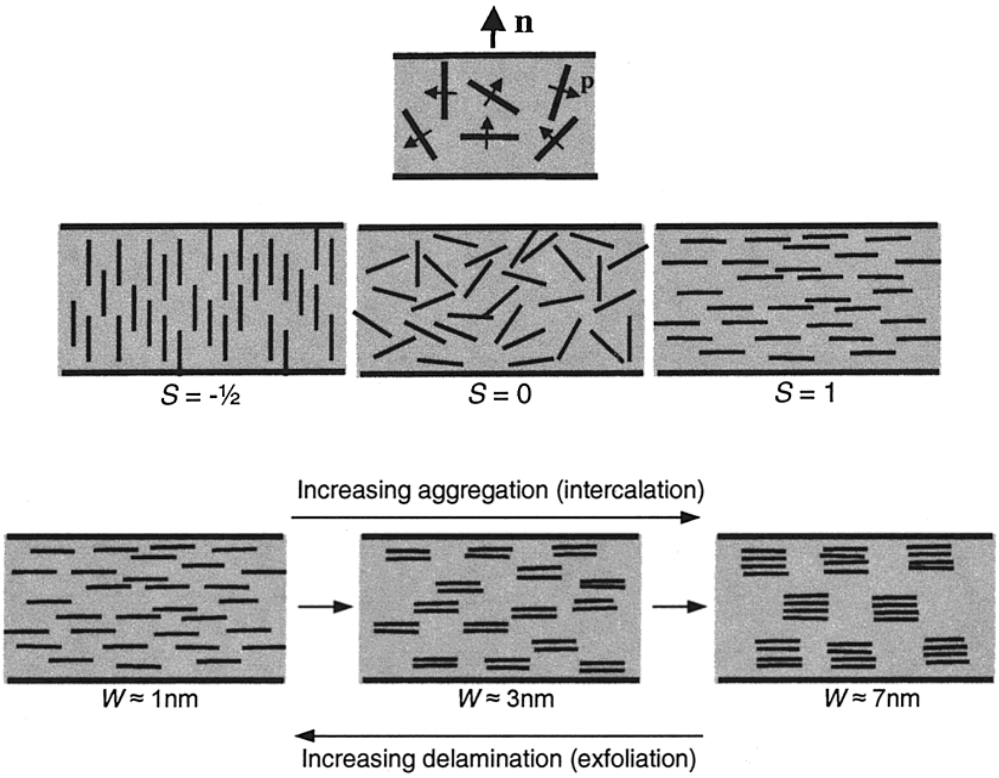

Figure 3.1. Illustration of how dispersion and alignment of fillers influence barrier properties [3]. Copied with permission

Ideally, the particles dispersed in the polymer matrix will have a very small value for W, suggesting good dispersion, and a value of 1 for S, which would describe perfect alignment of particles. When added to HDPE as in Chapter 2, a concentration of 10% volume (~20% wt.) GnP-M-15 should decrease the permeability by 98%. However, only a 77% reduction was observed. Scanning electron microscopy showed that there was significant agglomeration and misalignment of the platelets. Improving these two aspects should result in a composite that exhibits properties that are closer to the theoretical calculations.

There are many processing approaches that could result in improved dispersion and alignment of GnP in HDPE. Four approaches have been identified for further study, including microlayer co-extrusion, solution mixing, cryomilled-HDPE, and the coating of GnP prior to incorporating into HDPE. Figure 3.2 illustrates each method.

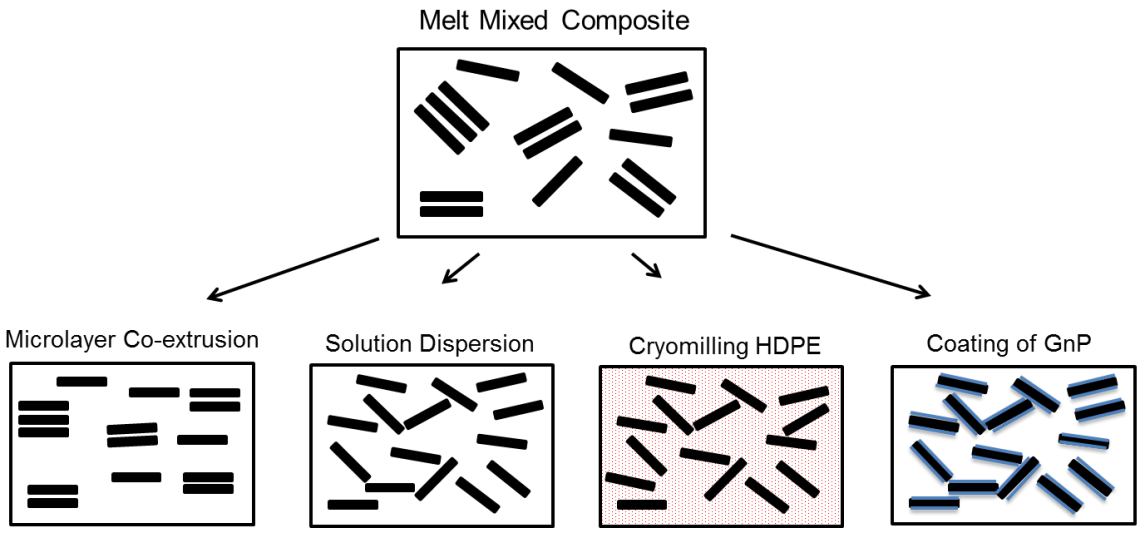

Figure 3.2. Alternative processing approaches

Microlayer co-extrusion (MCE) is a method that has been shown to result in highly aligned particles [4]. If perfect alignment is achieved, it should force the value of S to 1 in Equation 2, which would maximize the tortuous path and be optimal to prevent gas permeating through the matrix. The MCE process can be seen in Figure 3.3. In this process, the die takes a stream of polymer(s), slices it in half vertically, positions those two streams into a stack, and then compresses it into one stream. Each stage effectively doubles the number of "layers" within the stream. The forces on the particles from the repeated cutting and pressing should yield highly aligned GnP in an HDPE matrix. Since the mixing of the two materials is still done via melt extrusion, it would be expected to result in a similar dispersion as in melt extrusion followed by injection molding, as depicted in Figure 3.2.

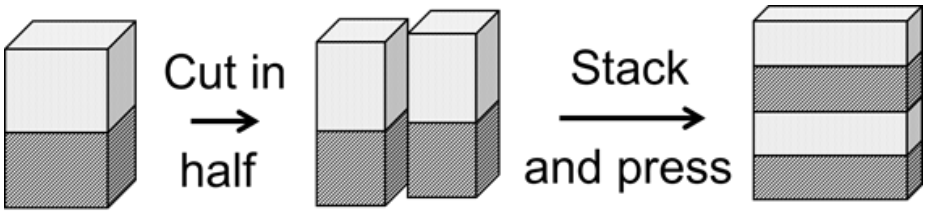

Figure 3.3. Microlayer co-extrusion process diagram.

To try to improve the dispersion of the GnP platelets in HDPE, it is important to make the surfaces of the platelets less attractive to each other and more attracted to the polymer matrix. One approach to achieve this is to coat the platelets with a material that is soluble in the matrix prior to using melt mixing for manufacturing the nanocomposites. It has previously been shown that a low molecular weight wax coating on the platelets improves the dispersion in an HDPE

matrix, which should result in enhanced properties [5]. Another coating that may provide benefits in dispersion and barrier properties is an elastomeric coating. Due to the potential difference in the coefficient of thermal expansion between the GnP and the HDPE matrix, small voids may form around the platelets during cooling [6]. Coating the platelets with an HDPE-compatible elastomer may help improve the interfacial adhesion between the GnP and HDPE, which would eliminate any potential voids and result in a matrix with better barrier properties.

The mixing environment of melt extrusion is very viscous, making it difficult to disperse the platelets effectively. When a nanofiller is added to the melt, the viscosity of the melt tends to increase even more [7]. In order to overcome this limitation, GnP and HDPE could be mixed in a solution based system. Using a solvent that HDPE is soluble in, such as xylene, it should be easier to disperse the platelets into the matrix. Once done, the solvent can be driven off, resulting in a dried material that can be further processed into samples. Ideally this would prevent larger agglomerates of GnP from forming, as depicted in Figure 3.2, resulting in a better overall dispersion of the nanofiller in the polymer matrix.

A third approach to improve the dispersion of the GnP in a polymer matrix is to cryomill the HDPE pellets into a finer powder prior to mixing [8]. Grinding the HDPE pellets into a size that is more similar to that of the GnP should result in improved dispersion prior to mixing, and less formation of agglomerates and concentrated areas of polymer. Additionally, in a fourth approach, a solution based approach could be combined with the cryomilling to coat the cryomilled HDPE particles with GnP platelets prior to melt mixing.

3.2 Materials and Methods

3.2.1 Materials

INEOS Olefins & Polymers USA again supplied the HDPE used, grade K46-06-185, with a density of 0.946 $g.cm^{-3}$. Two grades of GnP, GnP-M-15 and GnP-M-25, were supplied by XG Sciences (Lansing, MI, USA). The have diameters of 15 and 25 microns respectively and both have an average thickness of 6 nm and surface area of 120-150 $m2.g^{-1}$. The platelets were heated to 450 °C for 1 hour to remove volatile compounds from the manufacturing process. Two grades of wax were used to pre-coat the platelet. The first was a paraffin wax from Sigma Aldrich with a molecular weight of 500 $g.mol^{-1}$ and the second was from Sasol, trade name Sasolwax H1, with a slightly higher molecular weight of 800 $g.mol^{-1}$. The Sasol wax should be more stable at higher processing temperatures. A third coating was a Dow Chemical supplied polyolefin ethylene-octene copolymer elastomer with the trade name Engage 8200.

3.2.2 Microlayer Co-extrusion (MCE) Composite Processing

A Leistritz extruder with 25 mm co-rotating twin screws was used for large scale extrusion with a multi-layer slit die from Premier Dies Corporation. Extruding a film through the die results in a 16 “layer” structure. The screw configuration of the Leistritz can be seen in Figure 3.4. The melt is conveyed through the initial portion and then enters multiple kneading zones before being conveyed out to the film die. The temperature of the extruder and the die was set to 200 °C and the screw rotation speed was set to 20 rpm, which resulted in an overall pressure of 2000-2300 psi depending on the concentration of the platelets. The resulting film from the die was cooled on a three roll chill stack set to 100 °C and collected at a rate of two feet per minute. Two different

methods of mixing the composites were investigated. The first method was to mix the HDPE pellets and the GnP-M-25 powder in the extruder at a desired concentration and then immediately process it through the film die. The second method was to first make a 30% wt. masterbatch of GnP in HDPE using the same screw configuration and an open die. The extruded material was then chopped into pellets similar to the neat HDPE pellet size and used as a basis for making lower concentrations.

Figure 3.4. Screw configuration for the Leistritz extruder.

3.2.3 Solution Dispersion Composite Processing

To prepare the solution dispersed composites, GnP-M-15 was first dispersed in xylene with light sonication (20W) for 30 minutes. HDPE pellets were then added and the solution was stirred and heated to boiling under reflux conditions for 1 hour, after which the solution was allowed to cool to room temperature. Once cool, the HDPE/GnP mixture tends to precipitate out of solution. This material was dried under vacuum at 80 °C in a Binder oven to remove any trace xylene. The dried material was processed in two different manners. It was processed through the DSM as outline in Chapter 2 and films were compressed from flex specimens in the heated Carver Press. For comparison, films were also pressed directly from the dried composite.

3.2.4 Cryomilled HDPE Composite Processing

A Mikro-Bantam mill with a 0.02 inch filter was used with liquid nitrogen to cry-mill the HDPE pellets into a fine power. This powder was used in the DSM as outlined in Chapter 2 to make composites with GnP-M-15 for mechanical testing, and permeation properties were measured from a film compressed from a flex specimen in a heated Carver press. Alternatively, GnP and the HDPE powder were added to xylene at room temperature, and a light sonication of 20W was applied for 30 minutes in an attempt to coat the HDPE powder particles with GnP. The resulting material was dried in a vacuum oven at 80 °C and then pressed into a film using a heated Carver Press as outlined previously.

3.2.5 Coated GnP Composite Processing

Coating the platelets was done in a xylene solution. The coating material was first dissolved in xylene at room temperature, and then GnP-M-15 was dispersed using a light sonication of 20W for 30 minutes. The GnP platelets were coated at an 80:20 GnP to wax weight ratio for the Sasol and paraffin waxes. The platelets were coated at a 50:50 GnP to elastomer weight ratio for the Engage elastomer. Once coated, the material was dried in a vacuum oven at 80 °C to remove any trace solvent. The coated materials were then processed through the DSM as outlined in Chapter 2 with HDPE pellets. Films for permeation were again made by compressing a flex specimen in a heated Carver press.

3.2.6 Composite Characterization Techniques

Flexural properties were measured following ASTM D790 using a 100 lb load cell and a displacement speed of 0.05 $in.min^{-1}$ on a UTS SFM-20. The thickness to span ratio was 1/16. Izod impact specimens were measured according to ASTM D256. Notches were made in the samples with a motorized tooth notcher and samples were tested with a 1 lb hammer.

Thin films of the composites were tested for oxygen permeability using a Mocon OX-TRAN 2/20 ML. Films were conditioned 6 hours prior to testing and the resulting oxygen transmission rate was normalized with respect to film thickness.

A Zeiss EVO LS25 scanning electron microscope (SEM) was used to examine the cross-sections of Izod specimens and films that were cast in quick curing epoxy and polished. The acceleration voltage was 4 kV. To better expose the platelets for dispersion observations, samples were plasma treated in a 50-50 oxygen/nitrogen environment for 14 minutes with a power of 375W. The samples were coated with a 3 nm film of tungsten using a Leica EM MED020 sputter-coater to eliminate sample charging in the SEM.

3.3 Results and Discussion

3.3.1 Microlayer Co-extrusion Composites Results

When melt mixing is used to combine GnP-M-15 and HDPE, a noticeable improvement in barrier properties is achieved. Adding 10% wt. GnP to the matrix resulted in a 65% reduction in oxygen permeation and increasing the concentration to 15% wt. GnP resulted in 73% reduction

[9]. Modelling suggests there is still room for improvement with a better dispersion and alignment of the GnP. Using a MCE die during extrusion should result in films with perfect alignment. To improve the dispersion of the platelets, a masterbatch approach was taken. When starting with a masterbatch precursor, the composites see more mixing time and would be easier to re-process. SEM micrographs of the film cross-sections for 15% wt. GnP-M-25 in HDPE are seen in Figure 3.5.

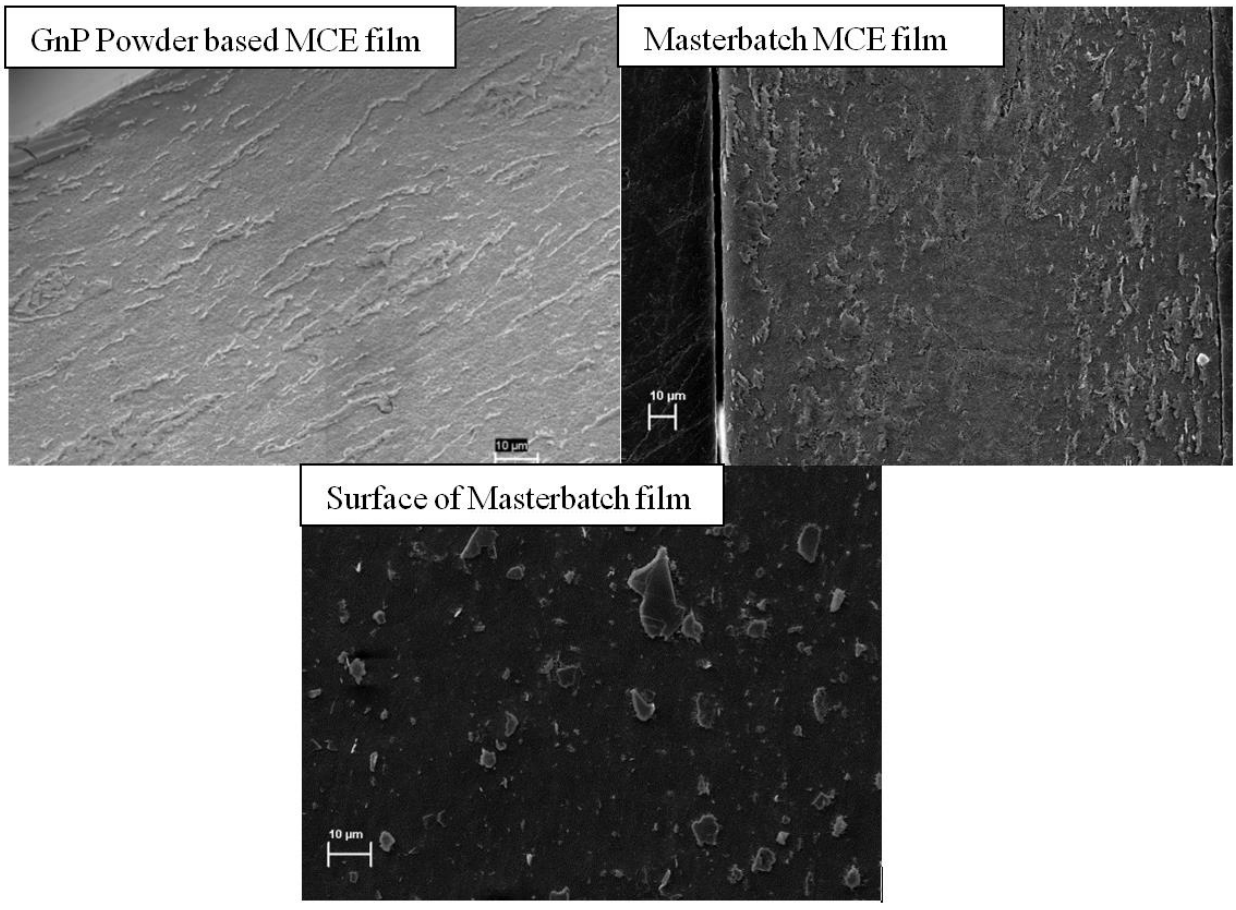

Figure 3.5. SEM observations of 15% wt. GnP-M-25 microlayer co-extrusion films.

As seen in the cross-sections of the MCE films, there is a nearly perfect alignment of the platelets along the flow plane. The images suggest that the S value in Equation 2 is approaching one, which should be optimal for increasing the tortuosity of the path permeating gas molecules follow. There is however a noticeable difference in the appearance of the films that were made directly from GnP-M-25 in powder form and the films that were produced from the concentrated 30% wt. GnP-M-25 masterbatch in HDPE. The cross-section and surface of the films extruded from the masterbatch based composites show GnP particle sizes that are much smaller. The extra processing that occurred during production of the masterbatch must have helped to break the platelets down to smaller sizes, which would negatively affect the barrier property results as there will be more openings between the platelets. Based on the scale bars, many of the platelets have been broken down to diameters below 5 microns. This effect is not as pronounced in the films that were extruded directly from the GnP-M-25 powder. The oxygen permeation results show the effects of the size reduction and can be seen in Figure 3.6.

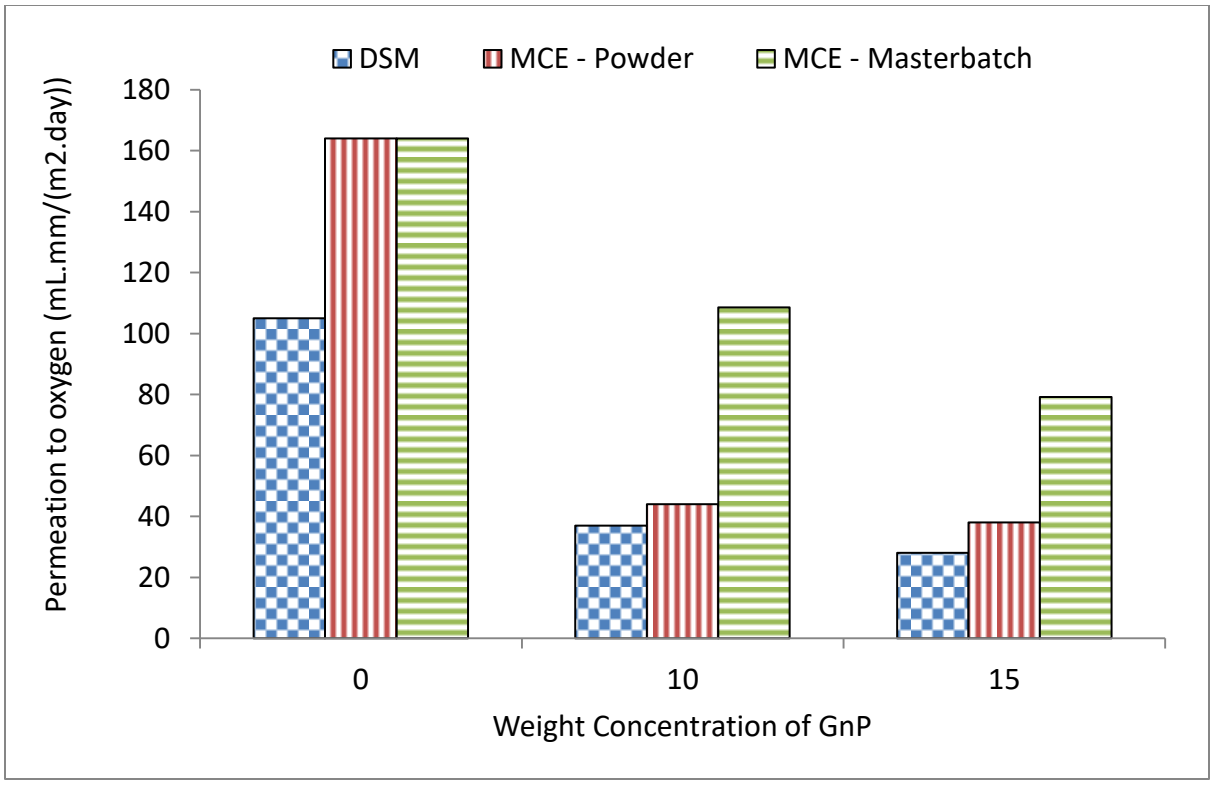

Figure 3.6. Oxygen permeation results of the MCE GnP-HDPE Composites.

In Figure 3.6, the blue bars represent GnP-HDPE composites that were processed through the DSM in chapter 2, the red bar represents the MCE composites made with GnP powder, and the green bar represents MCE composites made with the 30% wt. GnP masterbatch. Due to the processing differences, the neat HDPE that was extruded through the MCE die had a higher permeability than the films that were compressed from a flexural sample from the DSM processing. However, for the 10% and 15% GnP concentrations, there was a higher relative reduction in oxygen permeation, 73% and 76% respectively. The same limitations appear to be present, as the overall permeation values are similar. The dispersion of the platelets still limits the overall effect on the barrier properties. It is clear that the masterbatch approach did not

improve upon the dispersion, as the oxygen permeation results are nearly double that of GnP powder based composites. This is most likely attributed to the large amount of size reduction that occurred, reducing many of the platelets to below a 5 micron size.

3.3.2 Solution Dispersion Composite Results

An alternative approach to improving the dispersion of the platelets within the HDPE matrix is to use a solution dispersion approach. A major factor in the agglomeration issues when using melt mixing to compound the HDPE and GnP is that the very viscous environment makes it difficult to separate the platelets from each other. Using a solvent to dissolve the base matrix and then mixing in the GnP should help overcome the viscosity limitations on GnP dispersion. After dispersing the HDPE and GnP into xylene and subsequently drying the material, flexural and Izod specimens were made with the DSM micro-extruder. The results of the flexural properties can be seen in Figure 3.7.

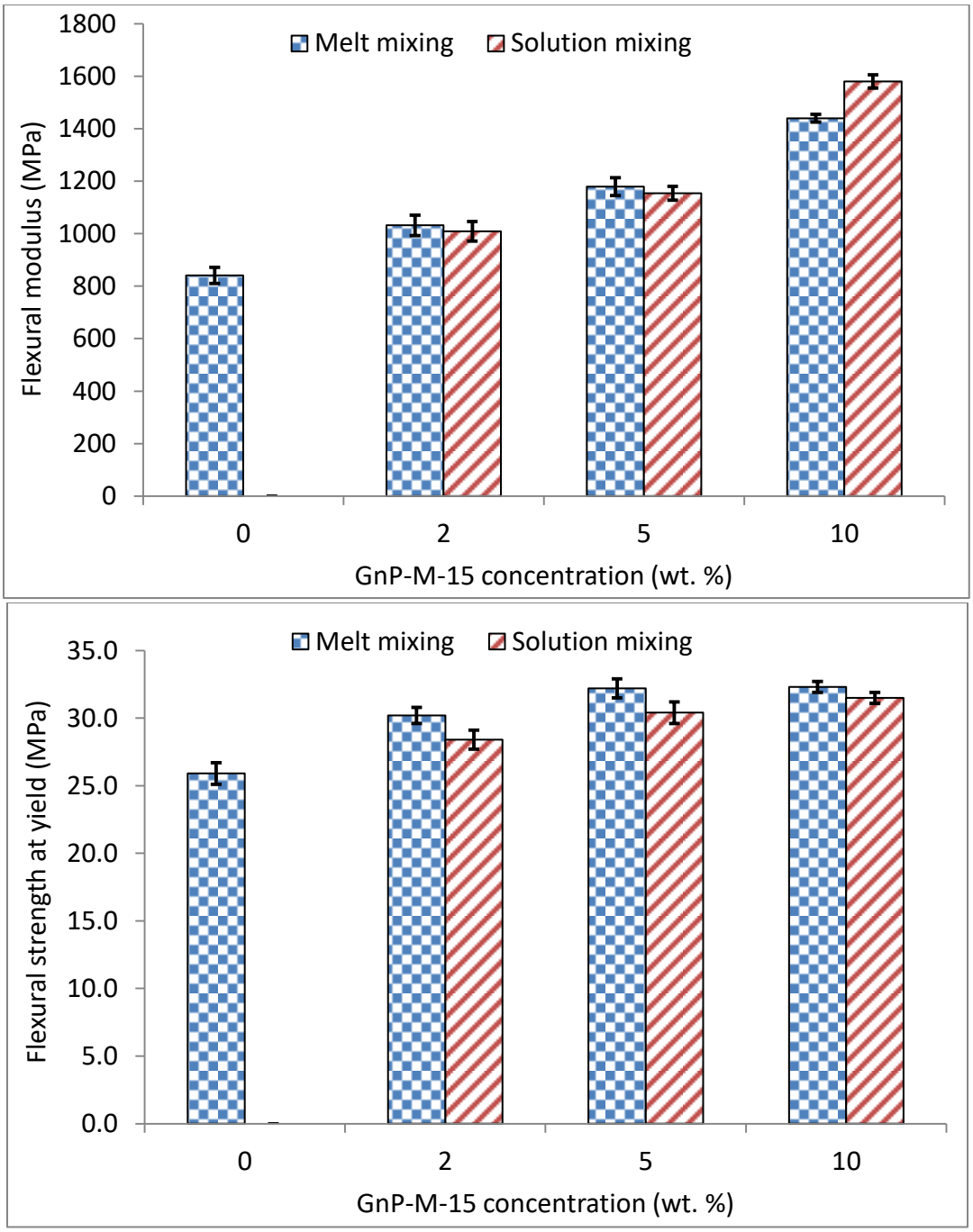

Figure 3.7. Flexural properties of solution dispersed vs. melt mixed HDPE-GnP composites.

There is little change in the flexural properties with a pre-processing of solution mixing the GnP and HDPE, shown by the majority of the error bars overlapping for both flexural strength and modulus. The only point at which there is a statistical difference in the properties is for the flexural modulus at 10% wt. GnP-M-15. The flexural results suggest that there is little improvement in the dispersion of the platelets when using solution dispersion as a pre-processing technique. The Izod impact resistance properties are seen in Figure 3.8.

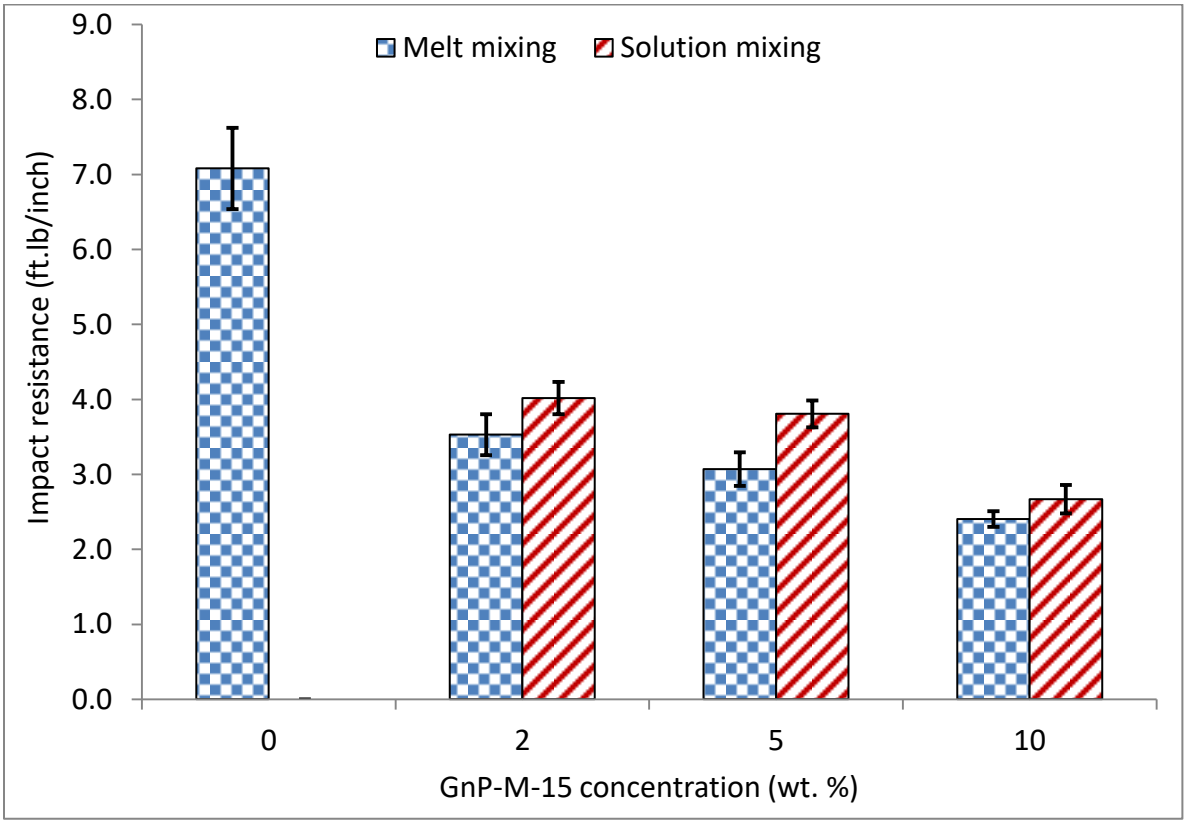

Figure 3.8. Izod impact resistance of solution dispersed vs. melt mixed HDPE-GnP composites.

There is a slight recovery of the lost impact resistance when using solution mixing to first mix the HDPE and GnP. This could be attributed to smaller agglomerates within the matrix, leading to smaller stress concentration sites. Another factor could be additional size reduction due to the pre-processing of the GnP with sonication. SEM analysis of the melt mixed composites versus the solution mixed composites can be seen in Figure 3.9.

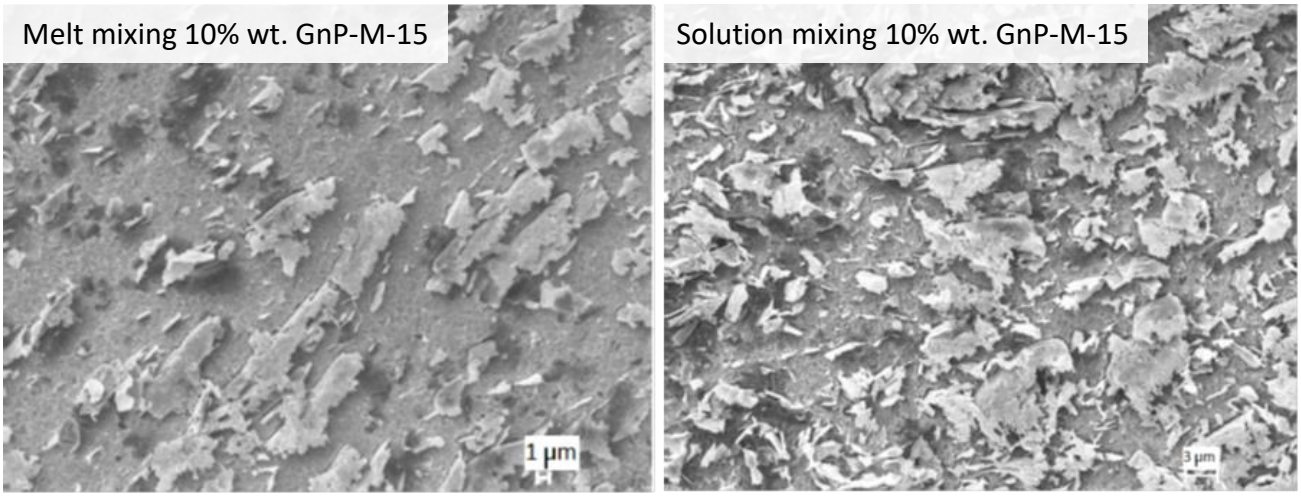

Figure 3.9. SEM observations of solution mixed vs melt mixed composites.

The SEM images help to explain some of the mechanical property results. Due to the additional processing and sonication during the solution dispersion, the GnP platelets are broken up into smaller averages sizes. This slightly improves the dispersion and results in a slight recovery of impact resistance due to smaller stress concentration sites. The smaller platelet size is not ideal for barrier properties, despite the resulting improved dispersion. The barrier properties of the composite can be seen in Figure 3.10.

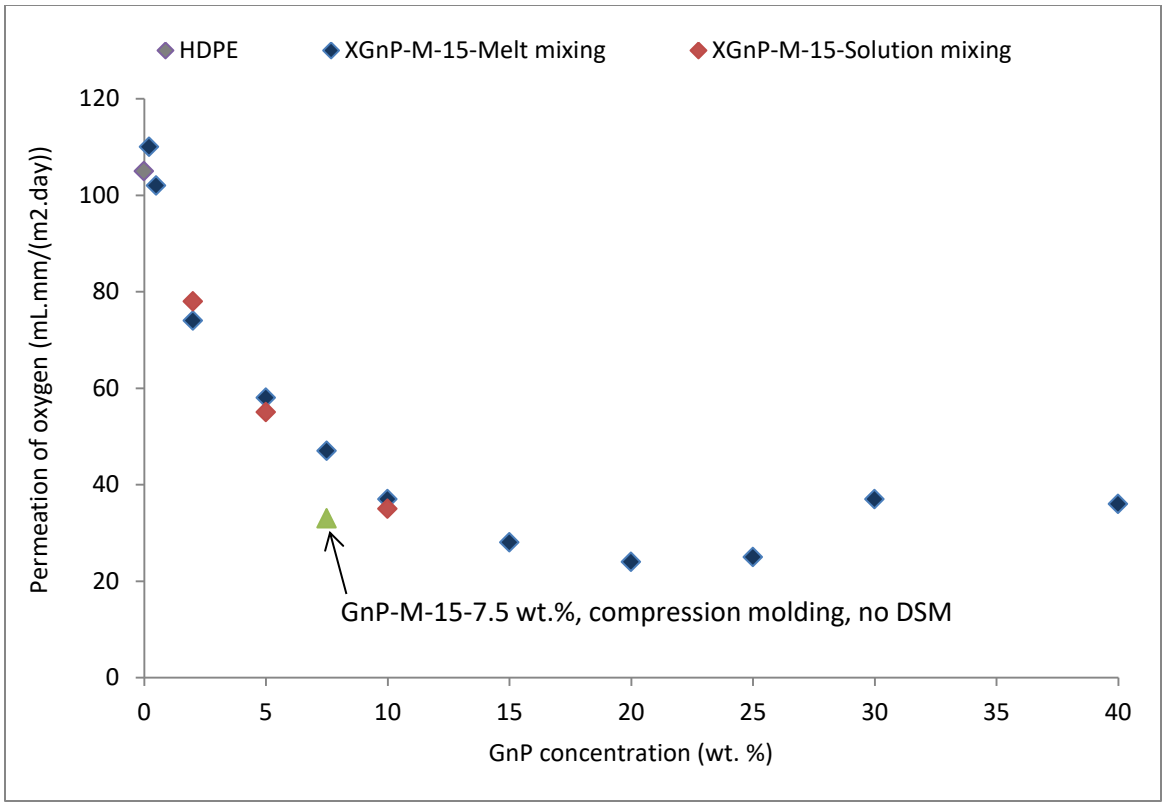

Figure 3.10. Oxygen barrier properties of solution mixed vs melt mixed composites.

In general the permeation results for the composites pre-processed with solution mixing follow the same trends as the composites that were just melt mixed. As seen in the SEM observations, there may be a small improvement in dispersion of the platelets, leading to slight improvements at the 5% and 10% weight GnP concentrations. However, the size reduction of the platelets counteracts this improvement, limiting the enhancement of the resistance to oxygen permeation. For comparison, a film was directly compression molded from the solution dispersed material at a 7.5% weight concentration. This film exhibited an additional 40% reduction in oxygen permeation compared to a melt mixed film of the same concentration. This suggests that the solution mixing process does result in a better GnP dispersion, but when the material is

reprocessed through a melt extrusion process, the advantage is lost and there is re-aggregation and further size reduction of the platelets, as discussed with Figure 3.9. The GnP in the melt mixed composites are overall much larger than those in the solution mixed composite that was re-processed through the DSM. The platelets were broken up even more with the double processing, and their sizes are much smaller, similar to what occurred with the masterbatch in the micro-layer co-extrusion process.

3.3.3 Cryomilled HDPE Composite Results

Mechanically altering the HDPE particle size to make it similar to the size of the GnP also offered a way to improve the dispersion of the matrix. By making the particle sizes closer to the same size prior to melt mixing, the platelets should be easier to disperse. The flexural properties of a 5% wt. composite made with the original pellet form and cryomilled HDPE powder are compared in Figure 3.11.

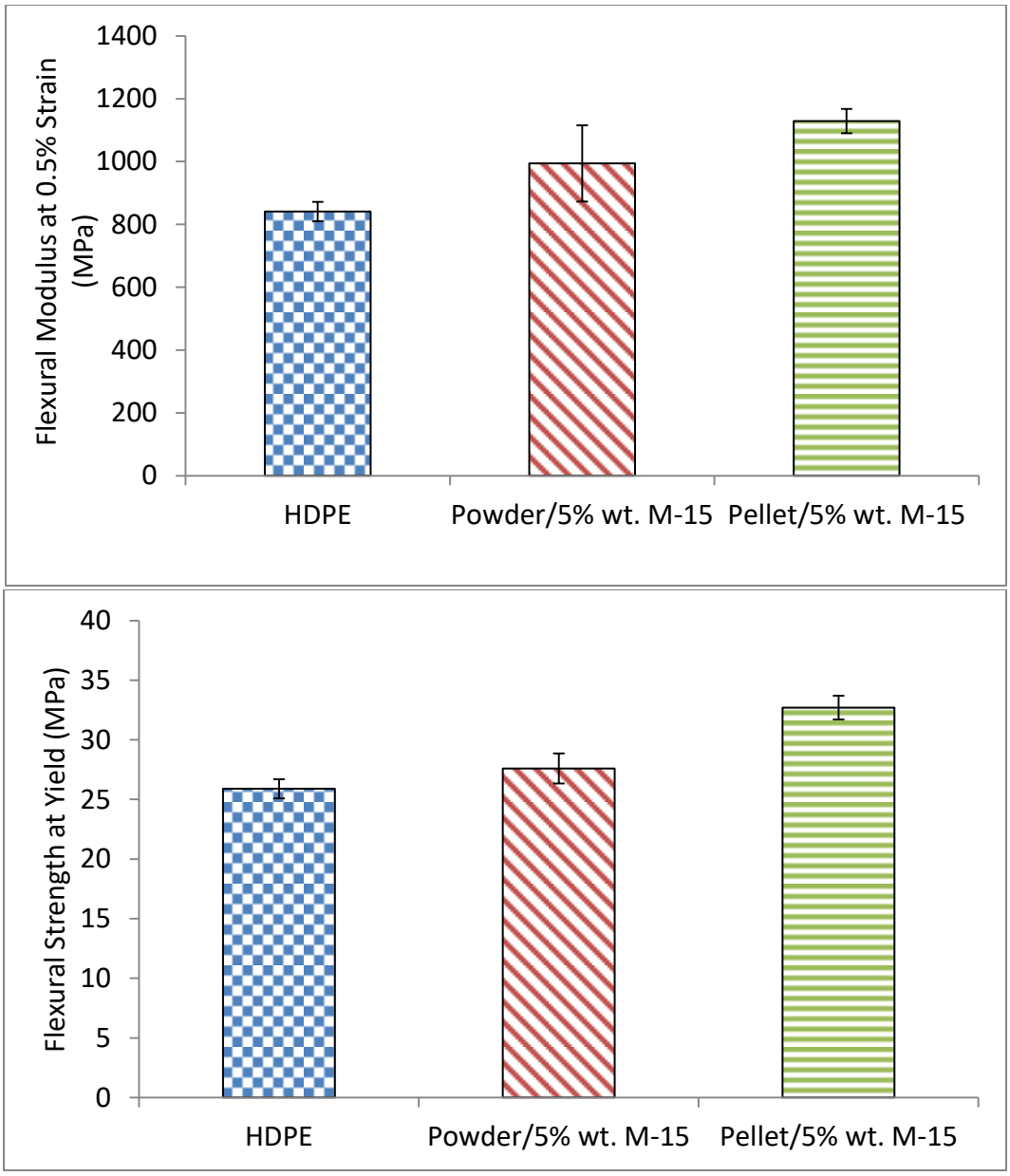

Figure 3.11. Flexural properties of cryomilled vs. pellet form HDPE-GnP composites.

The composites made from the cryomilled HDPE powder have a lower flexural modulus and strength than the equivalent composite melt extruded using the HDPE in pellet form. There is a 12% decrease in modulus and a 15% decrease in flexural strength for a 5% weight GnP composite. The reason for this decrease is attributed to breaking down the polymer during the cryomilling process. However, the composites made with the powder form still have improved flexural properties compared to neat HDPE. The Izod impact resistance measurements are shown in Figure 3.12 for the same compositions. There is negligible difference in the impact results. There is still a sharp drop of over 50% from the neat value when HDPE powder is used instead of HDPE pellets.

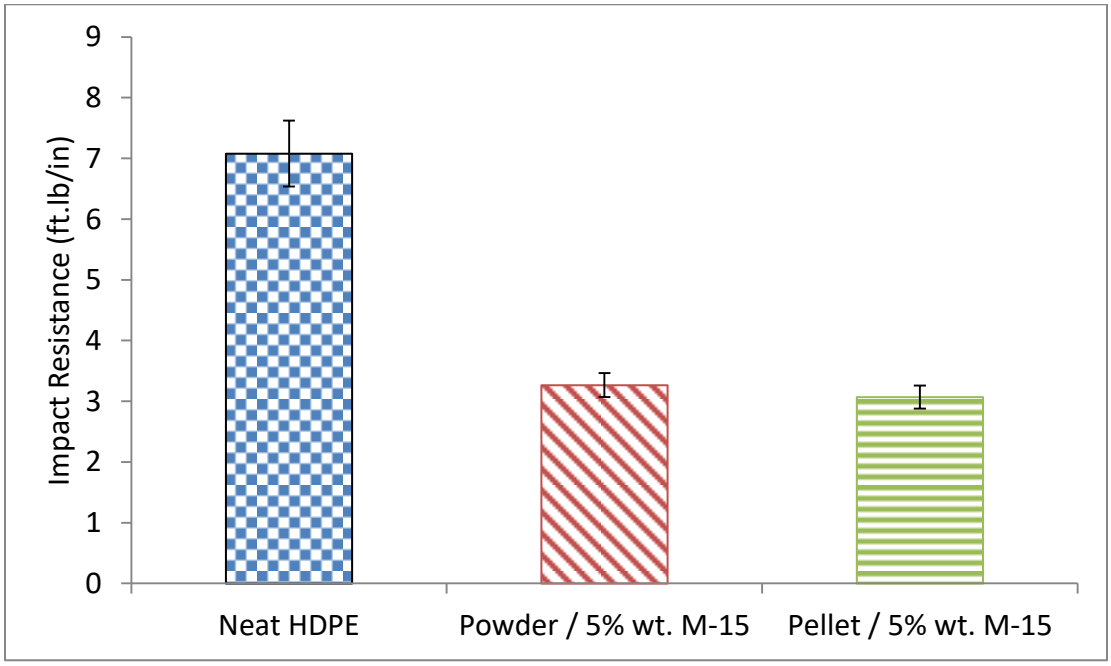

Figure 3.12. Izod impact resistance of cryomilled vs. pellet form HDPE-GnP composites.

The oxygen permeability results are shown in Figure 3.13. Two types of films were prepared for the powder based composite. The first was a flex specimen from the melt extrusion process that was compressed in a heated Carver press. Alternatively, the HDPE powder and GnP were dispersed into xylene with sonication, dried, and then compressed directly into a film with the heated Carver press. Compared to melt mixing the pellet form HDPE and GnP, melt mixing of the HDPE powder and GnP result in an additional 30% reduction in oxygen permeation for a 5% weight GnP composite. Compared to the neat HDPE value, there is a 65% reduction. There was little additional improvement from dispersing the HDPE powder and GnP in a solvent system and then pressing into a film. This is attributed to lack of uniformity of the GnP coverage of the HDPE particles, as seen in Figure 3.14. Agglomerations are still present and some particles have many more platelets on the surface than others. Overall, the powder based HDPE composites exhibited flexural properties that were equivalent to or exceeded the neat HDPE matrix, and resulted in an additional 30% reduction in oxygen permeation compared to the pellet form HDPE based composites.

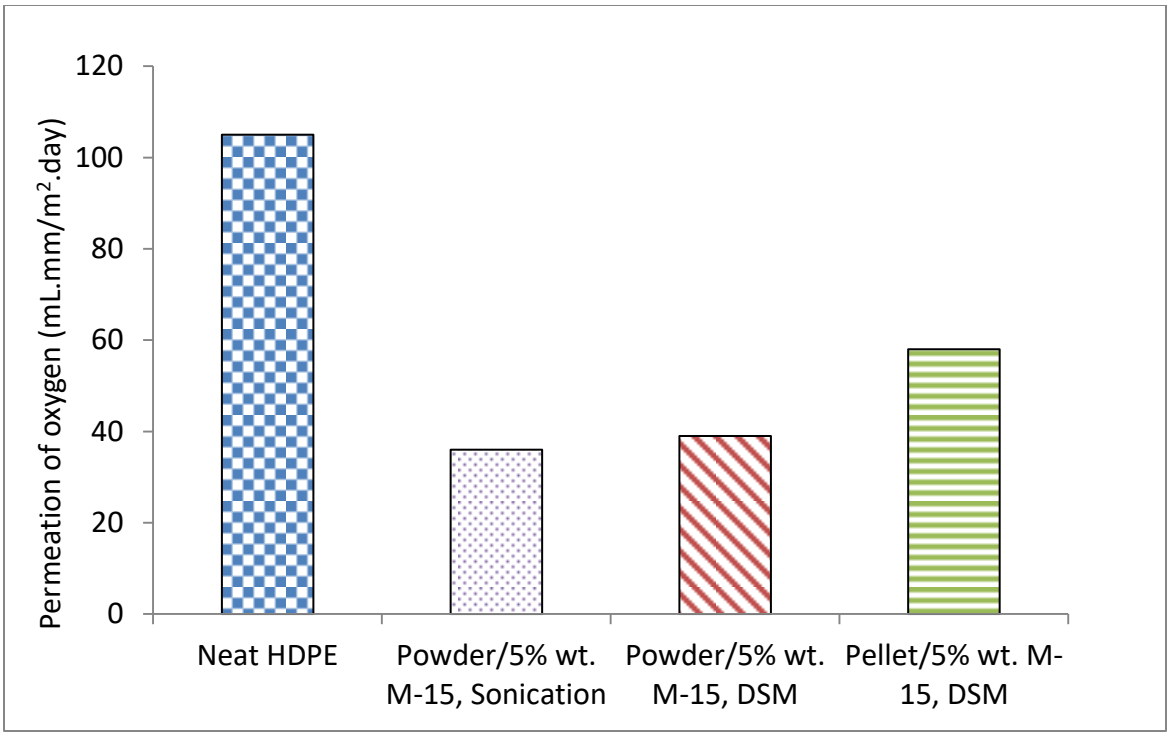

Figure 3.13. Oxygen permeation of cryomilled vs. pellet form HDPE-GnP composites.

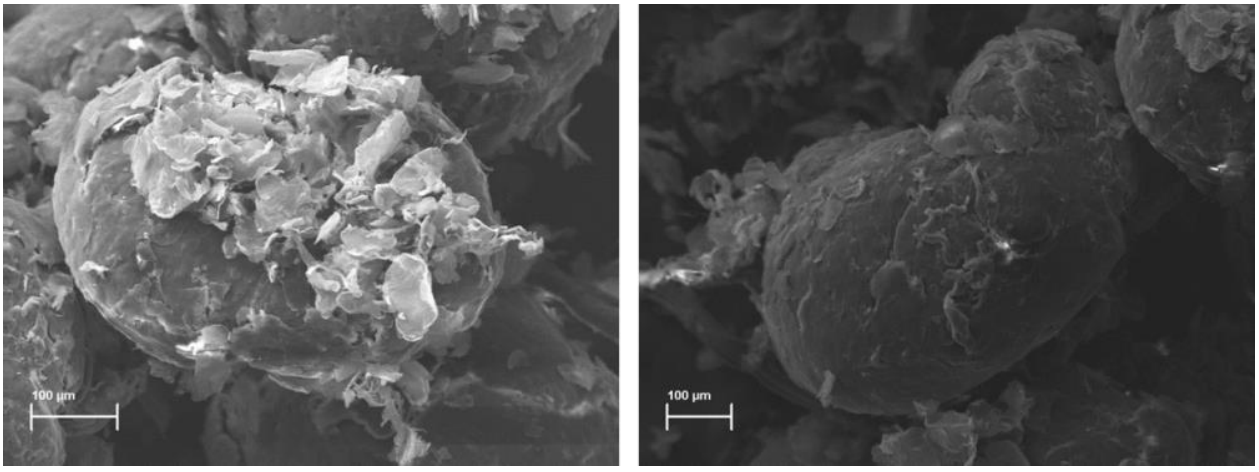

Figure 3.14. SEM of GnP coated HDPE particles.

3.3.4 Wax Coated GnP Composites Results

Another approach to improve the dispersion of the GnP in HDPE is to make the surfaces more compatible. This was done by coating the GnP with a low molecular weight wax prior to melt extrusion with HDPE. The platelets were coated at a GnP to wax ratio of 80:20. At this ratio, there is approximately a 2.2 nanometer thick coating on the platelets. The flexural properties for the two different wax coated GnP composites compared to the unmodified GnP composites made through melt extrusion can be seen in Figure 3.15. When using paraffin wax coated GnP, there is a decrease in flexural modulus and strength at yield of 37% and 26% respectively when compared to an unmodified GnP composite of the same concentration. The Sasol wax coated GnP composites yielded better results compared to the paraffin wax, but there was still a decrease of 19% in flexural modulus and 15% in flexural strength relative to the unmodified composite. The main explanation for these decreases in flexural properties is because the load transfer from the HDPE matrix to the GnP platelets is not as effective when there is an additional low modulus interface between the two. The coating is ineffective in transferring the load to the platelets.

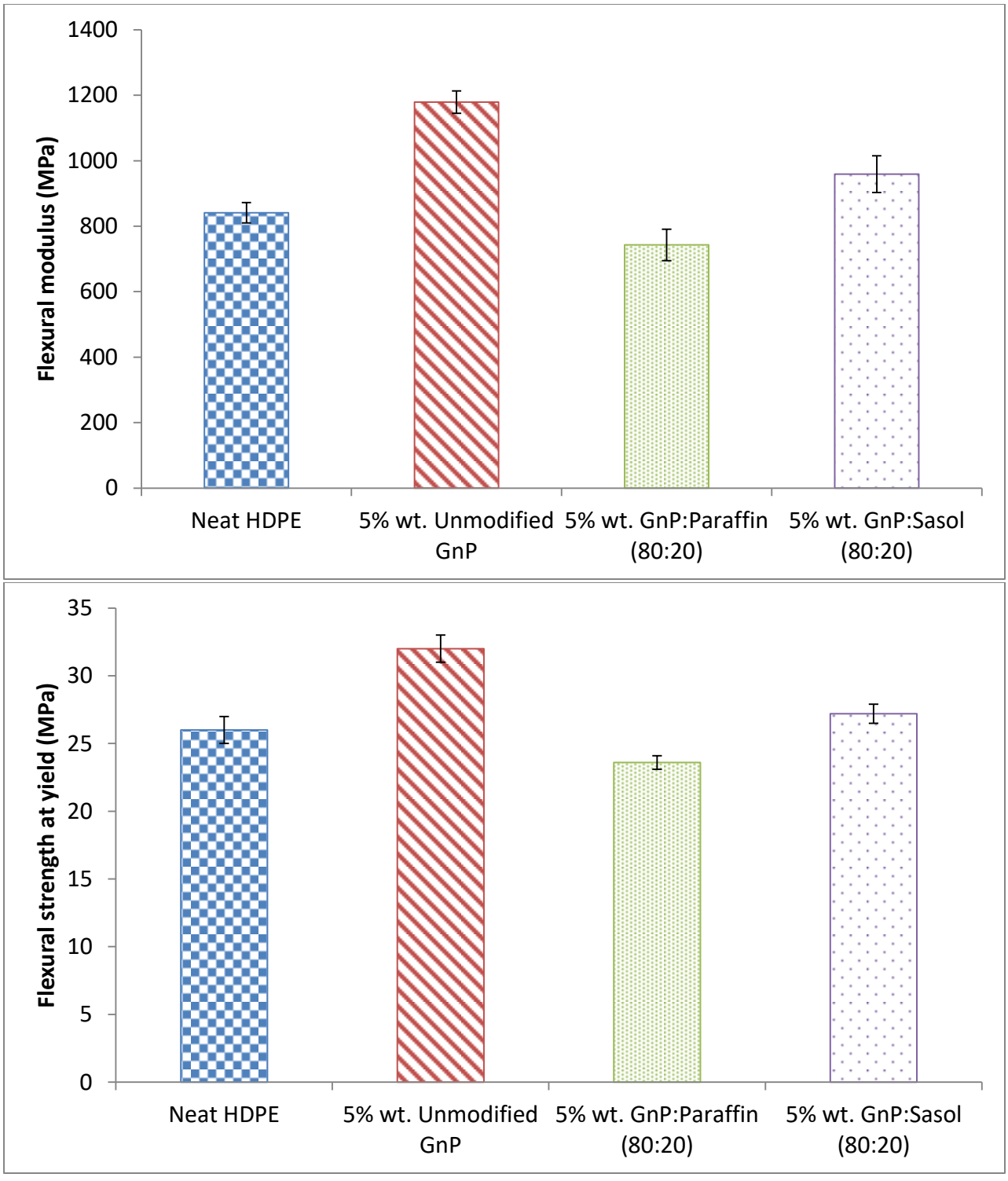

Figure 3.15. Flexural properties of wax coated GnP in HDPE composites.

The notched Izod impact resistance results for the wax coated GnP composites are shown in Figure 3.16. There is still a large drop from the neat polymer for a 5% wt. GnP composite, but the wax coated platelets resulted in a 25% recovery of the lost impact resistance compared to the unmodified GnP composites. This can be explained through SEM observation of the surface of the Izod break, shown in Figure 3.17. There is additional plastic deformation with the presence of the wax coatings, resulting in some recovery of the impact resistance. Part d of the figure shows the break morphology around an unmodified GnP platelet. In parts a through c, it is clear that there are elongated polymeric filaments, showing the increase in plastic deformation that is present. While the stiffness of the polymer is lessened, the impact resistance improves.

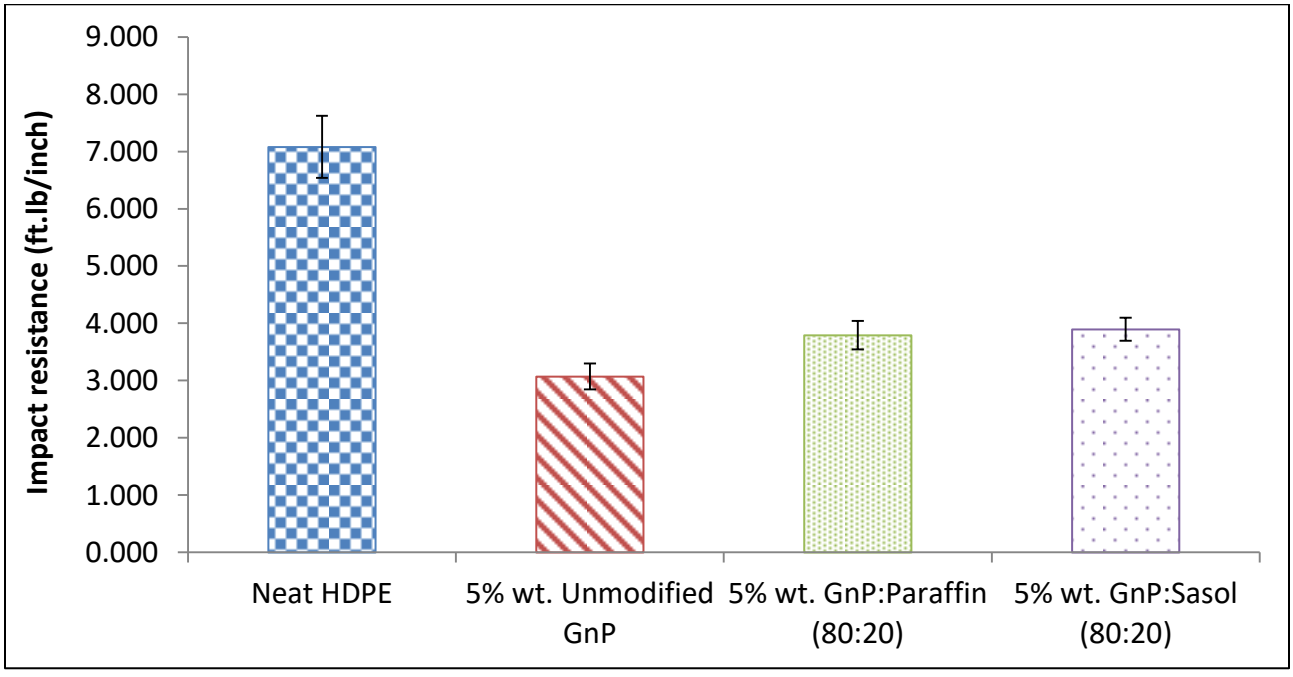

Figure 3.16. Notched Izod impact resistance of wax coated GnP in HDPE.

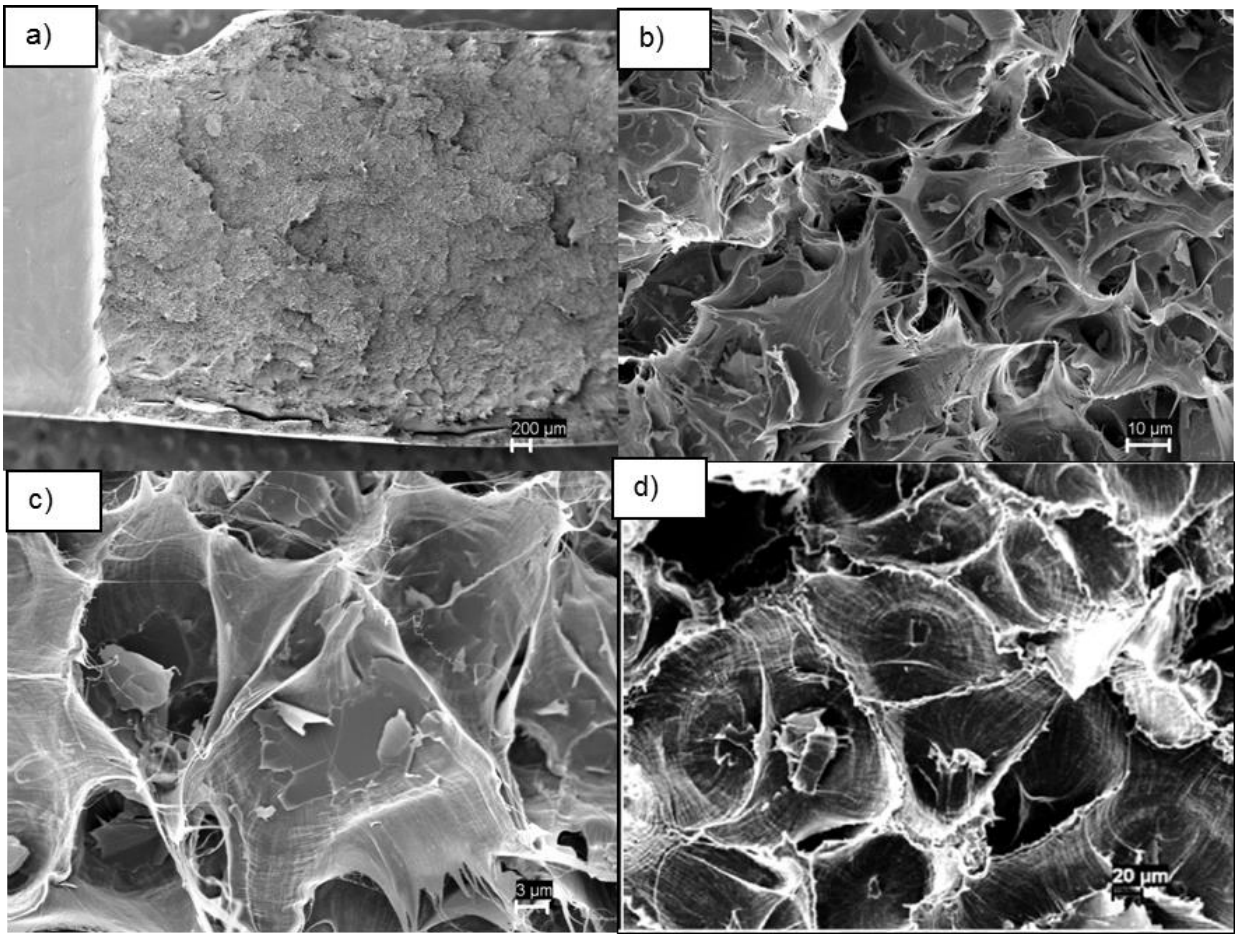

Figure 3.17. SEM Images of Izod impact fracture surface, a) overview of 5% wt. GnP coated with Sasol wax, b) and c) higher magnification of break, and d) 5% wt. unmodified GnP composite.

Figure 3.18 shows the oxygen permeation results for the wax coated platelets. There is no change in the oxygen permeation when the Sasol wax is used to coat the platelets. When the paraffin wax was used to coat the platelets, the resulting oxygen permeability was actually worse than the unmodified GnP composites A major reason for this could be that while the wax coating may help improve dispersion of the platelets within the polymer matrix, it also provides a path around

the platelets that permeating gases travel through more quickly. The bulk crystallinity of the material was the same as without the wax coating; however the crystallinity near the surface of the GnP may be lessened with the presence of the wax. While the wax coating of the platelets recovered some of the lost impact resistance, the effect of the platelets on flexural properties was lessened and the coating did not yield an improvement of the barrier properties.

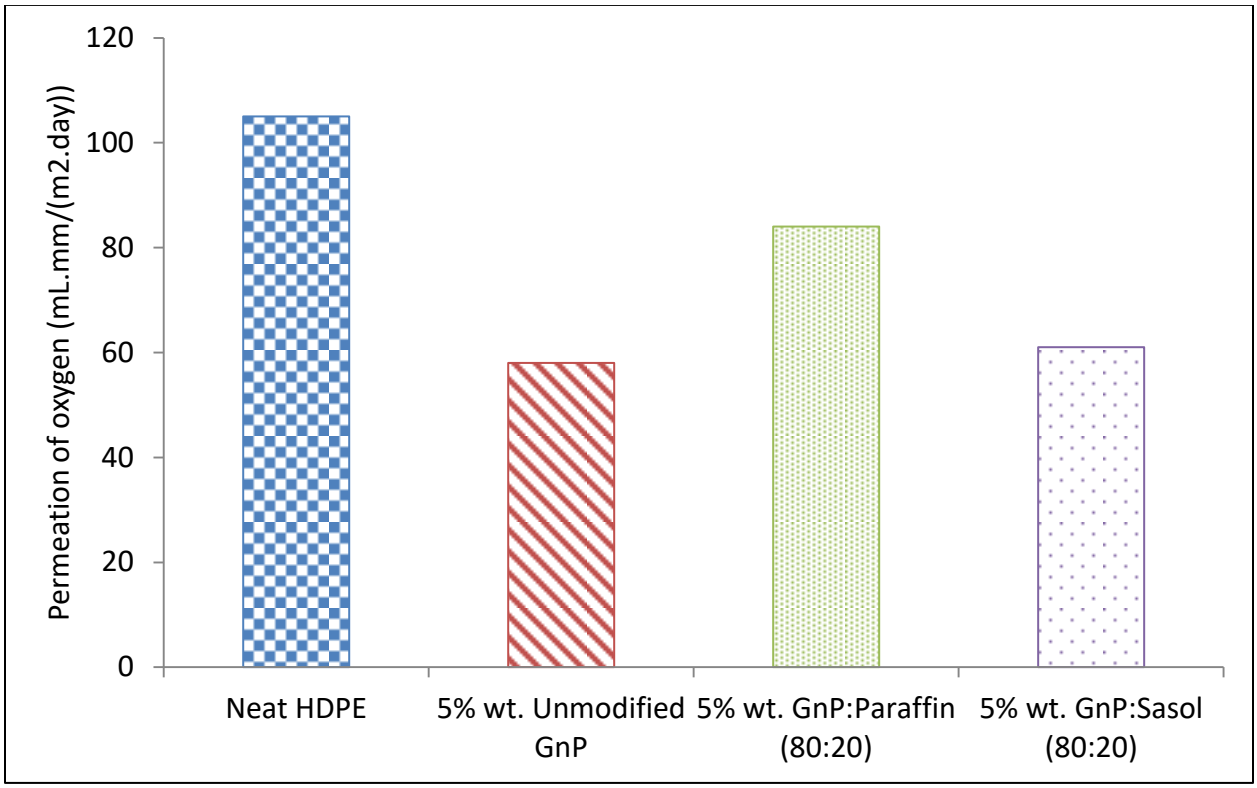

Figure 3.18. Oxygen permeation results of wax coated GnP in HDPE.

3.3.5 Elastomer Coated GnP Composites Results

Like the wax coating, the elastomeric coating of GnP was used to help improve dispersion by making the surface more compatible with HDPE, and also to overcome the difference of thermal expansion coefficients to ensure no voids form around the platelets during cooling. Voids near the GnP surface would allow for quicker permeation through the tortuous path created by the platelets. The GnP to elastomer ratio was 50:50, resulting in an estimated coating thickness of 9.5 nm. The flexural properties of the elastomeric coated GnP composites are shown in Figure 3.19. As with the wax coating, the additional low modulus interface between the GnP and the HDPE results in a reduction in flexural properties compared to the unmodified GnP composites. However, for both the 2 and 5 weight percent composites were equal to or better than the neat matrix for both modulus and strength.

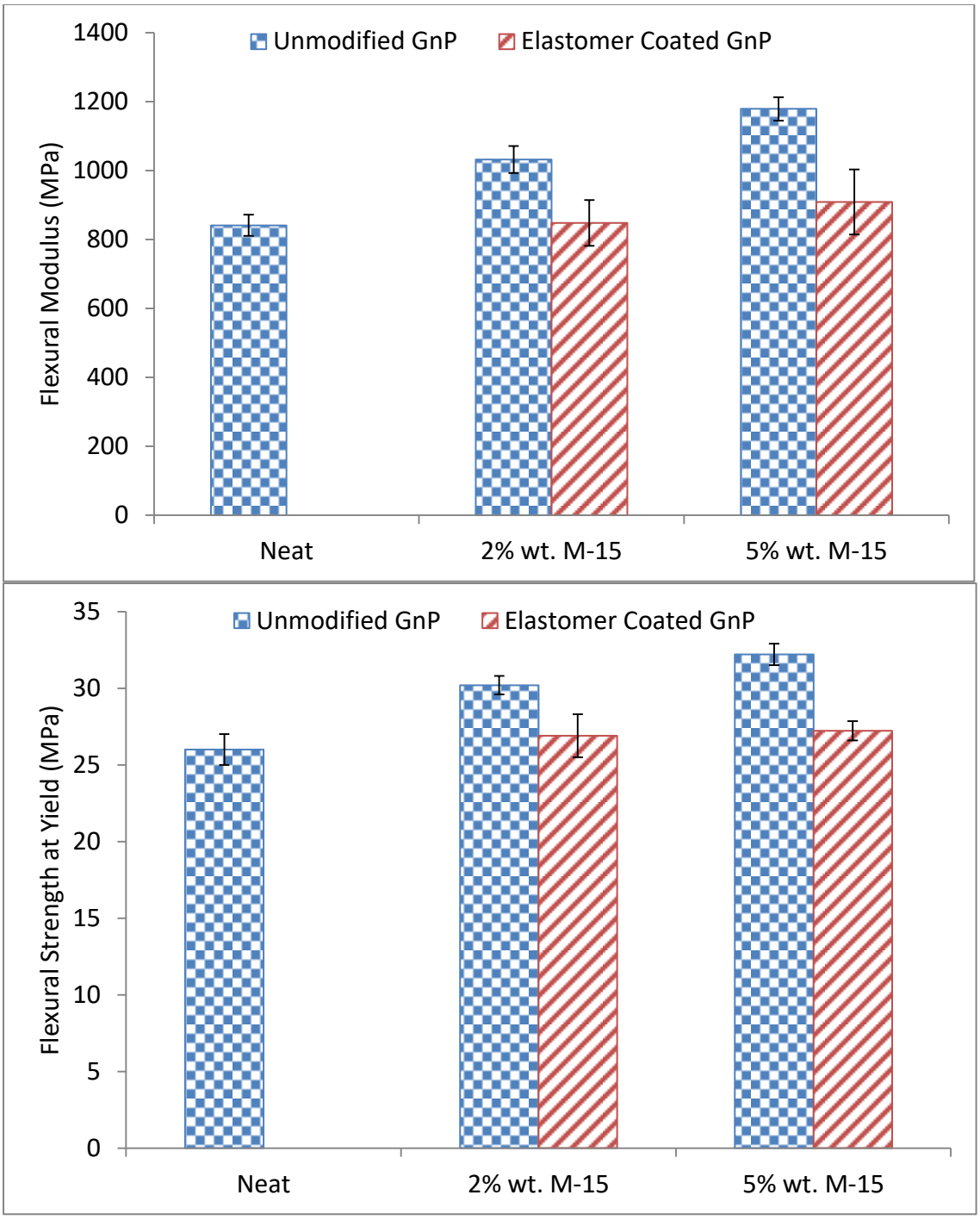

Figure 3.19. Flexural properties of elastomer coated GnP in HDPE composites.

The Izod impact resistance results are shown in Figure 3.20. For the 2 and 5% weight GnP composites, the impact resistance improved by 13% and 34% respectively when compared to the unmodified GnP composite. The reason do this improvement is similar to the reason that the wax coating improved the impact resistance. The elastomer undergoes a large amount of plastic deformation prior to breaking, as shown in Figure 3.21. This is evidenced by the long tendrils of elastomer that are present around the GnP platelets. As before, there is still a "cell" structure around the platelets, but the elastomer absorbs some of the stresses during the impact.

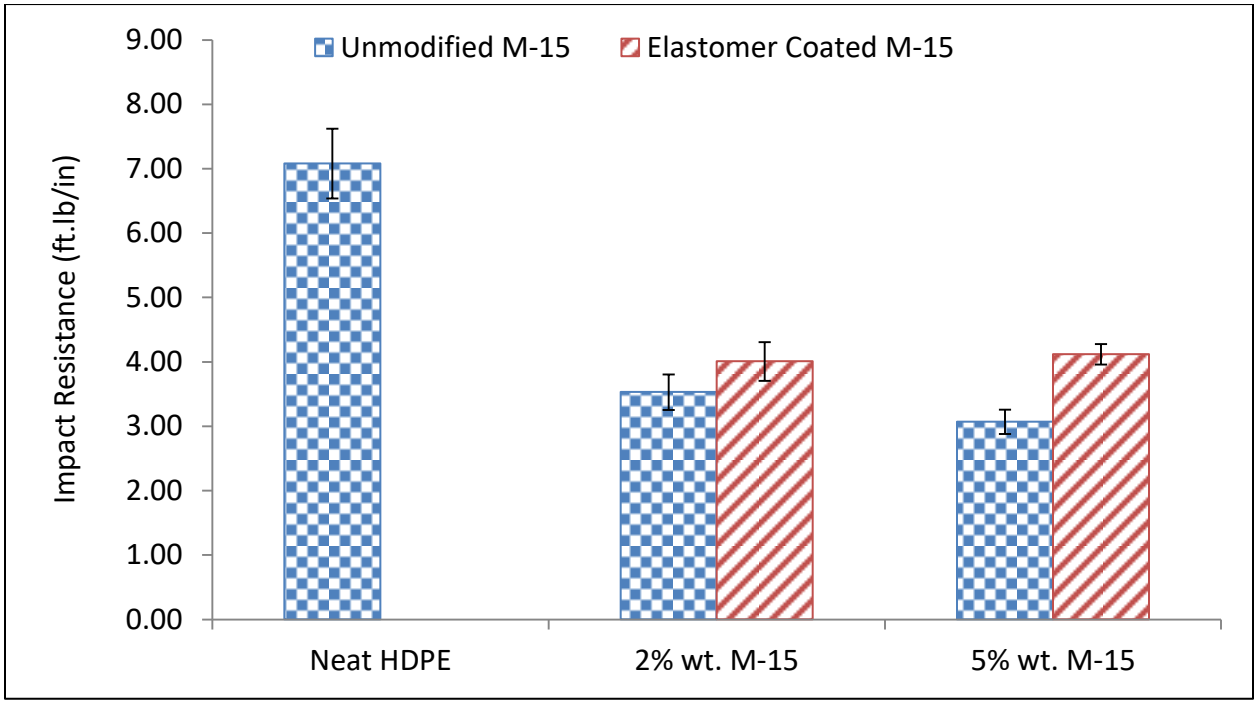

Figure 3.20. Notched Izod impact resistance of elastomer coated GnP in HDPE.

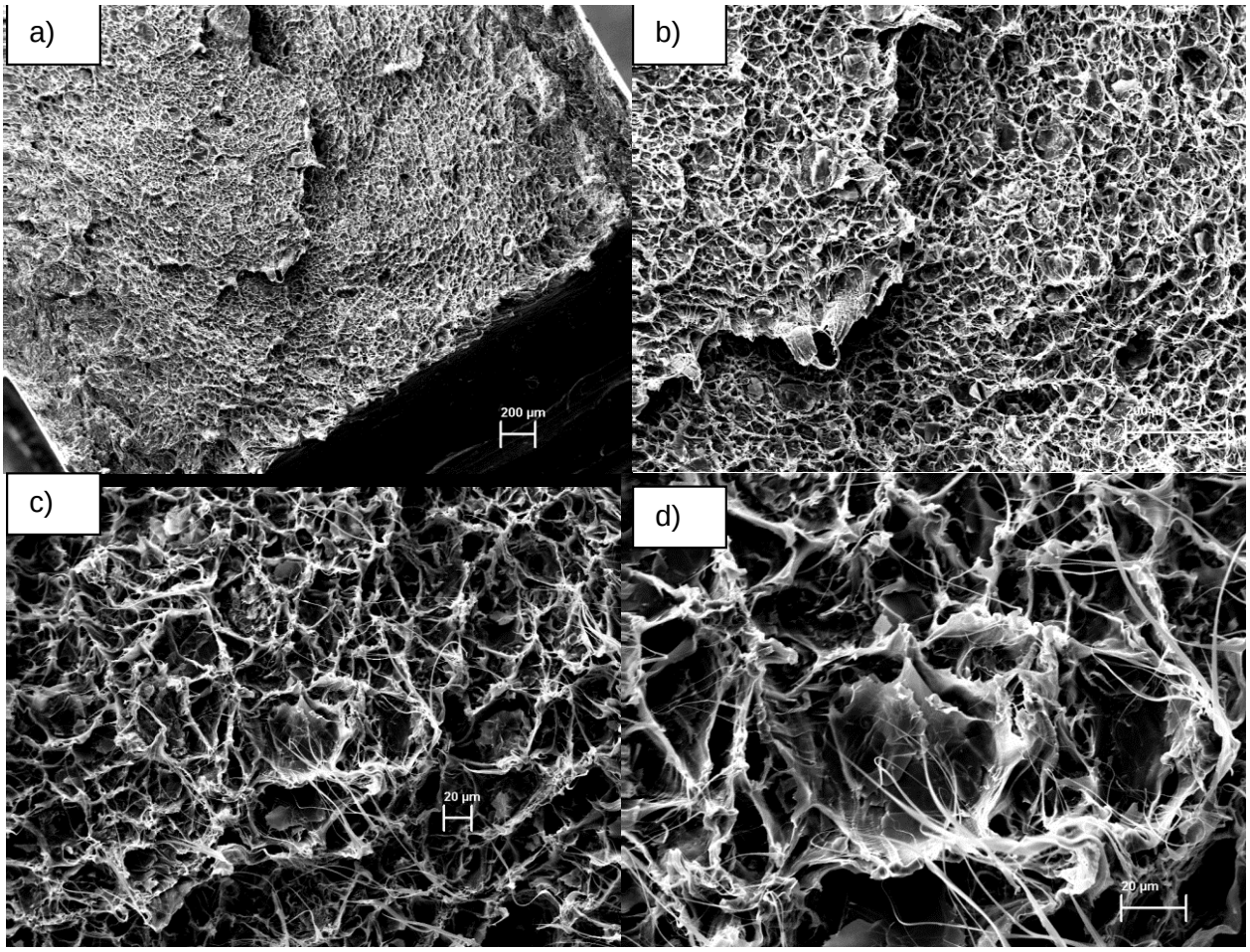

Figure 3.21. SEM images of the fracture surface after Izod impact test a) overview of 5% wt. elastomer coated GnP in HDPE, b) higher magnification of same composite, c) and d) ”cell” structure and plastic deformation of composite.

Figure 3.22 shows the barrier properties of the elastomer coated GnP composites compared to the unmodified ones. There is a marginal improvement in the barrier properties when using the elastomer coated GnP. For a 2% weight composite, there was a 23% improvement and for a 5% weight, there was a 9% improvement relative to the same loadings of unmodified GnP. The 5% wt. elastomer coated GnP has a 45% reduction in oxygen permeability compared to the neat HDPE. This suggests that the dispersion of the platelets may be slightly improved, though it did not yield a drastic change in the barrier properties.

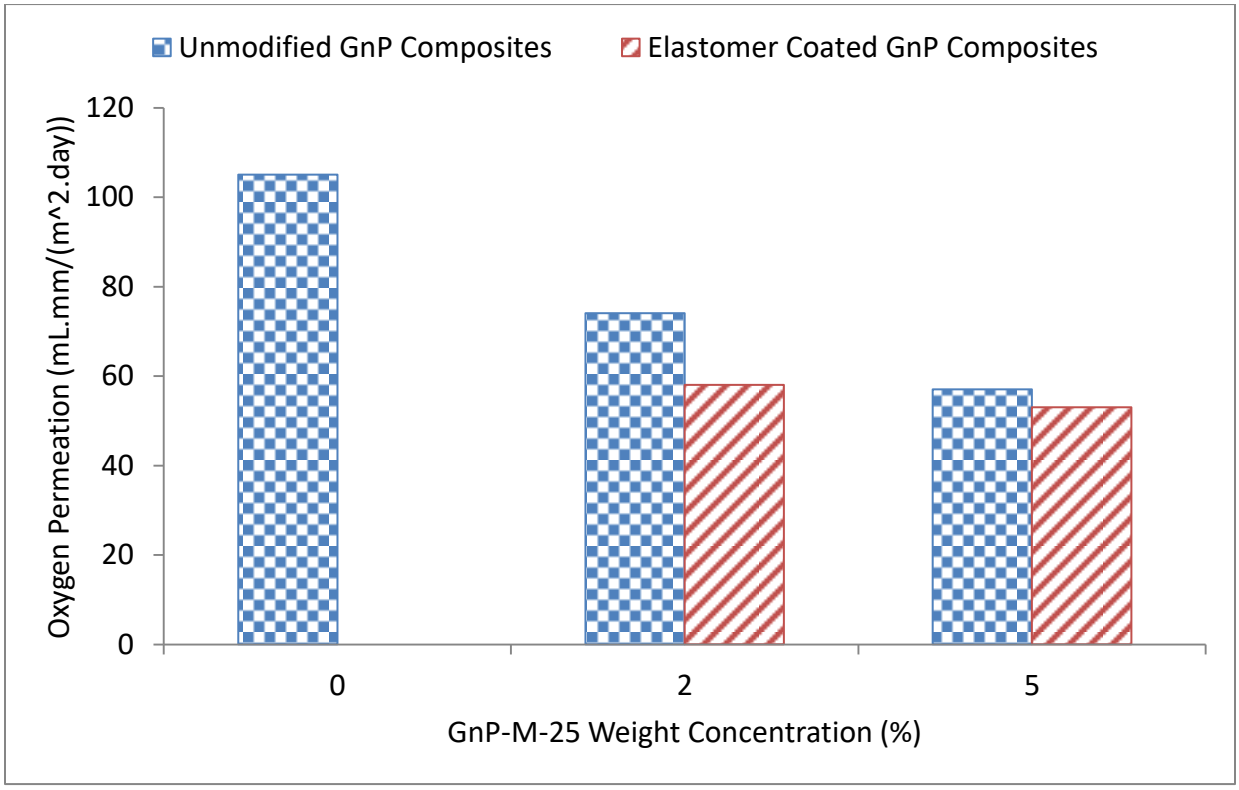

Figure 3.22. Oxygen permeation results of elastomer coated GnP in HDPE.

3.4 Conclusions

Multiple approaches to synthesizing graphene nanoplatelet (GNP)-high density polyethylene (HDPE) nanocomposites were taken to improve the alignment and dispersion of GnP. If perfect alignment and dispersion were achieved, there would be a large jump in barrier properties compared to melt mixing composites. With each attempt to improve barrier properties, the mechanical properties were also affected and examined. A summary of all the methods for a 5% weight composite can be seen in the spider plot in Figure 3.23. The percentages are relative to the neat HDPE polymer. With melt mixing, there is a clear decrease in oxygen permeation, an increase in flexural properties and a decrease in impact resistance. Microlayer co-extrusion (MCE) resulted in a higher relative improvement compared to simple melt mixing due to a higher degree of alignment of the GnP, but did not result in a better absolute value due to agglomeration issues still present. It was theorized that starting with e concentrated 30% wt. GnP in HDPE masterbatch would improve dispersion of the platelets in the MCE process; however the extra extrusion processing of the platelets caused the GnP to deform and be reduced in size yielding poorer oxygen permeation results. The solution mixing process did improve the dispersion and the oxygen permeation by 40% when compressed directly into a film, yielding the highest relative decrease, as seen in Figure 3.23. The advantages of the process were lost when the dried material was re-processed with melt extrusion. This was attributed to re-aggregation of the platelets and some additional size reduction. Cryomilling the HDPE into a size closer to that of the GnP did result in an improvement to barrier properties, but the mechanical properties were decreased due to modifying the HDPE. A low molecular weight wax coating on the surface of GnP prior to melt mixing resulted in some recovery of the lost impact resistance compared to the unmodified GnP composites due to increased plastic deformation, but had little benefit to the

oxygen permeation properties. The coating also caused the flexural reinforcement by the GnP to be reduced due to an extra, low modulus interface between the matrix and the GnP, but the results were still higher than the values for neat HDPE. An elastomeric coating of the GnP yielded very similar results to the wax coating, improving the impact resistance and reducing the flexural properties. However, the barrier properties with the elastomeric coating were also marginally improved. While all of these methods have their positive aspects, it is clear that melt mixing based methods of GnP are still limited by dispersion.

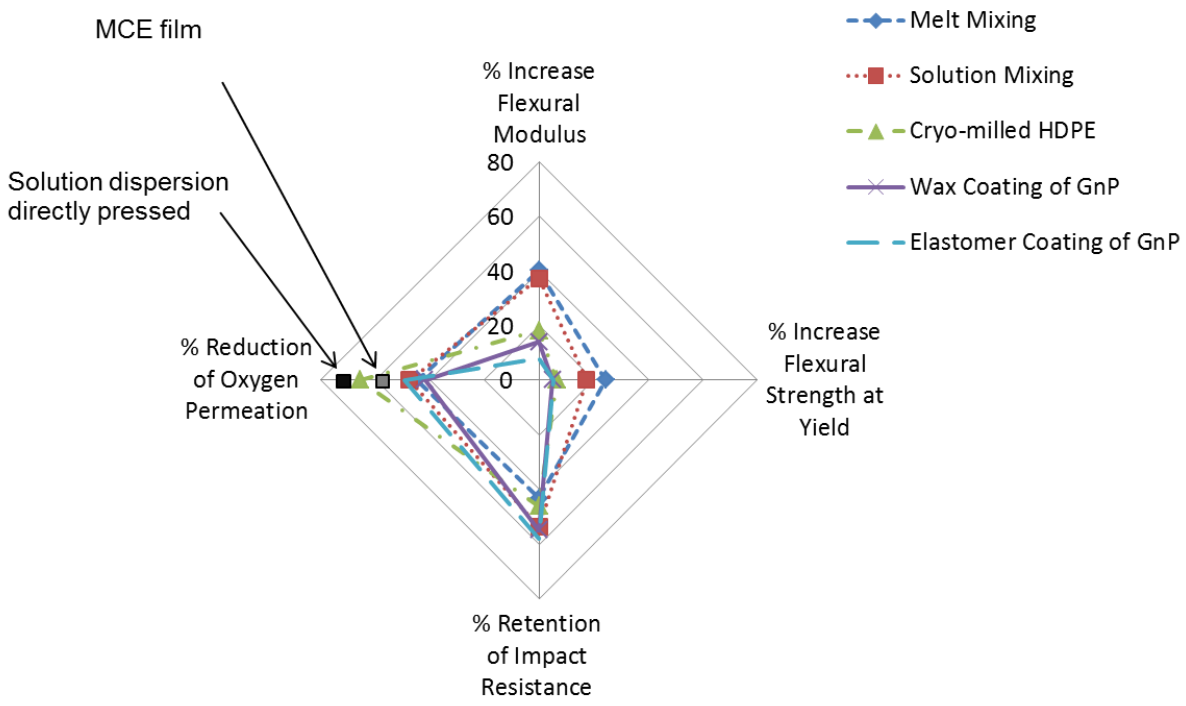

Figure 3.23. Spider plot for characterization of 5% GnP in HDPE composites using the different compounding techniques.

REFERENCES

REFERENCES

[1] D. R. Paul and L. M. Robeson, "Polymer nanotechnology: Nanocomposites," *Polymer (Guildf).*, vol. 49, no. 15, pp. 3187–3204, 2008.

[2] Z. Spitalsky, D. Tasis, K. Papagelis, and C. Galiotis, "Carbon nanotube-polymer composites: Chemistry, processing, mechanical and electrical properties," *Prog. Polym. Sci.*, vol. 35, no. 3, pp. 357–401, 2010.

[3] R. K. Bharadwaj, "Modeling the barrier properties of polymer-layered silicate nanocomposites," *Macromolecules*, vol. 34, no. 26, pp. 9189–9192, 2001.

[4] C. D. Mueller, S. Nazarenko, T. Ebeling, T. L. Schuman, A. Hiltner, and E. Baer, "Novel structures by microlayer coextrusion?talc-filled PP, PC/SAN, and HDPE/LLDPE," *Polym. Eng. Sci.*, vol. 37, no. 2, pp. 355–362, 1997.

[5] X. Jiang and L. T. Drzal, "Improving electrical conductivity and mechanical properties of high density polyethylene through incorporation of paraffin wax coated exfoliated graphene nanoplatelets and multi-wall carbon nano-tubes," *Compos. Part A Appl. Sci. Manuf.*, vol. 42, no. 11, pp. 1840–1849, 2011.

[6] B. M. Yoo, H. J. Shin, H. W. Yoon, and H. B. Park, "Graphene and graphene oxide and their uses in barrier polymers," *J. Appl. Polym. Sci.*, vol. 131, no. 1, pp. 1–23, 2014.

[7] Y. Li, J. Zhu, S. Wei, J. Ryu, Q. Wang, L. Sun, and Z. Guo, "Poly(propylene) Nanocomposites Containing Various Carbon Nanostructures," *Macromol. Chem. Phys.*, vol. 212, no. 22, pp. 2429–2438, 2011.

[8] X. Jiang and L. T. Drzal, "Multifunctional high-density polyethylene nanocomposites produced by incorporation of exfoliated graphene nanoplatelets 2: Crystallization, thermal and electrical properties," *Polym. Compos.*, vol. 33, no. 4, pp. 636–642, Apr. 2012.

[9] K. Honaker, F. Vautard, and L. T. Drzal, "Investigating the mechanical and barrier properties to oxygen and fuel of high density polyethylene–graphene nanoplatelet composites," *Mater. Sci. Eng. B*, pp. 1–8, 2016.

CHAPTER 4 - LAYER BY LAYER DEPOSITION OF GRAPHENE NANOPLATELETS

4.1 Introduction

Melt mixing of nanocomposites is a cost effective, scalable process for producing nanocomposites, but can clearly be limited by dispersion of the nanofiller. When incorporating graphene nanoplatelets (GnP) into high density polyethylene (HDPE), the barrier properties of the matrix can be improved by over 75% at a weight concentration of 20%, however increasing the concentration further did not yield further improvement [1]. It is difficult to achieve both a good dispersion and alignment when using melt mixing and extrusion.

One way to overcome the dispersion limitations of melt mixing is to instead use a coating method to deposit the nanofiller onto the surface of a polymer substrate, imparting multifunctional properties. Layer by layer deposition takes advantage of ionic charges to deposit alternating layers of a positively charged polymer and a negatively charged nanofiller. This process is shown in Figure 4.1 and has been well documented using nanoclays [2]–[6]. In those studies, the oxygen permeability of a Poly(ethylene terephthalate) (PET) substrate has been shown to decrease by over 90%, and in some cases was so low that commercially available oxygen sensing equipment could not measure the value.

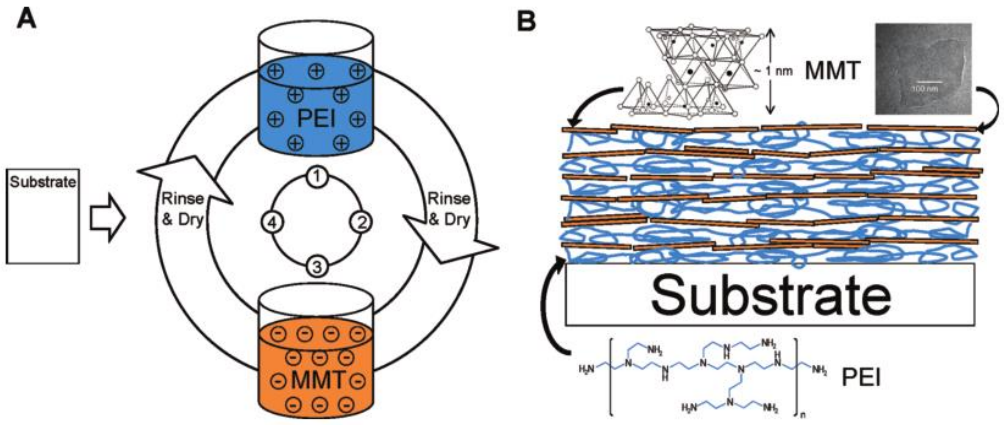

Figure 4.1. Layer by layer deposition diagram of a nanoclay and PEI. [3] Copied with permission.

Some layer by layer depositions of GnP onto a polymer substrate have been examined, but permeation was not measured [7], [8]. Coating the GnP with a material like sulfonated polystyrene (SPS) was shown to enhance the negative surface charge, which would pair well with a positively charged polymer. Due to the higher aspect ratio of GnP compared to nanoclays, it could be expected that similar performance in reducing oxygen permeability could be achieved with fewer layers of GnP. Additionally, the film may yield conductivity that would be able to dissipate a static charge.

An alternative way to form monolayers of GnP was presented by Biswas et al. [9]. In this study, graphene was dispersed in chloroform and then water was added to the dispersion. A light sonication was applied to the mixture, which causes the graphene to assemble into a layer at the chloroform/water interface. Air bubbles can then be used to carry the graphene to the water/air interface where it can be transferred onto a different substrate. Utilizing this method, layers of aligned GnP could be used to coat a polymer substrate and impart enhanced barrier properties.

4.2 Materials and Methods

4.2.1 Materials

High density polyethylene (HDPE) was supplied by INEOS Olefins and Polymers USA under the trade name K46-06-185 and was used as received. It has a density of 0.946 g.cm-3 (ASTM D4883) and a melt index (190 ºC/21.600 g) of 4.2 g/10 min (ASTM D1238). Branched polyethylenimine (PEI) was obtained from Sigma Aldrich with a molecular weight of 25,000 $g.mol^{-1}$. Sulfonated polystyrene (SPS) with a molecular weight of 70,000 $g.mol^{-1}$ was also obtained from Sigma Aldrich. Poly(diallyldimethylammonium chloride) (PDAC), obtained from Sigma Aldrich, had a molecular weight of 200,000 $g.mol^{-1}$. Poly(ethylene terephthalate) (PET) film with a thickness of 200 microns was obtained from Tekra. Reagent grade chloroform was purchased from Sigma Aldrich. Two grades of graphene nanoplatelets (GnP-M-25, GnP-M-5 and GnP-C-750) were obtained from XG Sciences (Lansing, Michigan, USA). Grades GnP-M-25 and GnP-M-5 have a surface area of 120-150 $m^2.g^{-1}$, an average thickness of 6 nm, and average diameters of 25 μm and 5 μm respectively. Grade GnP-C-750 has a surface area of 750 $m^2.g^{-1}$, an average thickness of 6 nm, and a diameter comprised between 300 nm and 1 μm. All GnP samples were heated for 1 hour at 450 °C in an air circulating oven to remove any trace volatile compounds remaining from the manufacturing process.

4.2.2 Layer by Layer Deposition Method

Layer by layer deposition was performed on a PET surface utilizing a process combined by those presented by Priolo et al. and Lu et al. [3], [7]. PET was first plasma treated in a 50% oxygen environment with 275W power for 30 minutes to induce a negative surface charge. For the positively charges polymer layers, two polymers were tried. A PEI solution was made by adding 1 gram of PEI into 400 mL of DI water and allowing the solution to mix overnight. A PDAC solution was made by adding 20 millimoles of PDAC into 500 mL of a 0.1M NaCl solution and allowing stirring overnight. For the GnP dipping solution, either GnP-M-5 or GnP-C-750 was dispersed in 500 mL of a 0.1M NaCl solution. 0.02 weight percent SPS was added and 0.05 weight percent of GnP was added. The solutions were bath sonicated for 30 minutes and then tip sonicated at 70W power for an additional 30 minutes with a 7 second on, 7 seconds off cycle. The resulting solution was centrifuged at 4000 rpm for 2 minutes, the supernatant was collected and stirred for 24 hours prior to use. When used with PDAC, the pH of the solution was left at 6, the result of mixing. When used with PEI, the pH of the solution was modified to 10 with 1.0M NaOH.

The dipping process was done by first dipping the plasma treated PET substrate into the polymer solution for 5 minutes, after which the substrate was rinsed and dried with an air brush. The sample was then dipped into the SPS coated GnP solution for 5 minutes, and then rinsed and dried again. Each subsequent dip was done for 1 minute, followed by rinsing and drying the polymer. This process was repeated until the desired number of layers had been deposited. After the layer by layer process was done, the films were heated to 60 °C for 1 hour prior to testing. A resulting film can be seen in Figure 4.2. The dark tint to the film clearly demonstrates that GnP has been deposited onto the surface.

Figure 4.2. PET substrate with a 40 bilayer system of PDAC/SPS-GnP deposited on the surface.

4.2.3 Self Assembled GnP Layers Deposited onto Polymer Surface

The procedure for this method was adapted from a processes developed by Biswas et al. [9]. To prepare the GnP layers, 10 mg of GnP-M-25 was added to 100 mL of chloroform and sonicated with 40W power for 10 minutes. The solution was then allowed to rest overnight, which allowed the large GnP agglomerates to settle out of solution. The upper 80% of this solution was transferred to a new beaker and 30 mL of water was added to the top. A very light sonication was applied to the mixture for 2 minutes. The disturbances to the chloroform force the GnP to assemble in a monolayer at the chloroform/water interface. Air bubbles were then introduced into the chloroform phase with a pipette. The air bubbles carry the GnP from the chloroform/water interface to the water/air interface. From there, the GnP layer was transferred to a thin HDPE film (produced from the extrusion through the multilayer film die in Chapter 3). This process was repeated until the desired number of layers was deposited. The resulting film was then compressed between two more neat layers of HDPE using a heated Carver press with

the following setup: Mirror finished steel plate/Neat HDPE/Sample/Neat HDPE/Mirror finished steel plate. 300 micron aluminum spacers were used to ensure the film was not compressed too thin. The press was heated to 150 °C, and the press was closed until a very small amount of pressure was applied. The resulting films before and after pressing can be seen in Figure 4.3. During the pressing process, the film tends to spread slightly.

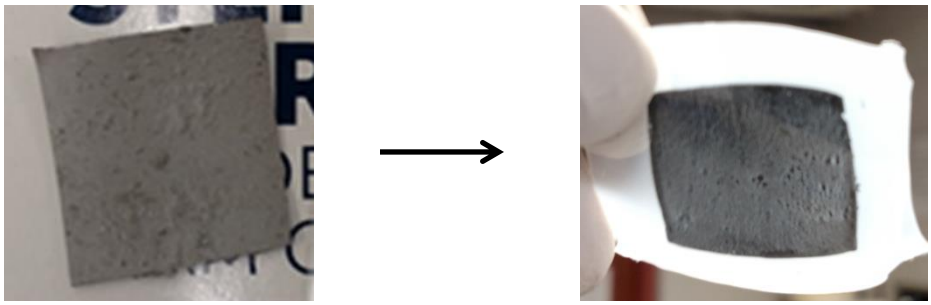

Figure 4.3. 15 layers of GnP deposited onto an HDPE film, and then pressed between two more layers of HDPE.

4.2.4 Characterization Techniques

Oxygen permeation testing was performed with a Mocon OX-TRAN 2/20 ML. Active individual zeros were performed for each cell prior to measuring the oxygen transmission. The resulting steady state transmission rates were normalized for film thickness.

Thermogravimetric analysis (TGA) was used to estimate the amount of GnP deposited onto the polymer surface. Samples were heated to 600 °C at a rate of 10 °C.min^{-1} in air using a TA Instruments Q500 machine.

Scanning electron microscopy was used to examine the surface of the layered GnP depositions. A Zeiss EVO LS25 was used with an acceleration voltage of 4 kV for analysis of the surfaces. To avoid sample charging, samples were coated with a 3 nm film of tungsten with a Leica EM MED020 sputter-coater.

4.3 Results and Discussion

4.3.1 Layer by Layer Deposition Results

Since nanoclays demonstrated such a large enhancement of barrier properties with as few as 40 bilayers using a layer by layer approach, it was theorized that the larger GnP-M-5 platelets could result in similar enhancements with fewer layers. The larger aspect ratio should result in a more tortuous path for the permeating gases to follow. 40 bilayer samples, 1 layer of SPS-GnP and 1 layer of polymer, were created with PEI as the cation polymer. This was done for both GnP-M-5 and GnP-C-750. The resulting oxygen permeation values can be seen in Figure 4.4. It is clear from the results that GnP-M-5 and GnP-C-750 result in similar barrier properties, despite the larger aspect ratio of the GnP-M-5. This can partially be explained by the SEM images in Figure 4.5. The surface of the film with GnP-M-5 results in few platelets actually being attached to the polymer substrate. On the other hand, the surface of the GnP-C-750 films show many platelets deposited, even if many of them are under 1 micron in diameter. A 41% reduction in oxygen transmission was observed with the 40 bilayer SPS-GnP-C-750/PEI samples.

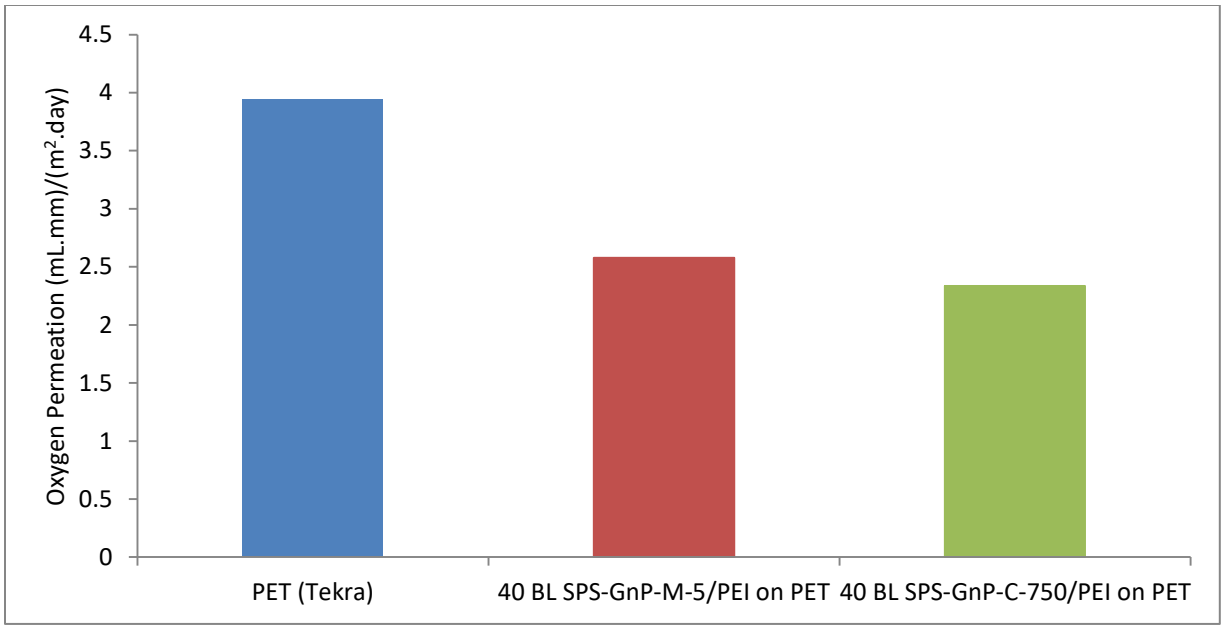

Figure 4.4. Oxygen permeation of SPS-GnP/PEI layer by layer deposition on PET.

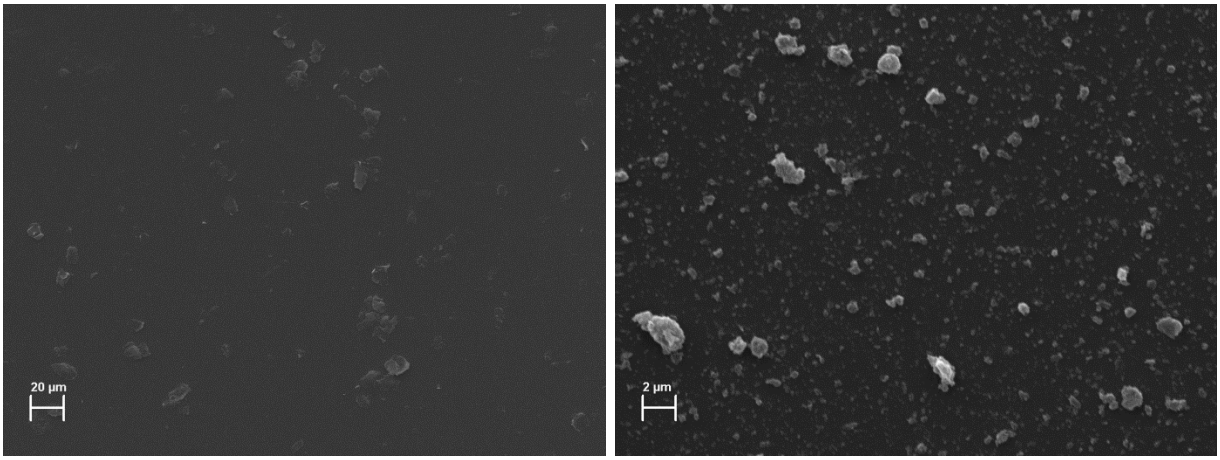

Figure 4.5. SEM of the surface of 40 bilayer samples of GnP-M-5 and GnP-C-750 with PEI.

Another cationic polymer, PDAC, exhibits a similar positive charge to PEI and was investigated with layer by layer deposition. It was alternated in layers with SPS-GnP-C-750. The oxygen transmission of the resulting composite films can be seen in Figure 4.6. By synthesizing a sample without GnP, the effects of SPS and PDAC could be assessed. A 40 bilayer system of SPS and PDAC resulted in a 30% reduction in oxygen permeation values. Adding GnP-C-750 results in an additional 30% reduction, resulting in an oxygen permeation value 60% less than neat PET film. Alternating the GnP-C-750 with PDAC instead of PEI resulted in an additional 20% improvement in barrier properties. Using SEM to analyze the cross-section of a deposited film on PET, it can be seen that the total thickness of the deposited film is less than 2 microns, shown in Figure 4.7. The thinness of this film emphasizes the effect that a small amount of material can have on the barrier properties of a system. In order to achieve 60% reduction in barrier properties via melt mixing in HDPE, it was necessary to add over 10 weight percent GnP to the system [1]. However, there are disadvantages to layer by layer deposition. It is a very time intensive process compared to melt mixing, and the additional polymers and equipment used for processing would be a costly investment. Scaling the process to a large scale environment, like would be necessary for production of fuel tank and line systems, would not be straightforward.

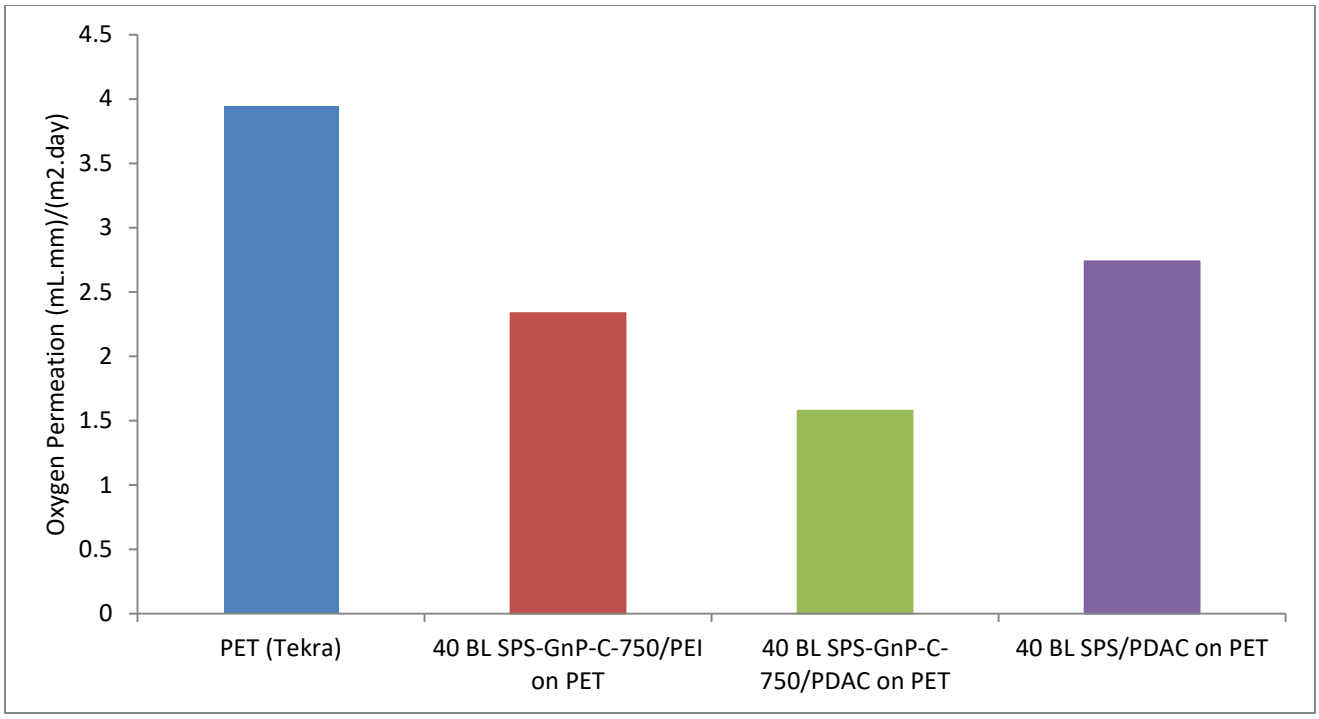

Figure 4.6. Oxygen permeation of SPS-GnP-C-750 and a cationic polymer: comparing PEI and PDAC as the alternating polymer.

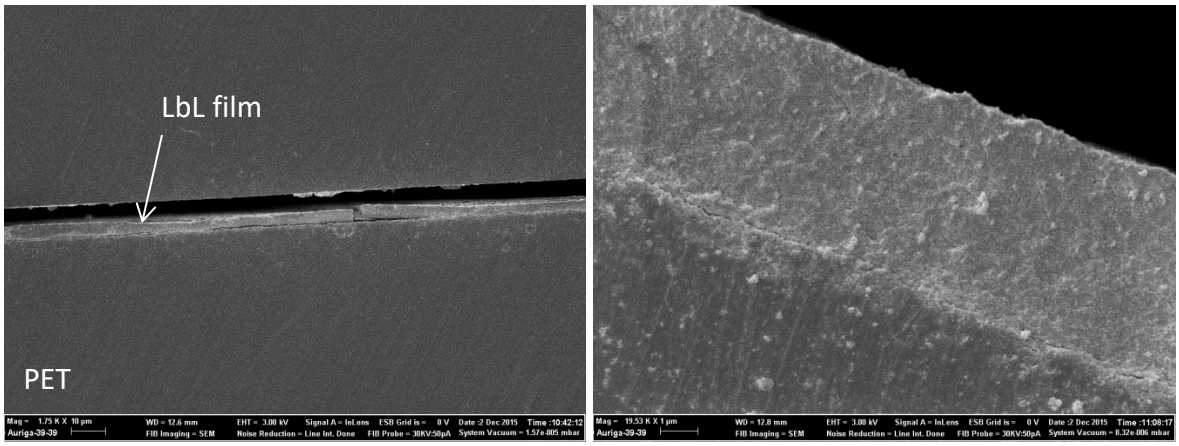

Figure 4.7. SEM cross-section of deposited 40 bilayer SPS-C-750/PDAC film on PET.

4.3.2 Self Assembled GnP Layer Deposition Results

While layer by layer deposition yielded good results for oxygen permeation, another method was investigated that did not utilize a secondary polymer for the deposition of GnP onto a surface. Utilizing differences in surface energies, GnP will self-assemble at a chloroform/water interface, as discussed earlier [9]. Air bubbles can then be used to transfer the GnP monolayer to the water/air interface. The resulting GnP monolayer that was bubbled was transferred to a glass slide and analyzed with SEM, seen in Figure 4.8. For the majority of the film, there is a continuous GnP monolayer covering the gaps. There are some small aggregates scattered, but the overall layer is very uniform. Small areas with no GnP are present, but depositing multiple layers of GnP onto a polymer substrate would result in overlapping platelets covering all areas.

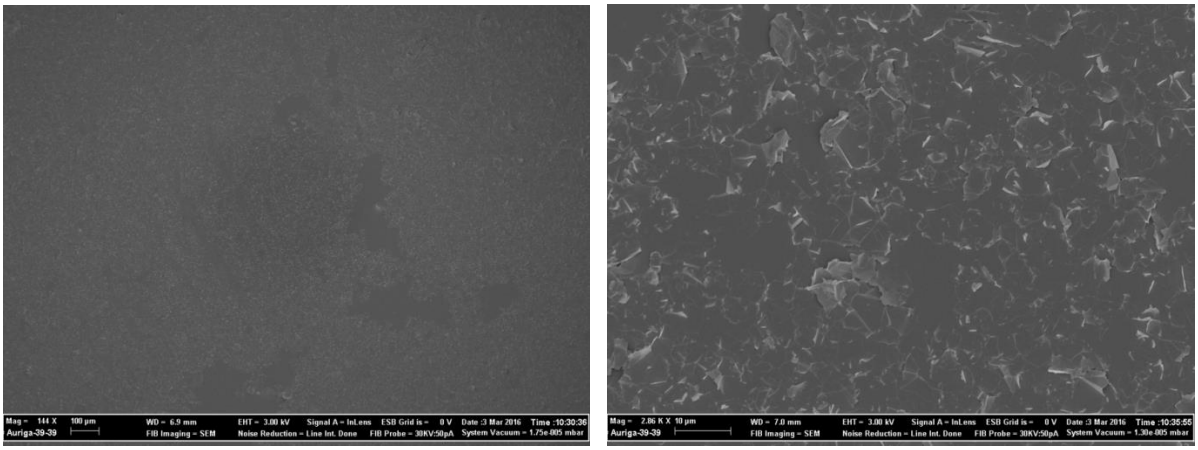

Figure 4.8. SEM of GnP monolayer deposited on glass substrate.

A sample was made with 15 layers of GnP deposited onto the HDPE surface and pressed between two more layers of HDPE, as described in the methods section, and shown in Figure 4.3. The resulting film was tested for oxygen permeation, and the results are found in Figure 4.9. Seen in the chart is a comparison between the resultant film, neat HDPE and a 2% wt. GnP-M-15 melt mixed composite, as presented in Chapter 2. The amount of GnP present in the sample was estimated through thermogravimetric analysis. When a neat HDPE sample was heated to 600 °C, there was 0.26% weight remaining as ash. When the 15 layer GnP sample was put through the same heating rate to 600 °C, there was 1.13% weight remaining. It is estimated that the 15 layer GnP composite contained less than 1% wt. GnP. This highly aligned, low concentration of GnP sandwiched between layers of HDPE resulted in a 60% decrease in oxygen transmission compared to neat HDPE. This is nearly double the relative decrease of the 2% wt. GnP composite that was prepared through melt mixing. This highlights the theory presented on barrier properties in Chapter 1. The densely packed platelets are highly aligned and well dispersed within their monolayers, creating a very tortuous path with relatively no gaps between the platelets. While these are promising results using a very small amount of GnP, it would still be challenging to scale up to an industrial level in a cost effective manner.

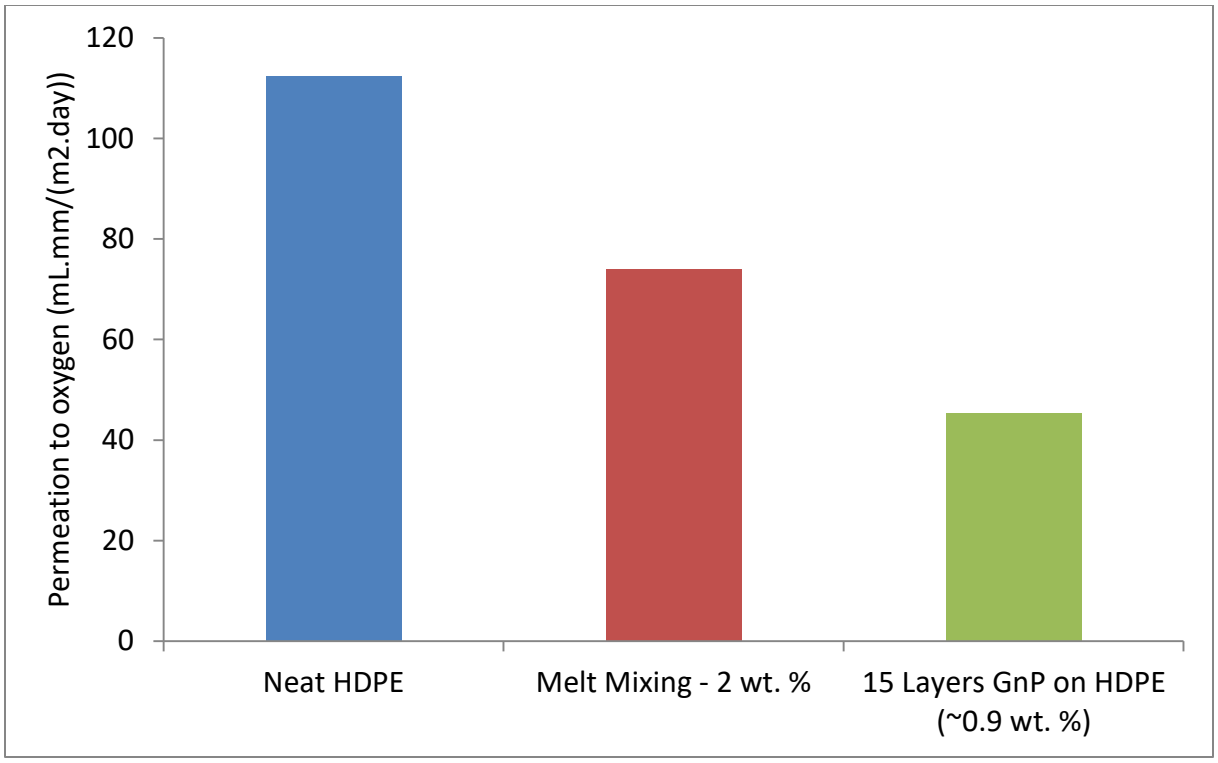

Figure 4.9. Oxygen permeation results of 15 layers of self-assembled GnP deposited on HDPE.

4.4 Conclusions

In this chapter, methods for depositing thin films with GnP were investigated, as well as the resulting barrier properties. In the first method, ionic charges on polymers were used to alternate a positively charged polymer, either PEI or PDAC, and a negatively charged, SPS coated, GnP to build up a layer by layer structure. This processes had shown promise in reducing barrier properties with nanoclays, and did result in large reductions in oxygen permeations with little amount of material. Layered structures made with PDAC yielded better results than those made with PEI. With a 40 bilayer system of PDAC and SPS-GnP-C-750, a film with a thickness of less

than 2 microns was formed, and there was a 60% reduction compared to the neat polymer film. Little difference was noticed between using GnP-M-5 and GnP-C-750 despite the larger aspect ratio of GnP-M-5. This could potentially be due to the greater forces required to deposit the larger platelets on the surface, resulting in less coverage with GnP-M-5 compared to the samples with GnP-C-750, verified with SEM observation. Alternatively, self-assembled GnP was deposited onto a polymer surface by taking advantages of the difference in surface energies between chloroform and water. After depositing 15 monolayers of GnP onto an HDPE surface, it was found that there was also a 60% reduction in oxygen permeation. Through thermogravimetric analysis, it was estimated that this composite film contained less than 1% GnP by weight. The barrier properties of this low weight content film exhibited 30% better resistance to oxygen transmission than a 2% weight GnP melt mixing composite. While both of these methods show promise in utilizing a very small amount of GnP to improve the barrier properties of a polymer, scaling up to an industrial level of processing is not straightforward and could be costly. However, if GnP could be delivered to the surface in dilute concentrations through a coating or spraying technique, it might be possible to produce the desired effect. Additional investigations into the efficiencies of the methods could be warranted.

REFERENCES

REFERENCES

[1] K. Honaker, F. Vautard, and L. T. Drzal, "Investigating the mechanical and barrier properties to oxygen and fuel of high density polyethylene–graphene nanoplatelet composites," *Mater. Sci. Eng. B*, pp. 1–8, 2016.

[2] M. A. Priolo, K. M. Holder, S. M. Greenlee, B. E. Stevens, and J. C. Grunlan, "Precisely tuning the clay spacing in nanobrick wall gas barrier thin films," *Chem. Mater.*, vol. 25, no. 9, pp. 1649–1655, 2013.

[3] M. A. Priolo, K. M. Holder, D. Gamboa, and J. C. Grunlan, "Influence of clay concentration on the gas barrier of clay-polymer nanobrick wall thin film assemblies," *Langmuir*, vol. 27, no. 19, pp. 12106–12114, 2011.

[4] M. A. Priolo, D. Gamboa, K. M. Holder, and J. C. Grunlan, "Super gas barrier of transparent polymer-clay multilayer ultrathin films," *Nano Lett.*, vol. 10, no. 12, pp. 4970–4974, 2010.

[5] D. Gamboa, M. A. Priolo, A. Ham, and J. C. Grunlan, "Note: Influence of rinsing and drying routines on growth of multilayer thin films using automated deposition system," *Rev. Sci. Instrum.*, vol. 81, no. 3, pp. 15–18, 2010.

[6] M. A. Priolo, D. Gamboa, and J. C. Grunlan, "Transparent clay-polymer nano brick wall assemblies with tailorable oxygen barrier," *ACS Appl. Mater. Interfaces*, vol. 2, no. 1, pp. 312–320, 2010.

[7] J. Lu, I. Do, H. Fukushima, I. Lee, and L. T. Drzal, "Stable Aqueous Suspension and Self-Assembly of Graphite Nanoplatelets Coated with Various Polyelectrolytes," *J. Nanomater.*, vol. 2010, pp. 1–11, 2010.

[8] T. Lee, S. H. Min, M. Gu, Y. K. Jung, W. Lee, J. U. Lee, D. G. Seong, and B. Kim, "Layer-by-Layer Assembly for Graphene-Based Multilayer Nanocomposites: Synthesis and Applications," *Chem. Mater.*, vol. 27, no. 11, pp. 3785–3796, 2015.

[9] S. Biswas and L. T. Drzal, "A novel approach to create a highly ordered monolayer film of graphene nanosheets at the liquid-liquid interface," *Nano Lett.*, vol. 9, no. 1, pp. 167–172, 2009.

CHAPTER 5 - INVESTIGATING MECHANICAL, ELECTRICAL, THERMAL AND BARRIER PROPERTIES OF BIOBASED POLYAMIDE-GNP NANOCOMPOSITES

5.1 Introduction

As the focus on protecting the environment grows, biobased materials gain more interest. Over 300 tons of plastics are manufactured each year, and the majority is synthesized from non-renewable materials, such as petroleum [1]. Many industries are seeking "green" alternatives for these polymers in the interest of finding a sustainable source for polymers and in protecting the environment. While the production of bio-based polymers has grown significantly recently, there are still challenges in implementing them into current applications. There can be a large disparity in performance of a biobased material versus a polymer synthesized from petroleum, which must be overcome if they are to be used widespread [2]. One way to improve the thermomechanical properties of the biobased polymers is to add a nanofiller, such as graphene or carbon nanotubes [3], [4]. Nanofillers have the potential to tailor the renewable polymers to fit what specifications are needed for a variety of applications.

One particular area of interest is in replacing the barrier polymers in automotive fuel tank and line systems. Currently, fuel tanks are made with a layered structure. Two layers of high density polyethylene (HDPE) have a layer of a barrier polymer sandwiched between them, with an adhesive bonding the layers together. The barrier polymer is typically ethyl vinyl alcohol (EVOH) or a polyamide, which both have excellent barrier properties to both oxygen and fuel. However, high humidity can typically cause these properties to decline [5]. Potential alternatives have recently been developed by Evonik Industries, synthesizing a polyamide from castor bean

oil. The castor bean plant is an abundant source around the globe and has been known to be a good basis for polymer synthesis [6]. These polymers are semi-crystalline in nature, exhibiting great chemical stability and base mechanical properties.

Challenges that arise in using these polymers is the fact that fuel tank and line systems need to be able to dissipate a static charge to eliminate the chance for fires to occur. Naturally, these polymers are insulating. It has been well documented that adding a conductive nanofiller like graphene can result in dramatic improvement to the overall conductivity of the composite [7]. This occurs when a percolated network is achieved, which theoretically is achievable at a low volume percent for graphene due to its high aspect ratio [8].

While single layer graphene is difficult to manufacture and still very costly, graphene nanoplatelets (GnP) are a cost effective alternative with similar properties. GnP consists of a few layers of graphene in a stack, and is made by rapidly heating sulfuric acid intercalated graphite, and then grinding the resulting expanded form into platelets [9]. Previous research has shown that incorporating these platelets into the HDPE layers of the fuel tank results in an improvement to the barrier properties due to the tortuous path established by the platelet morphology, as well as improvements to thermal stability and flexural properties [10].

5.2 Materials and Methods

5.2.1 Materials

Three different grades of bio-based polyamides were used, all supplied by Evonik Industries. Two polyamide 610 grades were used, trade name VESTAMID Terra HS16 (viscosity number of 160 cm^3/g) and HS22 (viscosity number of 220 $cm^3.g^{-1}$), each with a biobased content of 63%. One polyamide 1010 was used, trade name DS22 (viscosity number of 220 $cm^3.g^{-1}$), with a biobased content of 100%. Graphene nanoplatelets, trade name GnP-M-25, were obtained from XG Sciences (Lansing, Michigan, USA). These platelets have an average diameter of 25 microns, a surface area of 120-150 $m^2.g^{-1}$ and an average thickness of 6 nm. The GnP was heat treated for 1 hour at 450 °C in an air circulating oven to remove any trace volatile compounds remaining from the manufacturing process.

5.2.2 Nanocomposite Processing

All of the polyamides were dried at 80 °C for 4 hours and then stored in a dry room. Once removed from the dry room for use, the polymer was used within one hour to limit any moisture absorption. A co-rotating, twin-screw, DSM 15 cc extruder was used to process all of the nanocomposites. The melt temperature was set to 260 °C and the screws rotated at 100 rpm. This generated shear forces of 1200 N (HS16), 3500 N (HS22) and 4500 N (DS22) within the extruder. The composites were allowed to mix for 5 minutes to form a baseline. Mix times of 10 and 15 minutes were also investigated. After mixing, the extrudate was transferred to a holding barrel set to the same temperature as the melt, and a Daca Micro-injector was used to mold flexural and Izod samples. The mold temperature was set to 110 °C. The range of GnP

concentrations was varied from 0 to 15% weight. Film samples for oxygen permeation testing were made by compressing a flexural specimen between two mirror finished steel plates. The setup was sealed in a vacuum bag assembly to limit any generation of bubbles and heated to 260 °C in a heated Carver press. A pressure of 1 MPa was applied, resulting in films that were 250 microns in thickness.

5.2.3 Testing Procedures

A UTS SFM-20 testing machine was used for flexural testing of the composites using a 100 lb load cell. ASTM D790 was followed, the thickness to span ratio was 1/16 and the displacement speed was set to 0.03 $in.min^{-1}$.

A TMI impact apparatus was used to test the Izod impact resistance following ASTM D256. A 1lb hammer was used and the samples were notched with a motorized tooth notcher 24 hours prior to testing.

Crystallinity was estimated by Differential Scanning Calorimetry (DSC) with a TA Instruments Q2000 differential scanning calorimeter. Again, Equation 1 in Chapter 2 was used. To erase any thermal history, the samples were first heated to 260 °C at a rate of 20 $°C.min^{-1}$, and then held there for 5 minutes before being cooled to 40 °C. The same cycle was then used on the sample a second time and the melting enthalpy was calculated and used for estimation of the crystallinity. The melting enthalpy of purely crystalline PA610 is estimated to be 211 $J.g^{-1}$ and for PA1010 it is estimated to be 240 $J.g^{-1}$ [11].

Thermogravimetric analysis (TGA) was used to assess the thermal stability of the composites. A TA Instruments Q500 machine was used to heat the samples to 600 °C at a rate of 10 °C.min^{-1} in air. The rate of sample combustion was monitored over time to determine the stability.

Electrical conductivity was measured with a Gamry Potentiostat using flexural specimens for both in-plane and through-plane measurements. The in-plane direction is considered to be in the same direction as the polymer flow, while the through-plane is perpendicular. The Gamry measurement is made over two points across the sample. For in-plane measurements, flex samples were cut in half and the ends were trimmed off to make sure there was no thin, insulating polymer film at the surface. The ends were then painted with conductive silver paint, allowed to dry and then copper tape was applied to the ends and measurements with the Gamry were made. The same samples were then used for through-plane measurements. The ends with silver paint were trimmed off and then each side of the upper and lower surfaces of the specimen were plasma treated in 50:50 oxygen to nitrogen with a power of 375W for 15 minutes to remove a thin layer of polymer from the surface. Silver paint was then applied to the treated surfaces and copper tape was attached. The two point measurement was then taken for the through plane direction.

A Mocon OX-TRAN 2/20 ML was used to measure the oxygen permeation of the pressed films. Since all samples had a low oxygen transmission value, active individual zeros were done for each cell prior to measuring the oxygen permeation in order to establish a baseline for each assembly of samples. The resulting oxygen transmission rate was normalized to the film thickness for each value.

Scanning electron microscopy was used to examine the Izod impact resistance specimens, as well as cross-sections of the samples. Cross-sections of film samples were mounted in quick cure epoxy, polished, and then plasma treated for 15 minutes with 375W of power in a 50:50 oxygen/nitrogen atmosphere to expose the platelets. A Zeiss EVO LS25 was used with an acceleration voltage of 4 kV for analysis of the surfaces. To avoid sample charging, samples were coated with a 3 nm film of tungsten with a Leica EM MED020 sputter-coater.

5.3 Result and Discussion

5.3.1 Flexural Properties of PA-GnP Composites

The resulting flexural properties of the 5 minute mix time, melt extruded composites can be seen in Figure 5.1. For the base polymers, the HS16 and HS22 grades exhibit similar properties while the DS22 has a 10% lower value. This is probably due to the longer polyamide chains of the PA1010 versus PA610, which results in a more amorphous polymer. As expected, the flexural modulus increases with increasing GnP concentration. This is due to the fact that the GnP platelets are much stiffer than the polymer matrix and act as a reinforcement during a bending process. At a 10% weight concentration, there is a 100% improvement in modulus for the composites. This is similar to the improvement that results from incorporating GnP into HDPE through melt mixing [10]. The strength at yield results follow a similar trend, though the effect is less pronounced. As GnP concentration increases, the flexural strength also increases. At a 10% weight GnP concentration, there is a 25% improvement in strength. While the values between the

HS16 and HS22 composites differ, the relative effect of the platelets is still similar across the three grades of the biobased polyamides.

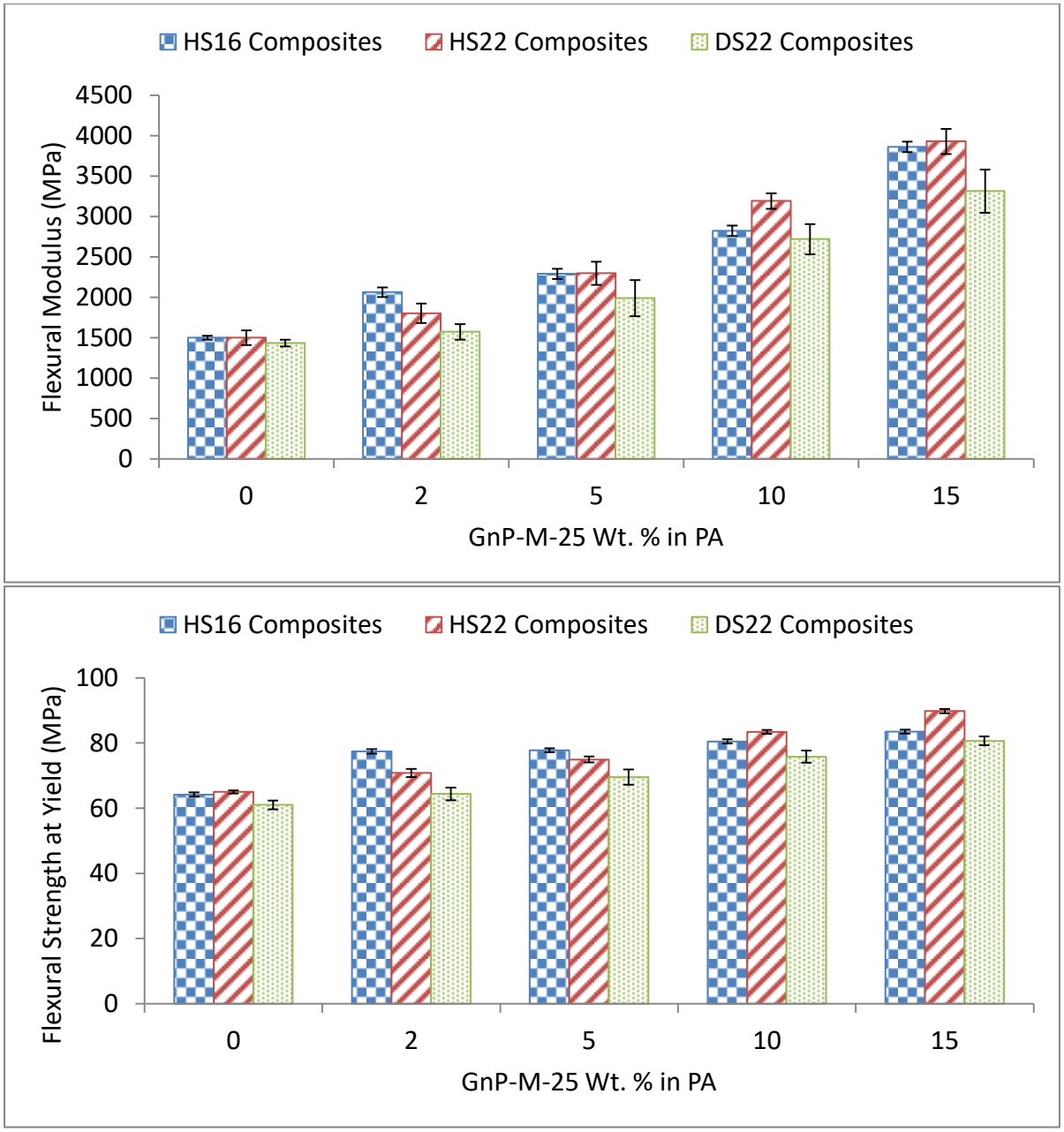

Figure 5.1. Flexural modulus and strength at yield as a function of GnP weight concentration for polyamide-GnP composites.

5.3.2 Izod Impact Resistance of PA-GnP Composites

While GnP had a great reinforcement effect of flexural properties, typically there can be a decrease in the Izod impact resistance. This is evident in Figure 5.2. As the GnP concentration increases, the impact resistance of the samples decreased. The reason for this decrease is that the GnP acts as a stress concentration site, resulting in a more brittle fracture. This was most prevalent for the HS16 composites, yielding a 50% decrease in impact resistance for a 10% weight GnP sample. At the same loading, there was a 33% decrease for the HS22 composites and a 17% decrease for the DS22 composites. The longer chains of the DS22 composite most likely resulted in a more amorphous structure, which would explain the better impact retention of those composites. The SEM analysis of the fractures supports these explanations. Figure 5.3 shows the Izod fractures for various concentrations of GnP in HS16. The neat polymer exhibits a glassy fracture; however there is still some plastic deformation present. As the concentration of GnP increases, the fracture surface becomes more and more brittle. It is also shown that there were some small voids present, which would reduce the impact resistance as well. Upon closer examination of the platelets in the matrix, it is clear that there is no polymer left on the GnP surface, suggesting poor adhesion of the GnP to the matrix. Improving this adhesion would result in recovery some of the lost impact resistance. The fracture surfaces for HS22 exhibited similar characteristics to HS16. Figure 5.4 shows the fractures for the DS22 composites. While similar to the HS16 surfaces, the neat polymer exhibits more plastic deformation, explaining the higher impact resistance. There still appears to be some residual polymer on the GnP after the break, which helps to explain why there is a higher retention of impact resistance compared to the HS grade material.

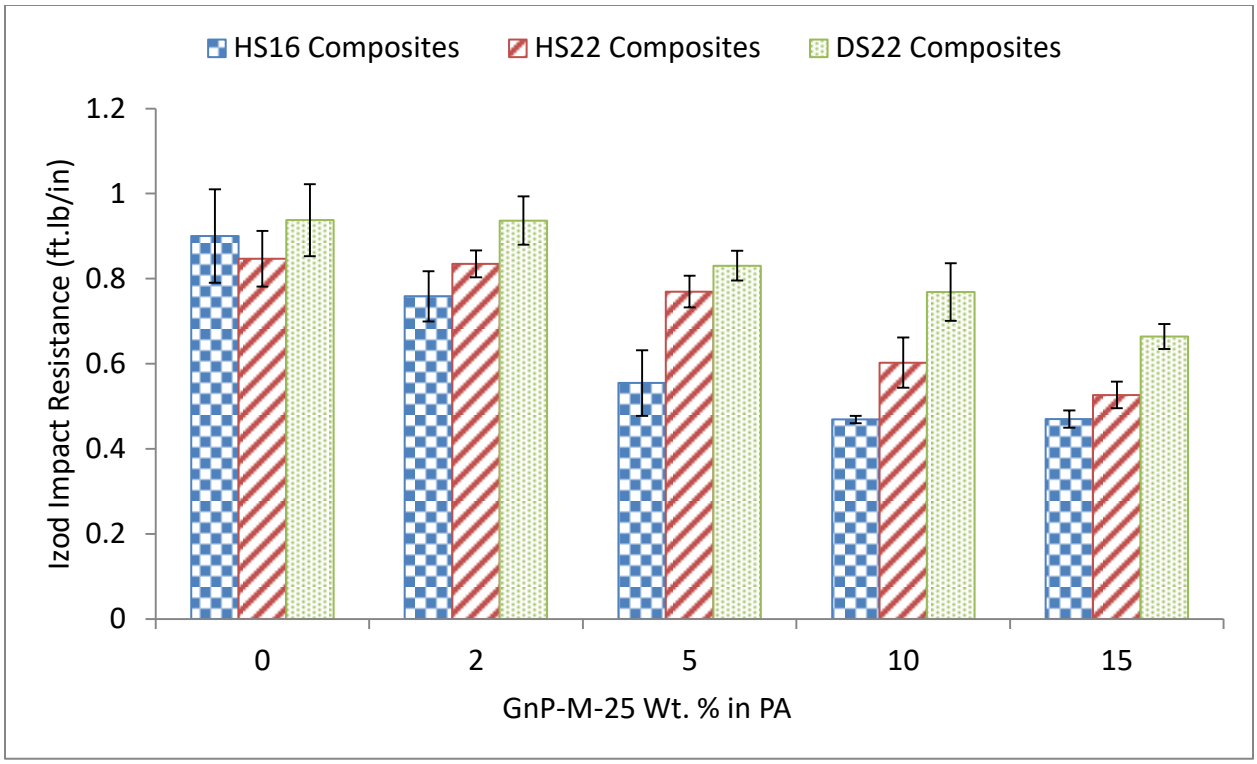

Figure 5.2. Izod impact resistance as a function of GnP weight concentration for polyamide-GnP composites.

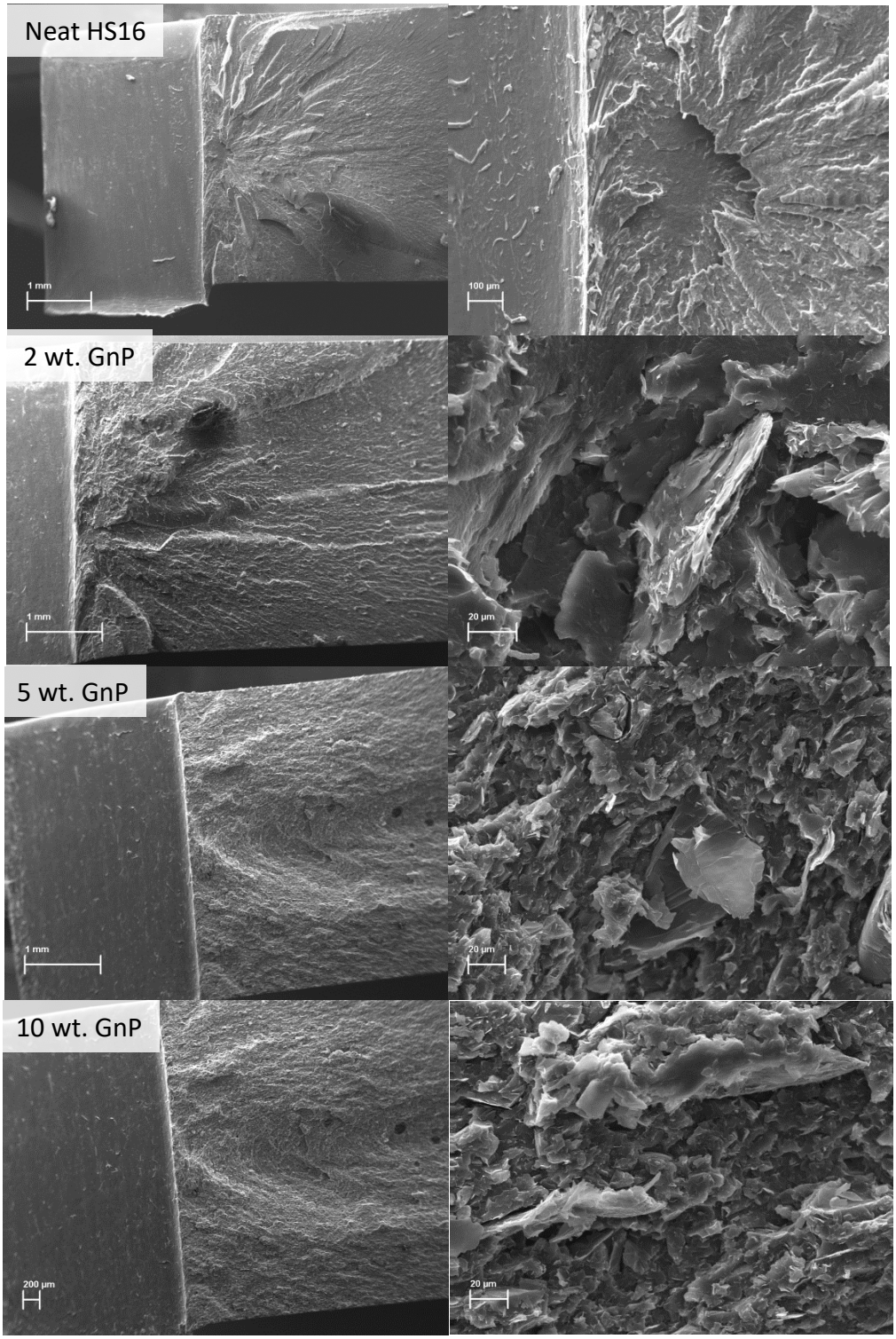

Figure 5.3. SEM images of the Izod fracture surface for 0 to 10% wt. GnP in PA610 HS16.

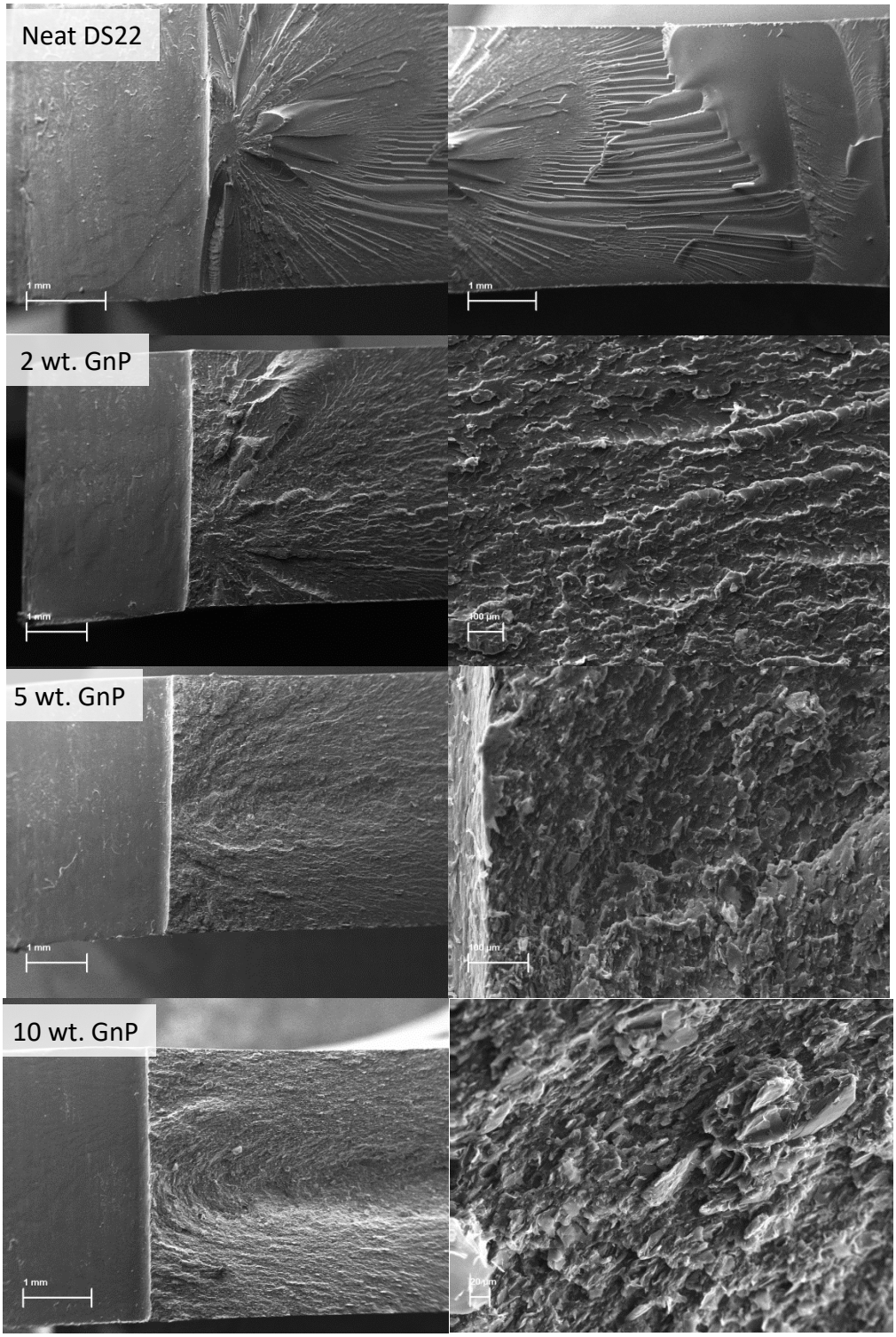

Figure 5.4. SEM images of Izod fracture surface for 0 to 15% wt. GnP-M-25 in PA1010 DS22.

5.3.3 Crystallinity of PA-GnP Composites

By using DSC to estimate the amount of energy absorbed during melting, the crystallinity of a material may be estimated using a theoretical melting enthalpy for a 100% crystalline material. These results are shown in Figure 5.5. In general, the HS grade based composites had a higher crystallinity than the DS composites. This reinforces the reason that the DS composites retain more of their impact resistance due to a more amorphous behavior. Previously it has been reported that GnP act as a nucleating agent when added to a semi-crystalline polymer at low concentrations, however that is seen for these biobased polyamide composites at concentrations of 2% or higher. For the majority of samples, adding GnP resulted in a decrease in the estimated crystallinity. This is most likely due to the fact that while the large platelets could act as a nucleating site, the amount of GnP present could hinder the mobility and diffusion of the polyamide chains, resulting in a lower overall crystallinity.

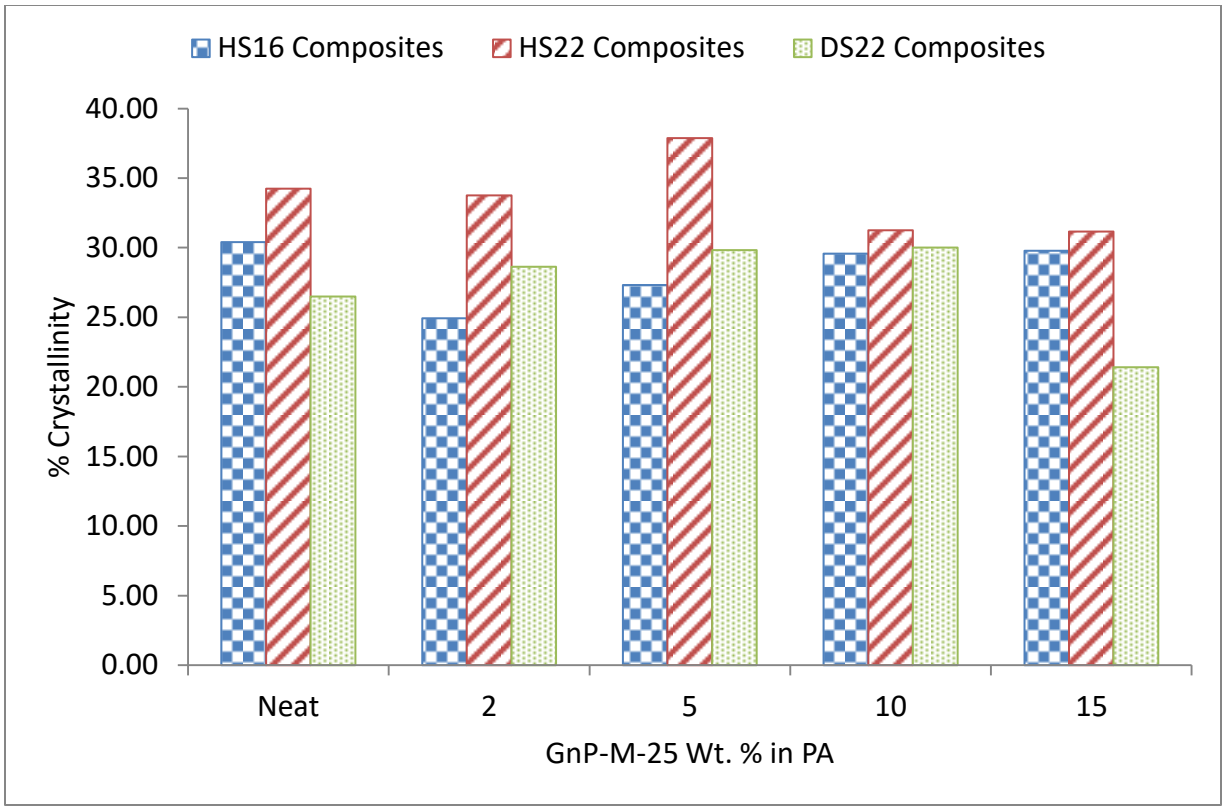

Figure 5.5. Crystallinity estimations for polyamide-GnP composites.

5.3.4 Thermal Stability of PA-GnP Composites

The thermal stability of the polyamide composites is represented by Figure 5.6. The DS22 grade is shown, but the results are representative for all three grades. As the weight concentration of the GnP increases, the composites become more thermal stable. This is because GnP is an excellent conductor of heat, helping dissipate heat from the matrix. The improved thermal stability is especially evident in the fact that at a 15% weight GnP concentration, the degradation temperature has been deflected by 50 °C. Even with a lower 2% weight concentration, there is a 10 °C offset before degradation occurs.

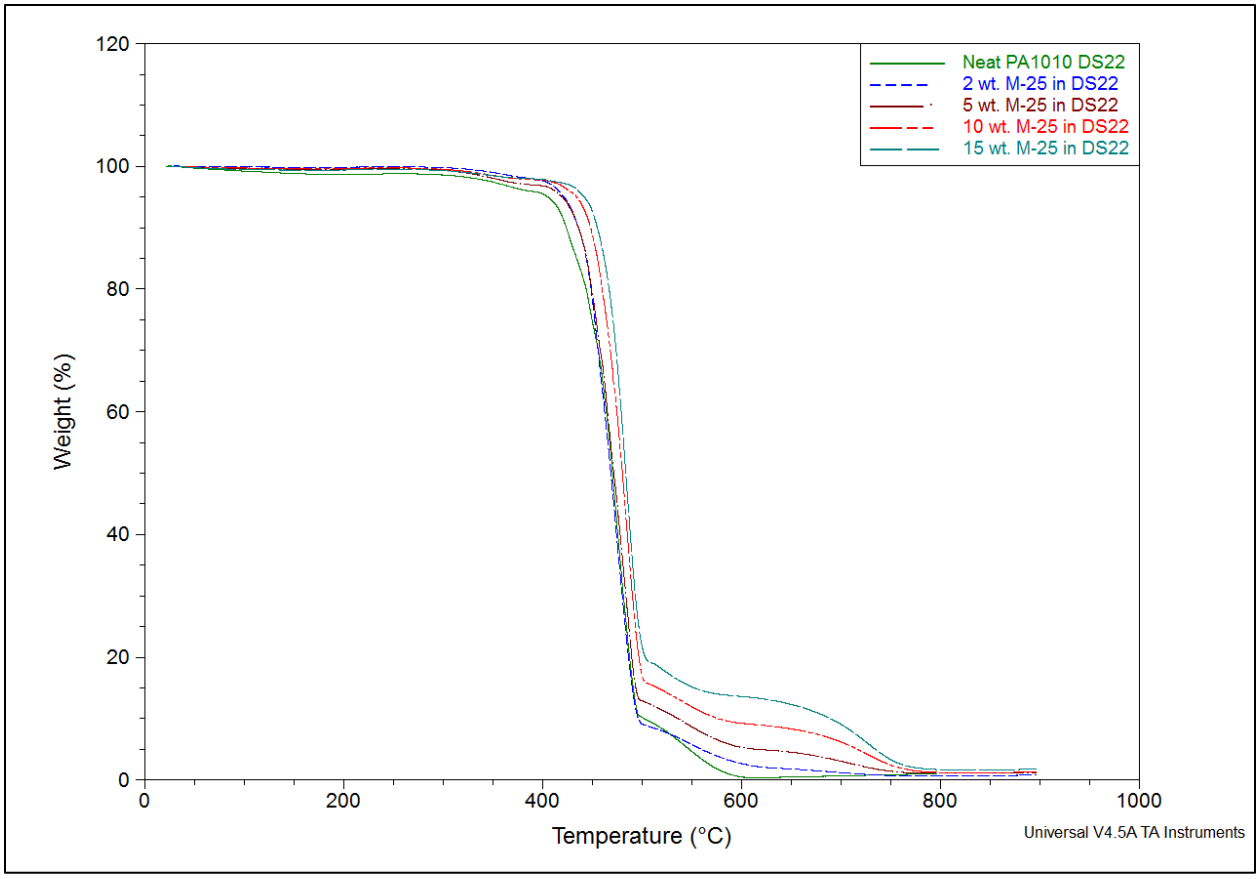

Figure 5.6. Thermal stability of polyamide-GnP composites.

5.3.5 Electrical Conductivity of PA-GnP Composites

Electrical conductivity is important if it is necessary for a material to be able to dissipate a static charge. While polyamides are insulating in nature, adding a conductive nanofiller like GnP could result in a conductive composite if the percolation threshold is reached. The in-plane conductivity is shown in Figure 5.7 and the through plane conductivity in Figure 5.8. There is little change for any of the composites for any GnP concentration 10% weight or less for either in or through-plane conductivity. At 15% weight, there is a change for only the HS16 polymer, probably since it is the least viscous and easiest to disperse the GnP in. At a 15% weight

concentration, there is over a 3 order of magnitude increase for both in and through plane conductivity of the HS16 based composites. The in-plane conductivity is still two orders of magnitude higher than the through-plane conductivity. This is due to the fact that the GnP platelets have a large, 2D aspect ratio and tend to orient themselves with the flow of the polymer. This generally results in many platelets touching along the in-plane axis, but less so in the direction perpendicular to the flow. While there is a marked improvement in the conductivity, there is still room for improvement if the platelets could be interconnected with another nano-filler, such as carbon black or carbon nanotubes.

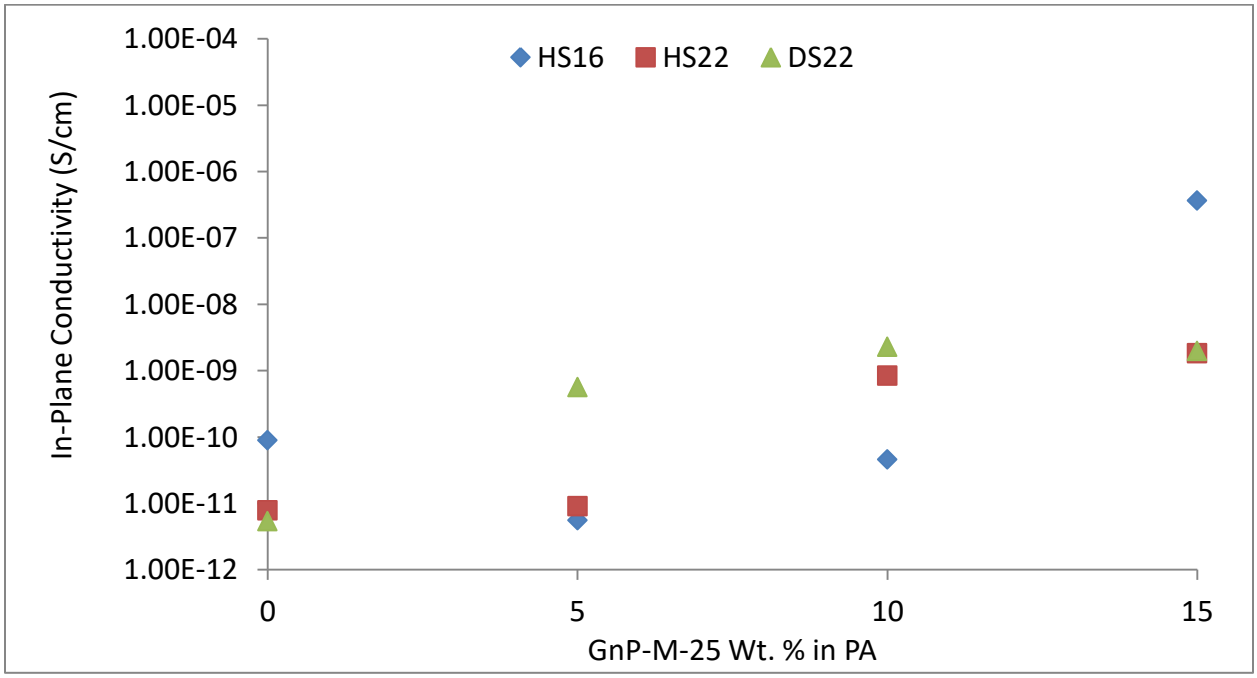

Figure 5.7. In-plane conductivity of polyamide-GnP composites.

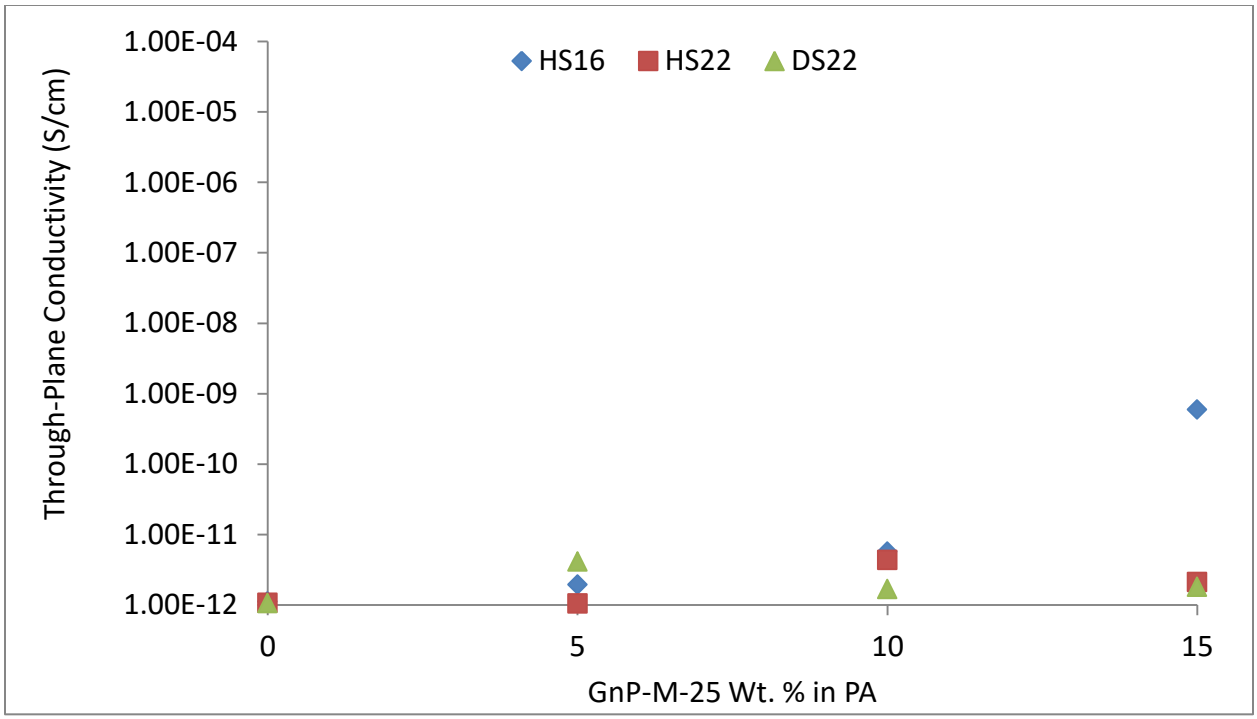

Figure 5.8. Through-plane conductivity of polyamide-GnP composites.

5.3.6 Oxygen Barrier Properties of PA-GnP Composites

Polyamides tend to have excellent barrier properties, which is why they are used in many applications where limiting permeation is valued. Adding GnP to the polymer should enhance those properties even further. The oxygen permeation results are seen in Figure 5.9. For the neat polymers, the HS grades performed better than the DS grades. This could be attributed to the more amorphous behavior of the DS grades. Neat HS22 had a permeation value that was half of that of HS16. This is most likely due to the higher density and molecular weight of the polymer. As the GnP concentration increases in the composites, the oxygen permeation decreases further. This is due to the tortuous path created by the platelets, resulted in an extended path of diffusion through the composite. For all three grades, there is a similar relative reduction in permeation. At

a 10% weight GnP concentration, there is a 40% reduction in permeation for the HS composites and a 50% reduction for the DS composites. The film cross-sections were mounted in a quick curing epoxy, polished, and plasma treated to better expose the GnP platelets. SEM analysis of the film cross-sections suggests there is still room for improvement in the barrier properties due to agglomeration issues that are clearly present in Figure 5.10. Shown are cross-sections from neat up to 15% wt. GnP-M-25. For the lower concentrated composites, there are not many large agglomerates of the platelets. However, at 10 and 15% wt. GnP, there are very large agglomerates present, which would help to explain why increasing past 10% weight does result in additional improvements to the barrier properties. It is clear that if the dispersion can be improved, the barrier properties would be further enhanced. One way to break up the agglomerates further is to allow for a longer mixing time during the extrusion process.

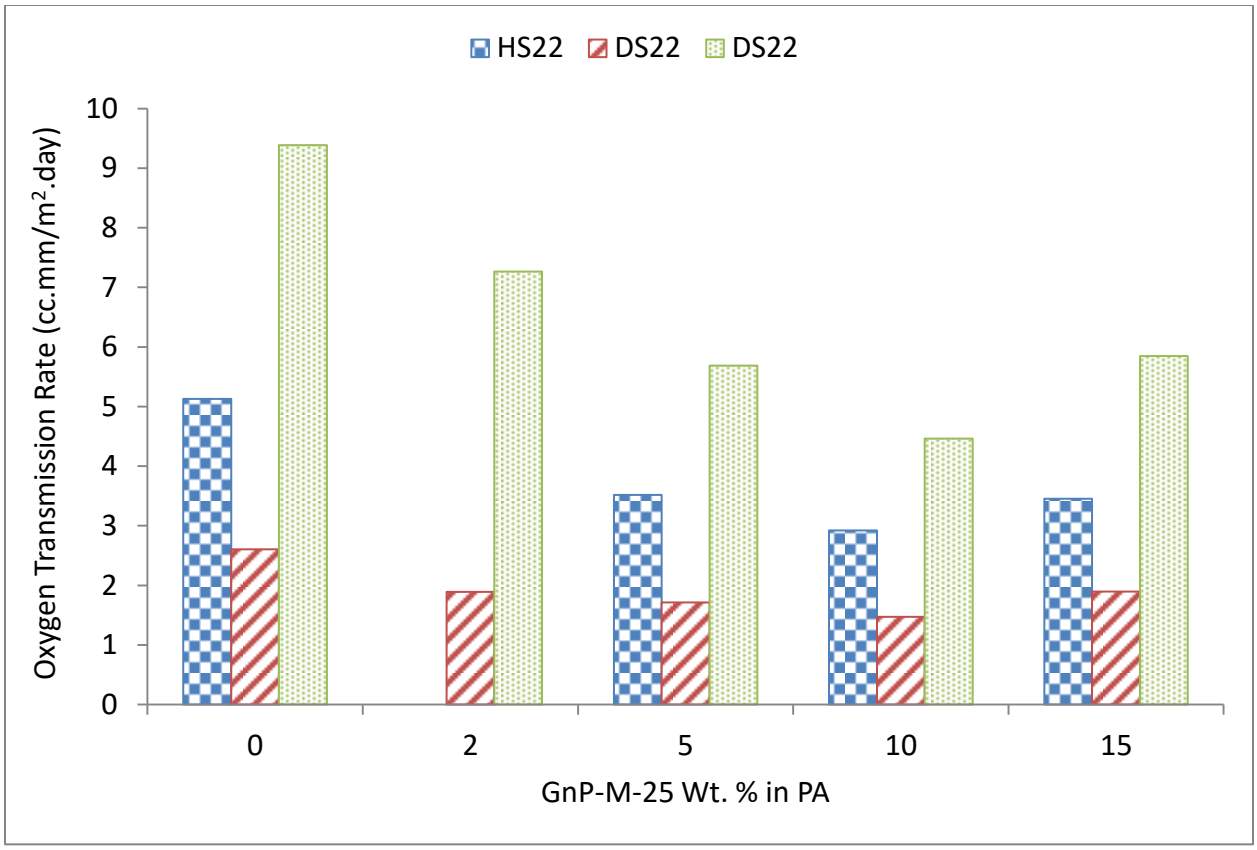

Figure 5.9. Oxygen permeation as a function of GnP weight concentration for polyamide-GnP composites.

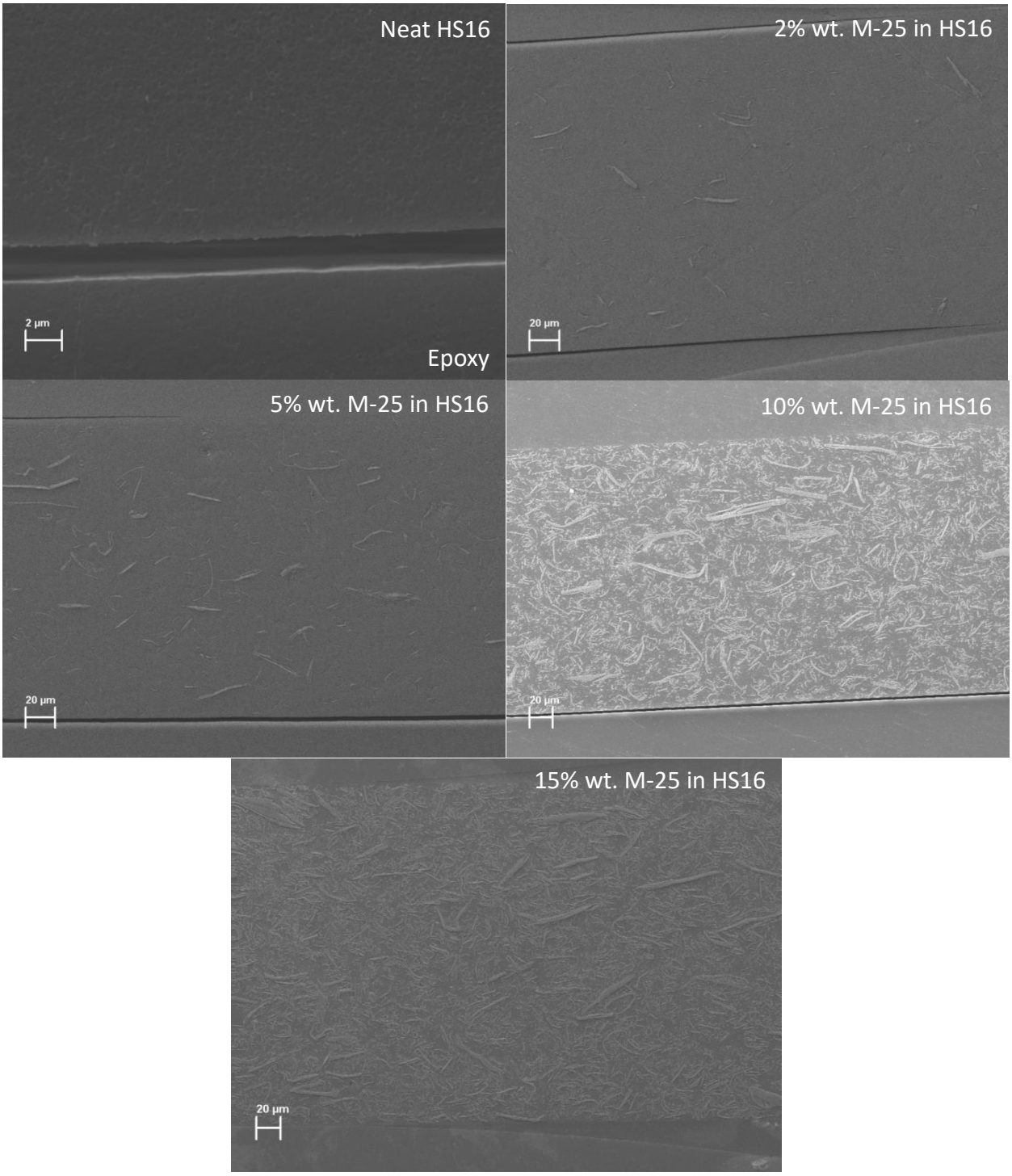

Figure 5.10. SEM of film cross-sections for a range of concentrations of GnP in polyamide HS16.

5.3.7 Effect of Mixing Time on HS16 PA-GnP Composites

In order to improve the dispersion of the platelets, a longer mixing time within the micro-extruder was examined for a 10% weight GnP-M-25 composite in polyamide HS16. Both ten and fifteen minute mix times were investigated to see if there would be some additional breakup of the large agglomerates clearly present in Figure 5.10. Flexural specimens were prepared, and films were pressed from them to test the oxygen permeation properties. The resulting flexural properties can be seen in Figure 5.11. With increased mixing time from five minutes to ten minutes, there is a small increase in both the modulus and strength, and another increase when going from ten minutes to fifteen minutes. This suggests that some of the agglomerates are being broken down, and a better dispersion is yielded.

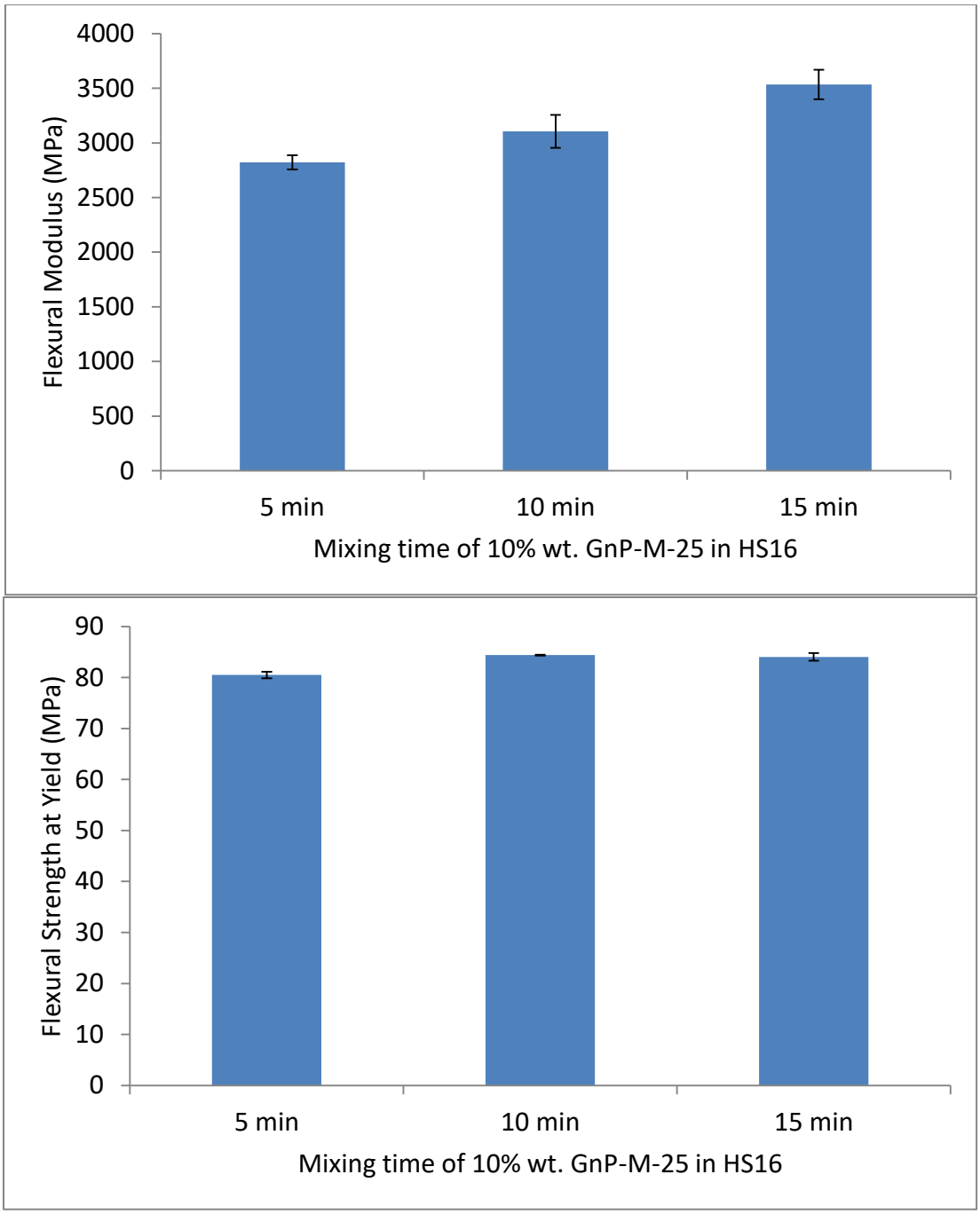

Figure 5.11. Influence of mixing time on the flexural properties of 10% wt. GnP in HS16 composites.

The oxygen barrier properties as a function of mix time for a 10% GnP in HS16 composite is shown in Figure 5.12. It is clear that the allowing for additional mixing time has an effect for these composites. Increasing from five to ten minutes mixing resulted in an additional 50% reduction in oxygen permeation – a 75% reduction overall compared to the neat polymer. Increasing to a 15 minute mix time resulted in a negligible difference for the barrier properties. There are two counteracting mechanisms at this point. Allowing for a longer mixing time breaks up the agglomerates even more, but also results in more size reduction. SEM analysis of the film cross-sections supports these results, shown in Figure 5.13. The first set of three images is an overview of the cross-section and the scale bar is 200 microns. The second set of three images is magnified and the scale bar is 50 microns. In the five minute mixed composites, it's clear there are many large agglomerates. While there are some agglomerates still present in the ten and fifteen minute mixed composites, many of them have been broken up into a smaller size. This is the reason that there are improved flexural and barrier properties with a longer mix time.

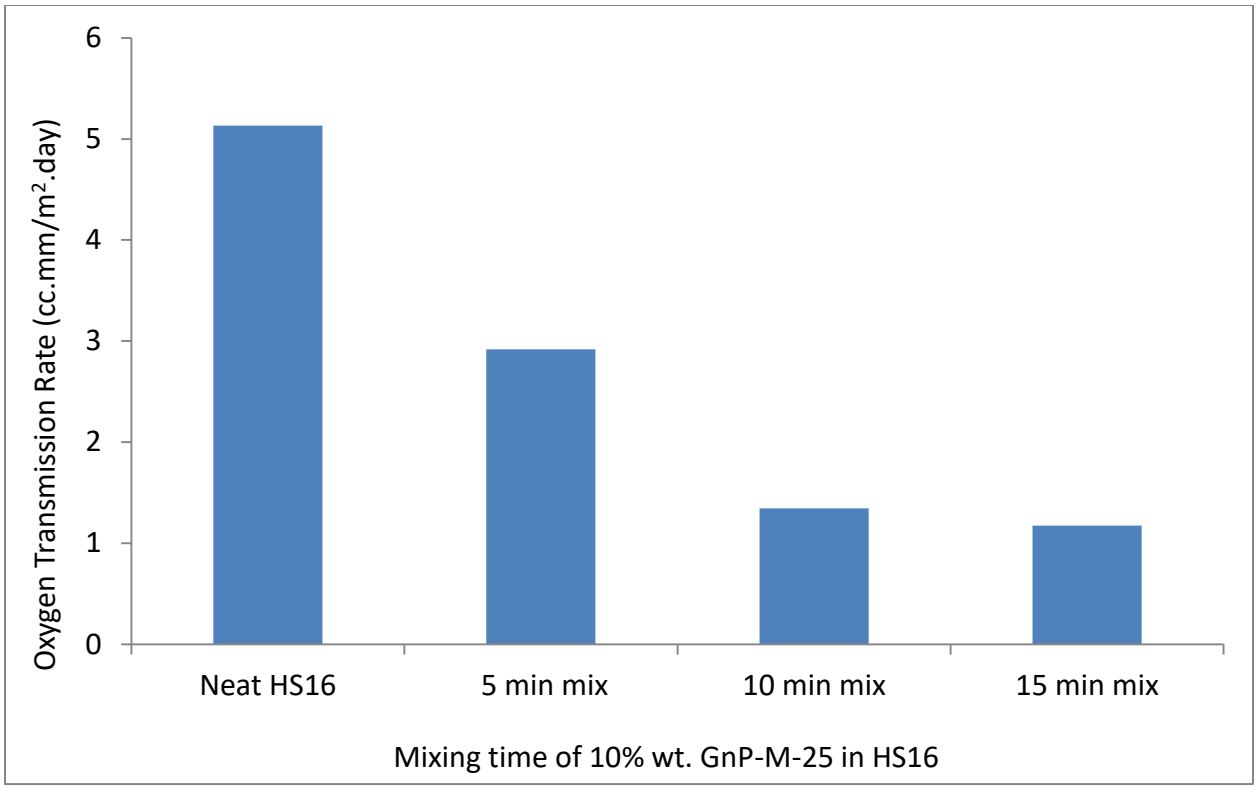

Figure 5.12. Oxygen permeation as a function of mixing time for a 10% wt. GnP in HS16 composite.

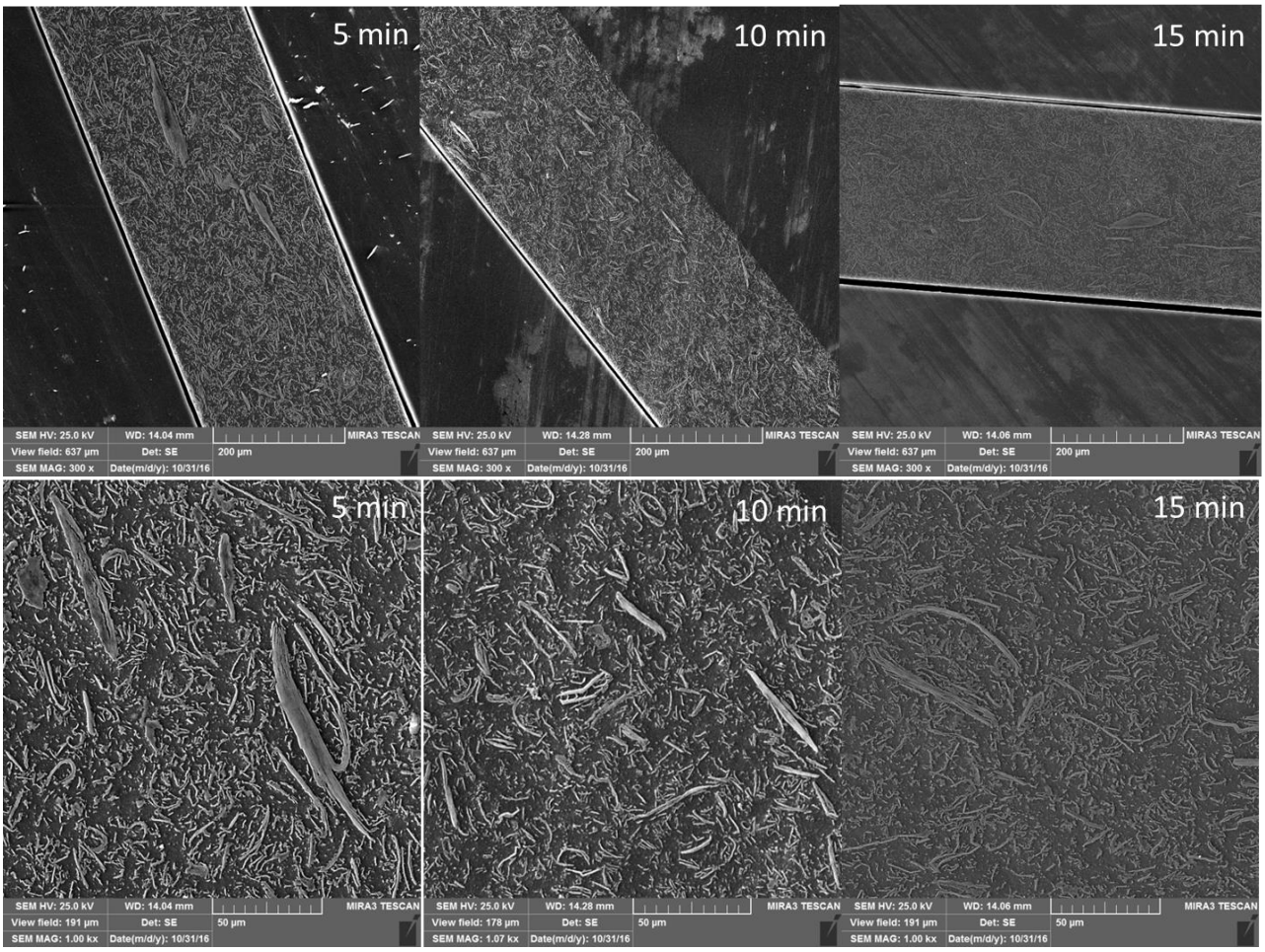

Figure 5.13. Film cross-section SEM of 10% wt. GnP in HS16 for varying mix times.

5.4 Conclusions

Graphene nanoplatelets (GnP) were investigated to see their effect on the mechanical, thermal, electrical and barrier properties of three different biobased polyamides to determine their viability in fuel systems for automotive applications. Two polyamide 610 polymers (HS16 and HS22) were investigated, and one polyamide 1010 (DS22). Composites were made by melt

extrusion with a five minute mix time. For all three grades, the flexural modulus and strength was improved with increasing GnP concentration. At a 10% wt. GnP concentration, there was a 100% improvement in the flexural modulus and a 25% improvement in the flexural strength at yield. Due to the GnP acting as a stress concentration site, there is a decrease in impact resistance with increasing GnP concentration. This was most prevalent for the HS16 composites, decreasing the impact resistance by 50% for a 10% wt. composite. There was a 33% and 17% for the HS22 and DS22 composites respectively for the same concentration. All samples had improved thermal stability due to the excellent thermal conductivity properties of GnP. Thermal decomposition was delayed by up to 50 °C depending on concentration. The electrical conductivity remained largely unaffected by GnP for concentrations up to 10% wt., however at 15% there was a 3 order of magnitude increase for both in-plane and through-plane conductivity for HS16 composites. Since GnP generally aligns with the flow of the polymer, the in-plane conductivity was two orders of magnitude higher than the through-plane. This difference could be overcome by incorporating a second nanofiller into the composite that would tend to be randomly oriented and interconnect the platelets. HS22 composites exhibited the best barrier properties, followed by HS16 and then DS22 composites. The presence of GnP affected each grade similarly, reducing the oxygen permeation by 40% for the HS grades and 50% for the DS grade at a 10% wt. GnP concentration. With a five minute mix time, increasing to 15% wt. GnP did not result in further improvement in the barrier properties due to agglomeration and dispersion difficulties, evident through SEM observation. It was theorized that increasing the mixing time within the extruder would result in better dispersion and further enhancement of the composite properties, so ten and fifteen minute mix times were investigated. Increasing the mixing time resulted in minor improvements to the flexural properties and great improvement to

the barrier properties. At a 10% wt. GnP concentration, there was a 75% reduction with a ten minute mix time relative to the neat polymer, 50% better than the five minute mix time composite. Increasing to fifteen did not result in further improvement for barrier properties. The micro-extruder is limited by only relying on shear forces to mix the fillers and matrix during extrusion. On a larger scale, specific mixing and kneading elements may yield similar results as increasing the mixing time within the micro-extruder.

REFERENCES

REFERENCES

[1] I. Vlassiouk, M. Regmi, P. Fulvio, S. Dai, P. Datskos, G. Eres, and S. Smirnov, "Role of hydrogen in chemical vapor deposition growth of large single-crystal graphene," *ACS Nano*, vol. 5, no. 7, pp. 6069–6076, 2011.

[2] C. Zhang, T. F. Garrison, S. A. Madbouly, and M. R. Kessler, "Recent Advances in Vegetable Oil-Based Polymers and Their Composites," *Prog. Polym. Sci.*, 2017.

[3] A. Ali, K. Yusoh, and S. F. Hasany, "Synthesis and Physicochemical Behaviour of Polyurethane-Multiwalled Carbon Nanotubes Nanocomposites Based on Renewable Castor Oil Polyols," *J. Nanomater.*, vol. 2014, no. 1, pp. 1–9, 2014.

[4] C. Wang, Y. Zhang, L. Lin, L. Ding, J. Li, R. Lu, M. He, H. Xie, and R. Cheng, "Thermal, mechanical, and morphological properties of functionalized graphene-reinforced bio-based polyurethane nanocomposites," *Eur. J. Lipid Sci. Technol.*, pp. 1940–1946, 2015.

[5] H. Kwon, D. Kim, and J. Seo, "Thermal and barrier properties of EVOH/EFG nanocomposite films for packaging applications: Effect of the mixing method," *Polym. Compos.*, vol. 16, no. 2, pp. 1–10, Dec. 2014.

[6] H. Mutlu and M. A. R. Meier, "Castor oil as a renewable resource for the chemical industry," *Eur. J. Lipid Sci. Technol.*, vol. 112, no. 1, pp. 10–30, 2010.

[7] X. Jiang and L. T. Drzal, "Improving electrical conductivity and mechanical properties of high density polyethylene through incorporation of paraffin wax coated exfoliated graphene nanoplatelets and multi-wall carbon nano-tubes," *Compos. Part A Appl. Sci. Manuf.*, vol. 42, no. 11, pp. 1840–1849, 2011.

[8] S. Stankovich, D. A. Dikin, G. H. B. Dommett, K. M. Kohlhaas, E. J. Zimney, E. A. Stach, R. D. Piner, S. T. Nguyen, and R. S. Ruoff, "Graphene-based composite materials," *Nature*, vol. 442, no. 7100, pp. 282–286, 2006.

[9] L. Drzal and H. Fukushima, "Expanded graphite and products produced therefrom," US Patent 7550529 B2, 2009.

[10] K. Honaker, F. Vautard, and L. T. Drzal, "Investigating the mechanical and barrier properties to oxygen and fuel of high density polyethylene–graphene nanoplatelet composites," *Mater. Sci. Eng. B*, pp. 1–8, 2016.

[11] M. R. Jian-bin Song, "Determination of Degree of Crystallinity of Nylon 1212 By Wide Angle X-Ray Diffraction," *Cheinese Journal of Polymer Science*, vol. 22. pp. 491–496, 2004.

CHAPTER 6 - CONDUCTIVE MULTIFUNCTIONAL COMPOSITES THROUGH SYNERGY OF MULTIPLE NANOFILLERS AND ALTERNATIVE PROCESSING

6.1 Introduction

As presented in Chapter 5, it is clear that biobased polyamides can be modified with graphene nanoplatelets (GnP) to form multifunctional composites. The barrier properties, mechanical flexural properties, and thermal stability all improve with increasing GnP content. One property that was not as improved as expected what the electrical conductivity. While the in-plane and through-plane conductivity was improved by 4 orders of magnitude compared to the base polymer, the theoretical percolation threshold for GnP should be much lower based on its aspect ratio [1]. The lack of improvement was attributed to poor dispersion and the fact that all of the platelets tend to align with the flow of the polymer due to the large aspect ratio. While excellent alignment of the platelets is beneficial for barrier properties, it means that there are often gaps between the platelets that break up the conductive pathway, especially in the through plane direction.

Percolation thresholds for carbon nanotubes (CNT) have been reported in the ranges of 0.1 to 3.0 weight percent [2], [3]. Their one dimensional structure allows for more entanglement in the polymer matrix, and their high aspect ratio results in a low percolation threshold. However, the lack of a two dimensional structure would not be advantageous for improving barrier properties, as has been demonstrated with carbon black and carbon fibers [4]. Combining a rod shaped nanoparticle, like CNT or carbon nanofibers (CNF), with a platelet structured nanoparticle like GnP may yield a composite that has excellent barrier properties and is also very electrically

conductive. Such a material would be ideal for use in automotive fuel tank and line systems. There may also be additional advantages to the mechanical properties with the incorporation of CNT into the matrix.

Another potential way the conductivity could be improved is through a plasma treatment of the composite surface. During molding of a composite sample, there is typically a thin layer of polymer that exists on the surface of the material. Since the polymer matrix tends to be insulating in nature, this thin layer could acts as a resistor when measuring the conductivity of a sample. One way to remove this layer is through an oxygen plasma treatment. This has been used before prior to observing a specimen with the SEM, because it has been known to etch away a thin layer of polymer while leaving the carbon based material in the composite intact. However, it has not been used to see the effect on the conductivity of a film before and after plasma treatment.

Another approach that may yield conductivity at low values is solution mixing. Formic acid is well known to dissolve polyamide polymers, and has been used before to disperse carbon base nanofiller and nanosilica [5], [6]. Utilizing a solution based mixing method may yield a better dispersion of the platelets, as discussed in Chapter 3. A better dispersion would result in a lower percolation threshold.

The following seeks to utilize these ideas to improve upon the properties of the biobased polyamide composites presented in Chapter 5.

6.2 Materials and Methods

6.2.1 Materials

A biobased polyamide 610 was obtained from Evonik Industries, trade name VESTAMID Terra HS16 (viscosity number of 160 cm^3/g), which has a biobased content of 63%. Graphene nanoplatelets, trade name GnP-M-25, were obtained from XG Sciences (Lansing, Michigan, USA). These platelets have an average diameter of 25 microns, a surface area of 120-150 $m^2.g^{-1}$ and an average thickness of 6 nm. The GnP was heat treated for 1 hour at 450 °C in an air circulating oven to remove any trace volatile compounds remaining from the manufacturing process. Carbon nanotubes, trade name NC7000, were obtained from Nanocyl. These nanotubes have an average diameter of 9.5 nm, and average length of 1.5 microns, and a surface area of 250-300 $m^2.g^{-1}$. Carbon nanofibers, trade name Pyrograf-III, grade PR-24-XT-HHT, were obtained from Pyrograf Products, Inc. These nanofibers have an average diameter of 100 nm and a surface area of 41 $m^2.g^{-1}$. Formic acid was obtained from Sigma Aldrich at >95% purity.

6.2.2 Nanocomposite Melt Processing

The polyamide HS16 was dried at 80 °C for 4 hours and then stored in a dry room. Once removed from the dry room for use, the polymer was used within one hour to limit any moisture absorption. A co-rotating, twin-screw, DSM 15 cc extruder was used to process all of the nanocomposites. The melt temperature was set to 260 °C and the screws rotated at 100 rpm. This generated shear forces around 1200 N in the extruder. Composites were allowed to mix for 10 minutes prior to molding flexural coupons. After mixing, the extrudate was transferred to a holding barrel set to the same temperature as the melt, and a Daca Micro-injector was used to

mold flexural and Izod samples. The mold temperature was set to 110 °C. Total nanofiller content was either 20% or 25% weight. Ratios of 10:0, 15:0, 20:0, 25:0, 8:2, 13:2 18:2, 23:2, and 20:5 of GnP to other nanofiller were investigates. The other nanofillers were CNT and CNF. Prior to melt mixing, the dry nanomaterial powders were mixed by hand for 60 seconds via stirring, then the polymer pellets were stirred in for 30 seconds by hand, then the mixture was fed into the DSM. Film samples for conductivity and oxygen permeation testing were made by compressing a flexural specimen between two mirror-finished steel plates. The setup was sealed in a vacuum bag assembly to limit any generation of bubbles and heated to 260 °C in a heated Carver press. A pressure of 1 MPa was applied, resulting in films that were 250 microns in thickness for the GnP and GnP/CNF composites. Composites containing CNTs resulted in generally thicker films, 375 to 400 microns in thickness.

6.2.3 Solution Mixing Method

A solution mixing method for GnP and polyamides was modified from Van Zyl et al. [5]. To make the composites, 0.5 grams of GnP-M-25 was added to 50 mL of formic acid and allowed to magnetically stir overnight. 4.5 grams of HS16 were then added to the solution and the polymer was allowed to dissolve for four hours. The solution was then poured into a petri dish and the formic acid was allowed to evaporate off. The resulting material was then dried at 80 °C under vacuum for 2 hours, and then pressed into films with the heated Carver press as described for the melt mixed composites.

6.2.4 Testing Procedures

A UTS SFM-20 testing machine was used for flexural testing of the composites using a 100 lb load cell. ASTM D790 was followed, the thickness to span ratio was 1/16 and the displacement speed was set to 0.03 $in.min^{-1}$.

A Mocon OX-TRAN 2/20 ML was used to measure the oxygen permeation of the pressed films. Since all samples had a low oxygen transmission value, active individual zeros were done for each cell prior to measuring the oxygen permeation in order to establish a baseline for each assembly of samples. The resulting oxygen transmission rate was normalized to the film thickness for each value.

Conductivity measurements were made on films pressed from flexural specimens. The method for conductivity calculations was the 4 point probe method. In order to calculate conductivity, the sheet resistivity is measured. This is done by touching the surface of the sample with 4 points, as shown in Equation 1. Current flows through the outer two probes and the voltage drop across the inner two probes is measured. Depending on the sample dimensions relative to the probe spacing, a correction factor will be applied in the sheet resistance calculation, which is below in Equation 1 [7], [8]:

$$\rho_s = \frac{V}{I} C \qquad \text{(Eqn. 1)}$$

where ρ_s is sheet resistance, V is the measured voltage, I is the current and C is the correction factor. Sheet resistance is proportional to bulk resistance over the thickness of the film [8]. The

correction factor is based on the sample dimensions a and d, shown in Figure 6.1 for both disk shaped films and rectangular films, compared to the probe spacing s. For all of these measurements, samples were trimmed from the pressed film to have an a/d ratio of 3.0 and a d/s of 3.0 as well. Based on the values presented in Table 6.1 as calculated by Smitt, the correction factor for all samples in this work was 2.7. A Keithley 2400 sourcemeter was used to supply the current and measure the voltage. A current of 1 μA was applied to the samples, the voltage was measured and the appropriate calculations were carried out to calculate the conductivity. The setup can be seen in Figure 6.2. Samples were tested on an insulating layer of plexiglass to ensure the base of the probe was not facilitating conductivity.

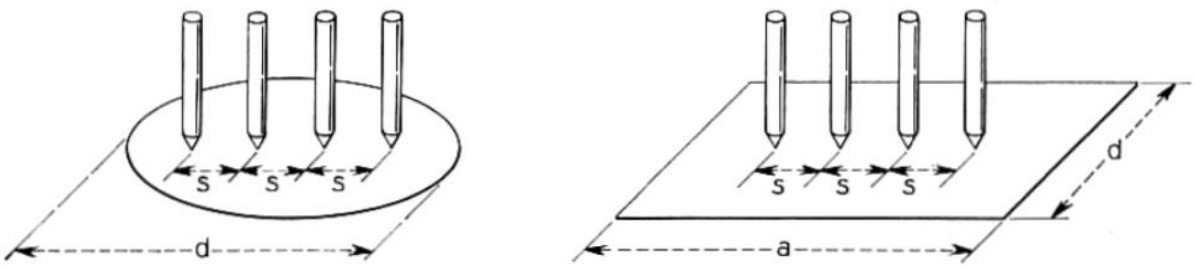

Figure 6.1. Diagram of 4 point probe conductivity measurement parameters. [7]

Table 6.1. Correction factors for various 4 point probe measurement geometries. [7]

d/s	circle diam d/s	$a/d = 1$	$a/d = 2$	$a/d = 3$	$a/d \geqq 4$
1.0				0.9988	0.9994
1.25				1.2467	1.2248
1.5			1.4788	1.4893	1.4893
1.75			1.7196	1.7238	1.7238
2.0			1.9454	1.9475	1.9475
2.5			2.3532	2.3541	2.3541
3.0	2.2662	2.4575	2.7000	2.7005	2.7005
4.0	2.9289	3.1137	3.2246	3.2248	3.2248
5.0	3.3625	3.5098	3.5749	3.5750	3.5750
7.5	3.9273	4.0095	4.0361	4.0362	4.0362
10.0	4.1716	4.2209	4.2357	4.2357	4.2357
15.0	4.3646	4.3882	4.3947	4.3947	4.3947
20.0	4.4364	4.4516	4.4553	4.4553	4.4553
40.0	4.5076	4.5120	4.5129	4.5129	4.5129
∞	4.5324	4.5324	4.5324	4.5325	4.5324

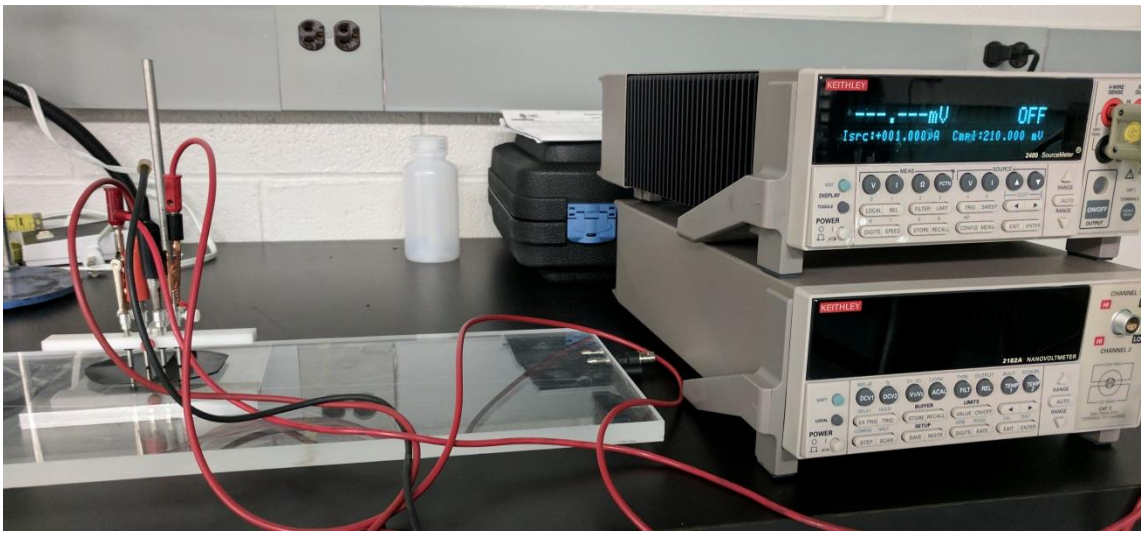

Figure 6.2. Four point probe conductivity test setup.

Scanning electron microscopy (SEM) was used to examine the cross-sections of films. The cross-sections were mounted in quick cure epoxy, polished, and then plasma treated for 15 minutes with 375W of power in a 50:50 oxygen/nitrogen atmosphere to expose the platelets. A Zeiss Auriga FIB-SEM was used with an acceleration voltage of 3 kV for analysis of the surfaces. To avoid sample charging, samples were coated with a film of platinum with a Denton Vacuum Desk II sputter-coater.

6.3 Results and Discussion

6.3.1 Flexural Properties – Melt Processed Composites

The effects of GnP on the flexural modulus and strength were reported in the previous chapter. It was shown that the modulus and strength of the composite tends to increase with increasing GnP concentration. It has also been demonstrated that adding CNT to a thermoplastic also can improve the mechanical properties [9]–[11]. The results of the flexural properties of the HS16 composites made with GnP and either CNT or CNF are shown in Figure 6.3. The modulus of the neat polymer is 1500 MPa, so each composite has a very large improvement over the neat. This is due to the high loading of the nanofillers in the composites, to achieve conductivity. Replacing a portion of the GnP with either CNT or CNF resulted in small additional improvements to the flexural modulus and strength, but many of the error bars are overlapping. The largest difference was the 27%% increase in flexural strength when 2% of the GnP was replaced with CNT at the lower loading of 10% material. This is most likely due to the fact that CNT have a larger surface area in contact with the polymer compared to the GnP, which should result in slight

improvements to the mechanical properties. At higher loadings, the strengths and modulus were similar across the composites.

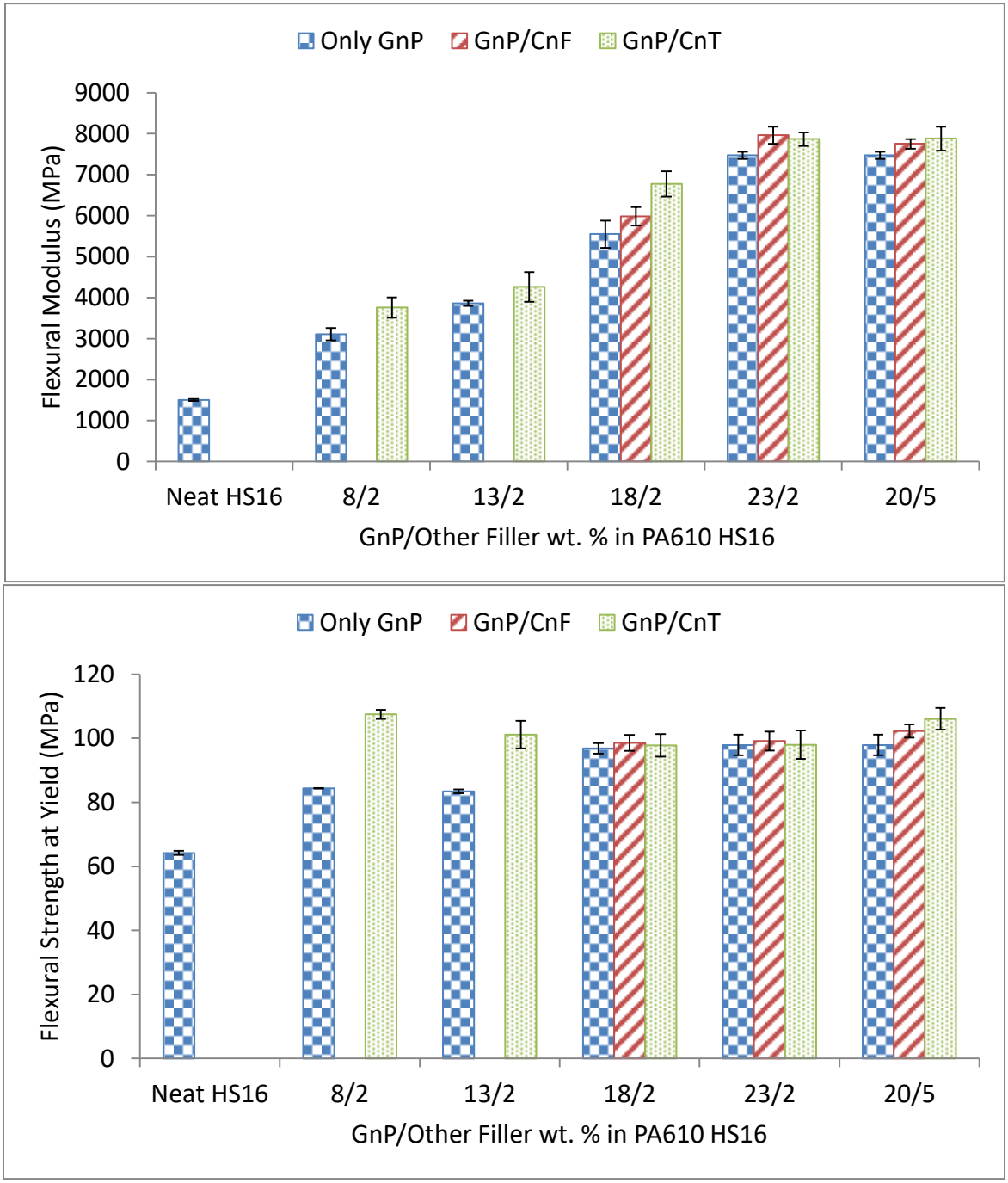

Figure 6.3. Flexural strength and modulus of GnP and either CNT or CNF in HS16 composites.

6.3.2 Four Point Probe Electrical Conductivity – Melt Processed Composites

The four point probe electrical conductivity results for both before and after a plasma treatment are shown in Figure 6.4. The blue bars represent a composite made with only GnP, while red has CNF added, and green has CNT added. Some clear trends are present. Before the plasma treatment, the composites with GnP only have the lowest conductivity, but are still seven orders of magnitude higher than the conductivity of neat HS16, which has a conductivity of $1x10^{-10}$ $S.m^{-1}$. There is a noticeable jump in conductivity going from 10 to 15 wt. percent, and another large increase going from 15 to 20 wt. percent, suggesting a percolated network is present. Substituting 2 wt. percent for CNF results in a doubling of the conductivity, however increasing this to 5 wt. percent doesn't yield any additional advantages. Substituting 2 wt. percent for CNT results in an order of magnitude increase for the conductivity, and increasing to 5 wt. percent results in some additional improvement. There is a lot of variance, probably due to a thin layer of polymer coating the surface where the probes contact. Utilizing a plasma treatment to etch away the insulating surface layer of polymer has a great effect on the conductivity of the films. An order of magnitude increase for all of the films was recognized. Substituting CNT into the composite still had the largest effect, and the 20/5 GnP to CNT composite had a conductivity 10 orders of magnitude higher than neat HS16. Even at low concentrations of 10 and 15 percent total weight, adding 2 wt. percent of CNT resulted in large increases in conductivity. After the plasma treatment, an increase from 2 to 5 wt. percent CNF now shows an increase in the overall conductivity. Composites of just 2 and 5 wt. percent CNT were made and tested with the same procedures to determine their effect on conductivity. After plasma treatment, the 2 wt. percent composite had a conductivity of 0.0009 $S.m^{-1}$ and the 5 wt. percent composite had a conductivity of .0412 $S.m^{-1}$. Clearly for conductivity purposes, the one dimensional nanofiller exhibits a lower

percolation threshold, as the 5 wt. CNT composite exhibited a higher conductivity than the 20% wt. GnP composite, and substituting a small amount of CNT for GnP into the composite resulted in large increases in conductivity. The reasons for this are supported by SEM observations.

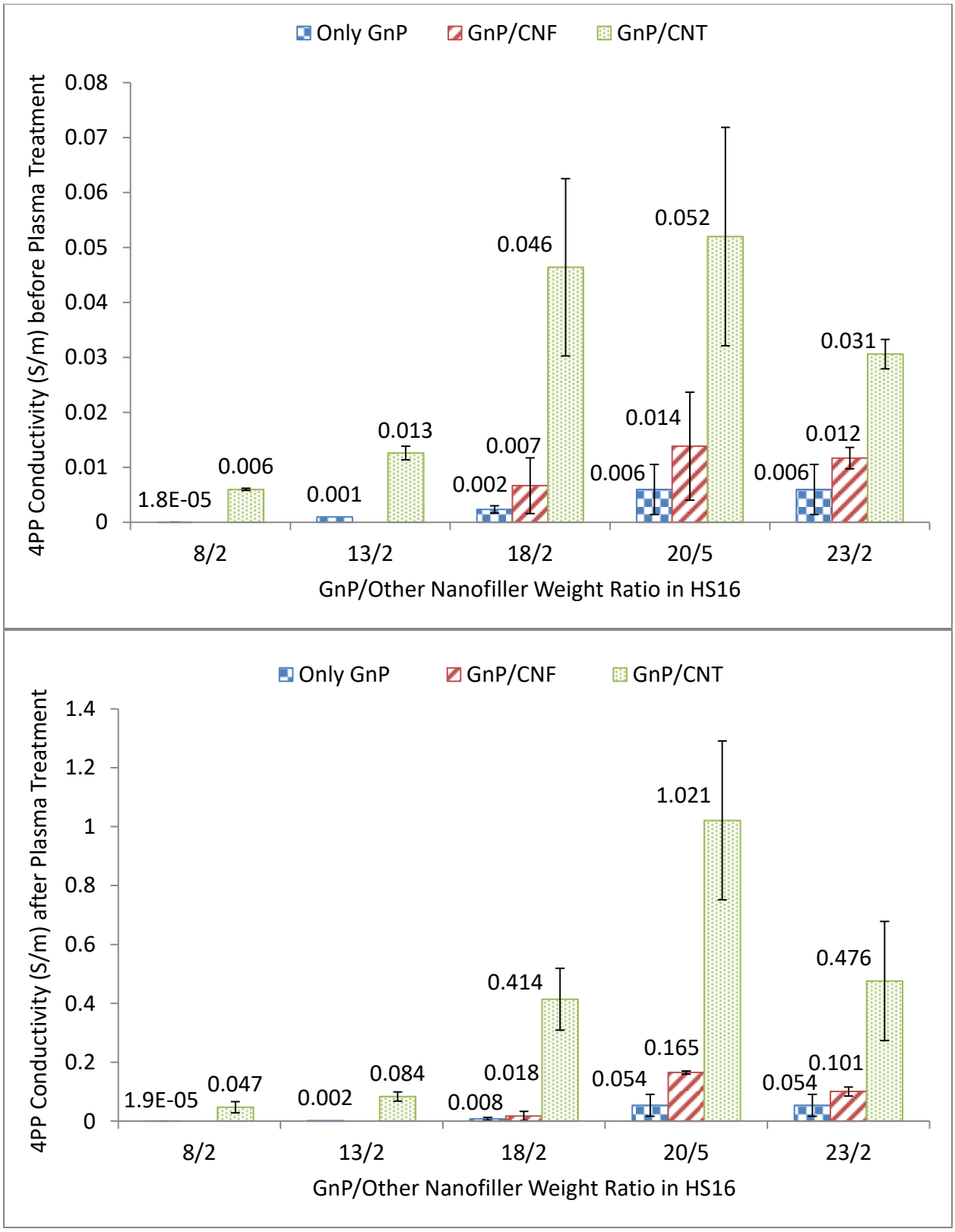

Figure 6.4. 4PP conductivity of GnP and either CNT :} or CNF in HS16 composites.

6.3.3 Scanning Electron Microscopy Observations – Melt Processed Composites

The morphology of the 25 wt. percent total nanofiller composites can be seen in Figure 6.5. There are some clear differences in the appearance of the surfaces when an additional nanofiller is added along with GnP. In the composites with only GnP, there are clearly large amounts of GnP that are isolated from each other in the polymer matrix, which would lead to a lower conductivity. As CNF or CNT is added, the morphology changes and there is clearly less polymer separating all of the GnP. Once 5 wt. percent of CNT is added, the GnP platelets almost all meld together due to the CNT covering all of the platelets. This explains the excellent conductivity of the samples doped with CNT, as there is clearly a conductive pathway formed within the composite. This interconnecting of the GnP with one dimensional particles becomes even clearer at high magnification. Figure 6.6 shows high magnification of a section of the 23/2 GnP to CNF ratio composite. The rod shaped CNF nanoparticles can be seen, scattered throughout the matrix, randomly oriented. Due to this random orientation, there are some additional connections between the GnP in the matrix, leading to a more conductive pathway through the composite. Figure 6.7 shows a high magnification look of the 23/2 GnP to CNT ratio composite. The 10 nm CNT can be seen covering the surface and filling in the gaps between the GnP throughout the composite. The CNT forms a web-like structure, leading to a percolated network and excellent conductivity for the composites relative to those with only GnP as the filler.

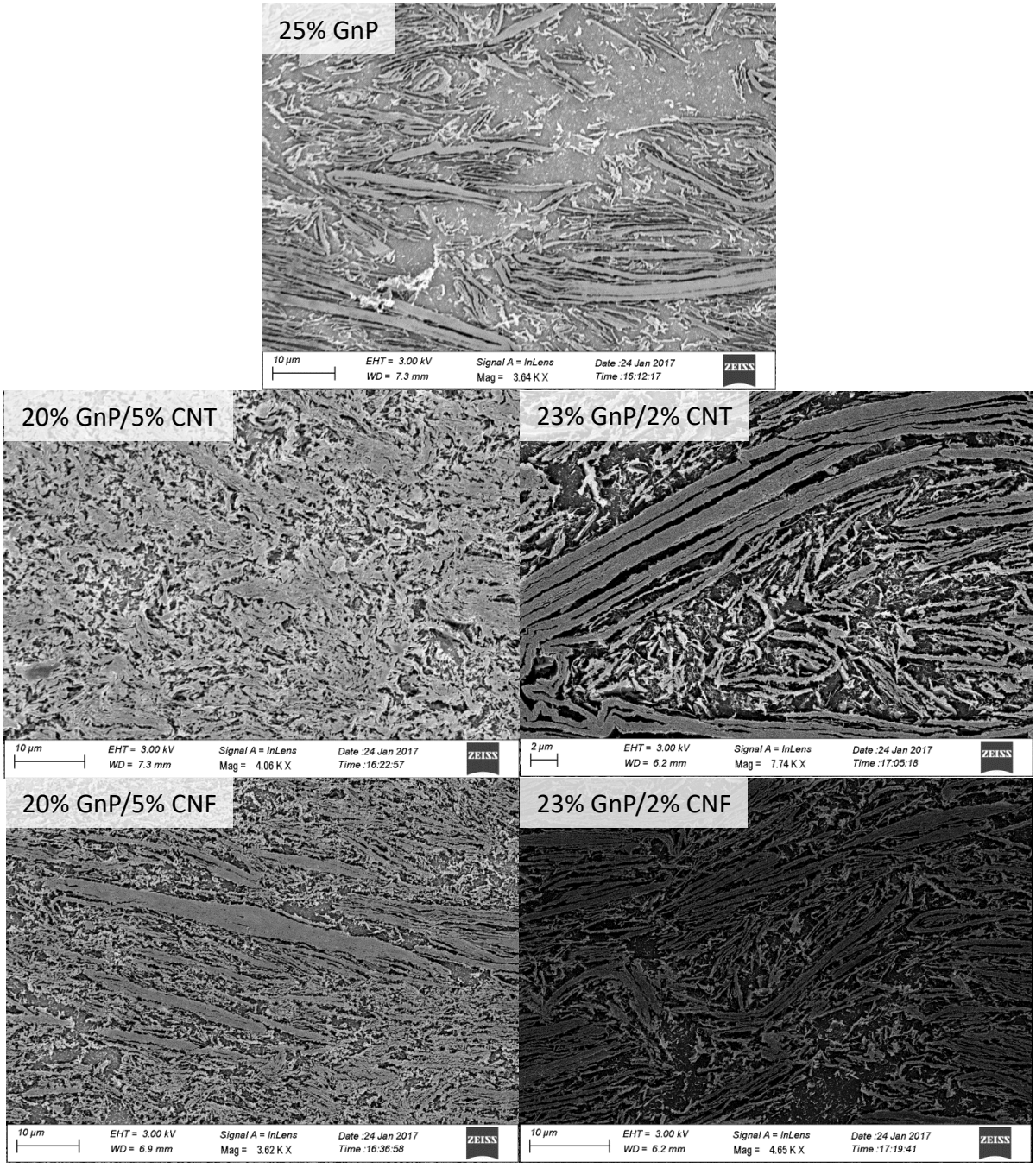

Figure 6.5. SEM overview of GnP and either CNT or CNF in HS16 composites.

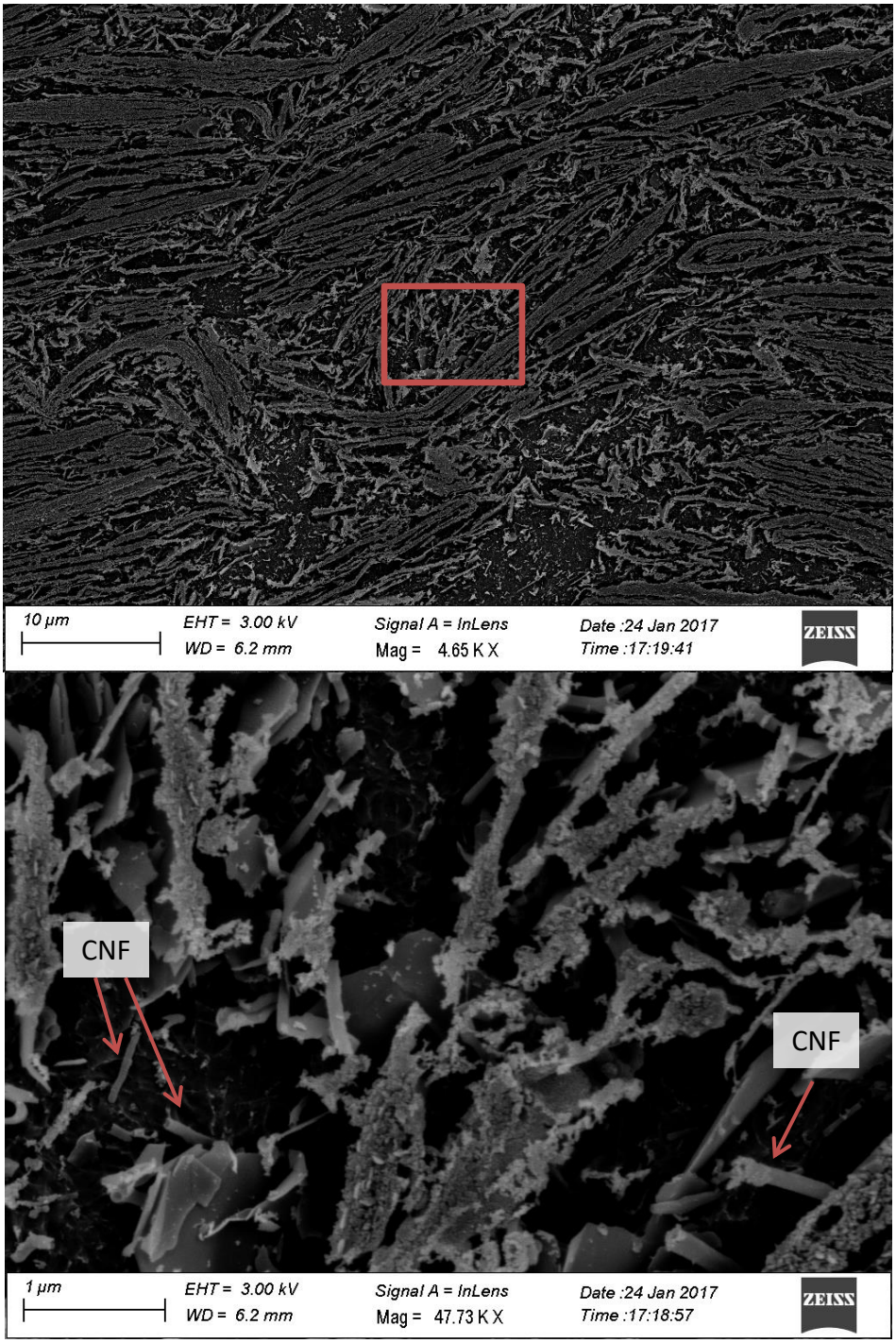

Figure 6.6. High magnification SEM of 23% GnP-M-25 and 2% CNF in HS16.

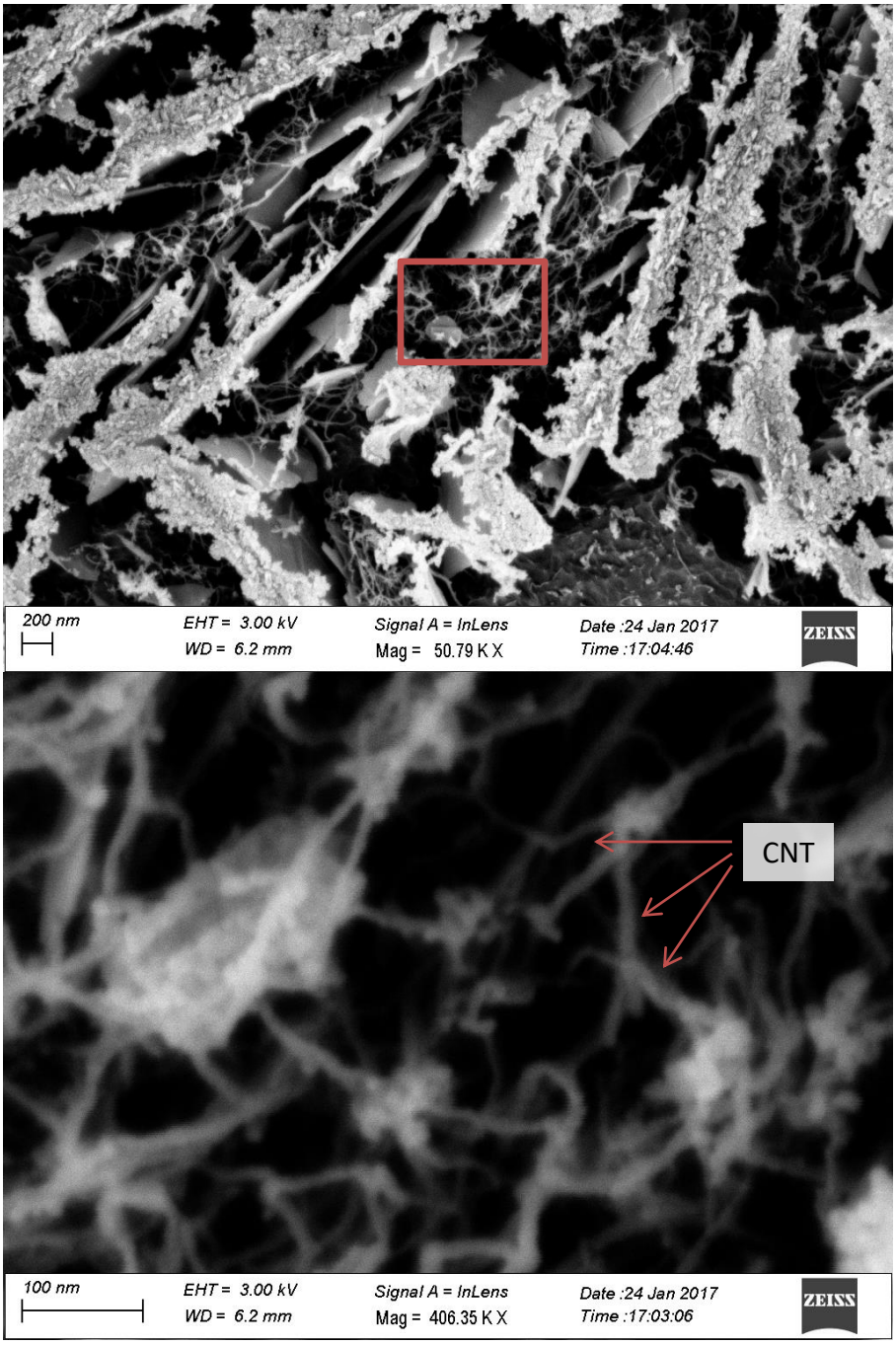

Figure 6.7. High magnification SEM of 23% GnP-M-25 and 2% CNT in HS16.

6.3.4 Oxygen Permeability – Melt Processed Composites

While the addition of a one dimensional nanoparticle helps to ensure a good conductivity in the composites, it is important that the barrier property enhancements due to the two dimensional GnP is still present. The oxygen permeability of the composites can be seen in Figure 6.8. With a 20% wt. GnP-M-25 composite, there is an 80% decrease in oxygen permeation. When 5 wt. percent CNF is also added to the matrix, there is still an 80% decrease in the oxygen permeability. This shows that the bulk of the barrier properties come from the GnP, and are relatively unaffected by the one dimensional nanoparticle. The 20/5 GnP to CNT ratio composite was also tested for oxygen permeability, but the resulting value was too low to be determined by the equipment. This is most likely due to the fact that the films containing CNT tended to be nearly double the thickness of the other films. While the transmission rates are normalized to film thickness, these thicker films resulted in oxygen transmissions that were too low to be accurately determined by the sensor. It would be expected that similar results to the CNF composites should be expected however. The barrier properties of the mixture of nanofillers can be expected to be approximately equivalent to those of just GnP based composites, as the one dimensional nanofiller additive does not add any additional tortuosity to the path that a permeating gas must follow.

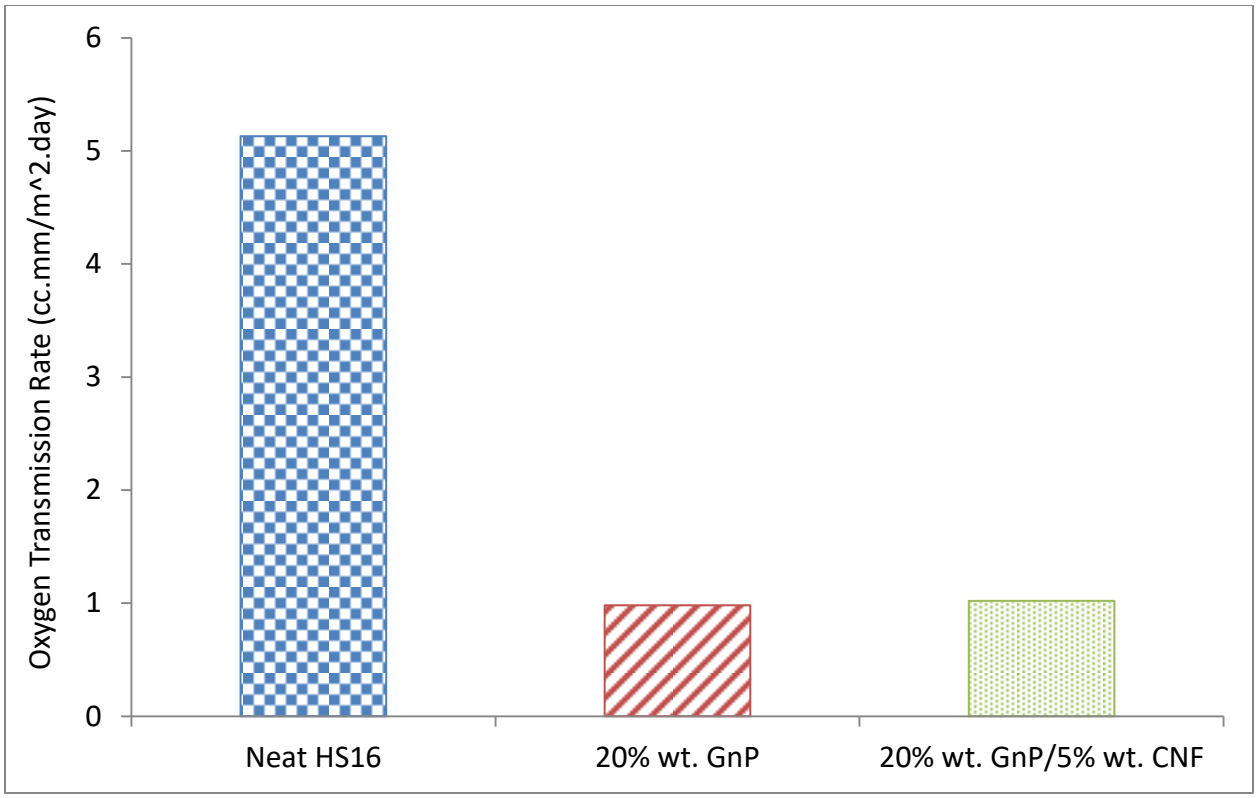

Figure 6.8. Oxygen permeability of GnP and either CNT or CNF in HS16 composites.

6.3.5 Solution Mixing Results

The films that were made from the solution mixing method were characterized for 4-point probe conductivity and oxygen permeation, and the cross-sections were analyzed with SEM. The results for the conductivity after plasma treatment of the 10 wt. percent GnP in HS16 films can be seen in Figure 6.9. From these results, it can be seen that the solution mixed film exhibits better conductivity than a melt mixed film with half the GnP concentration. Compared to a melt mixed composite of the same concentration, the 10 wt. percent GnP solution mixed film has a conductivity two orders of magnitude higher. Clearly there is a better dispersion of the GnP in the polymer matrix, resulting in a percolation at a much lower concentration when compared to

melt mixing. This is supported through SEM analysis of the film cross-sections, seen in Figure 6.10. In the melt mixed composite, there is a large amount of size reduction occurring, leading to many small platelets under 5 microns. There are also agglomeration issues present. In the solution mixed composite, there are much smaller agglomerates, and many of the platelets are well above 20 microns in diameter. The well dispersed, larger platelets are what lead to a much better conductivity at the same GnP loading when compared to the melt mixing process. However, the SEM analysis of the solution mixed films also clearly show fairly large voids present. This played a large role in determining the oxygen permeation through the films. Out of four films characterized, two films had low enough oxygen permeation that the sensor was unable to determine an accurate transmission rate, and two other films resulted in oxygen transmission rates that were high enough to cause the test to fail. From the SEM analysis of the cross-sections, it is pretty clear that the films that resulted in failed tests were most likely due to large voids present in the films. The voids are most likely present because when the formic acid evaporates off, the resulting composite is fairly porous, and when pressing, there may have still been trapped air bubbles present due to the porosity. Optimizing the pressing process of the solution mixture could potentially yield improved barrier properties and conductivity at lower loadings of GnP than melt mixing.

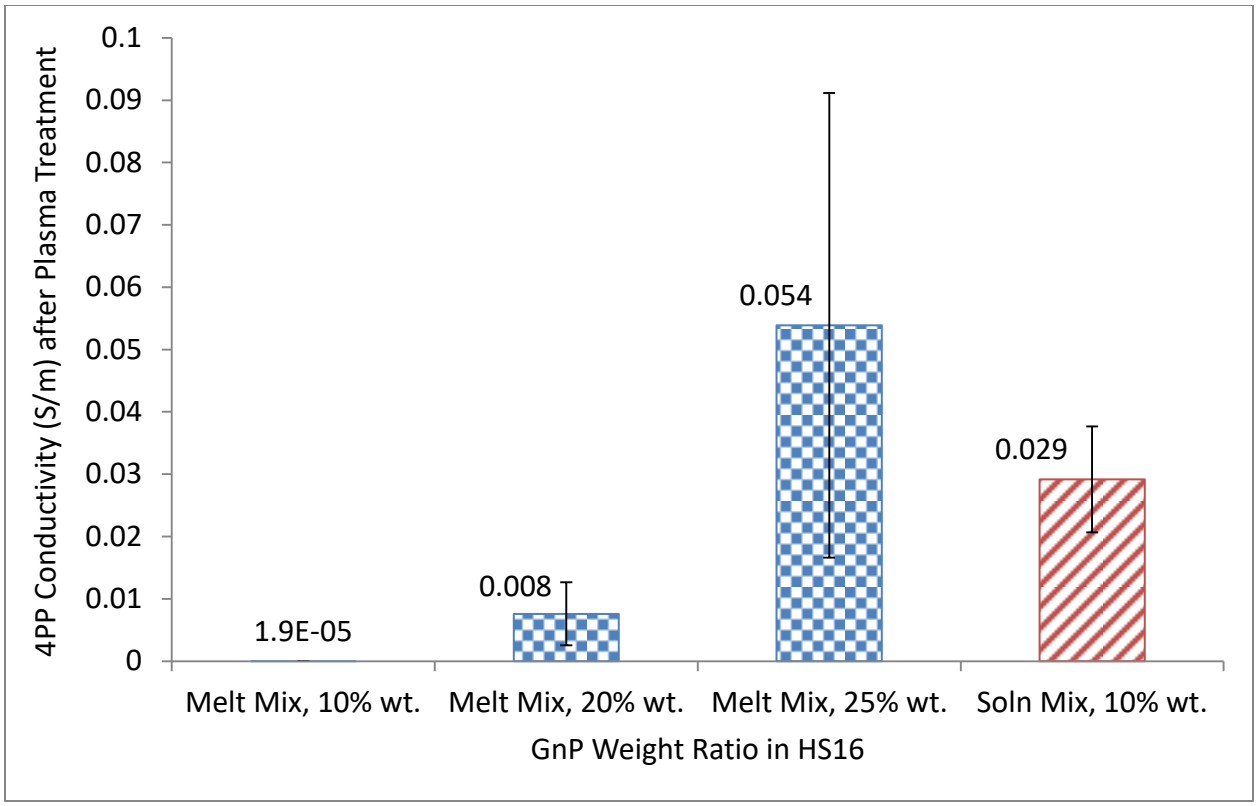

Figure 6.9. 4PP conductivity of solution mixed vs melt mixed composites.

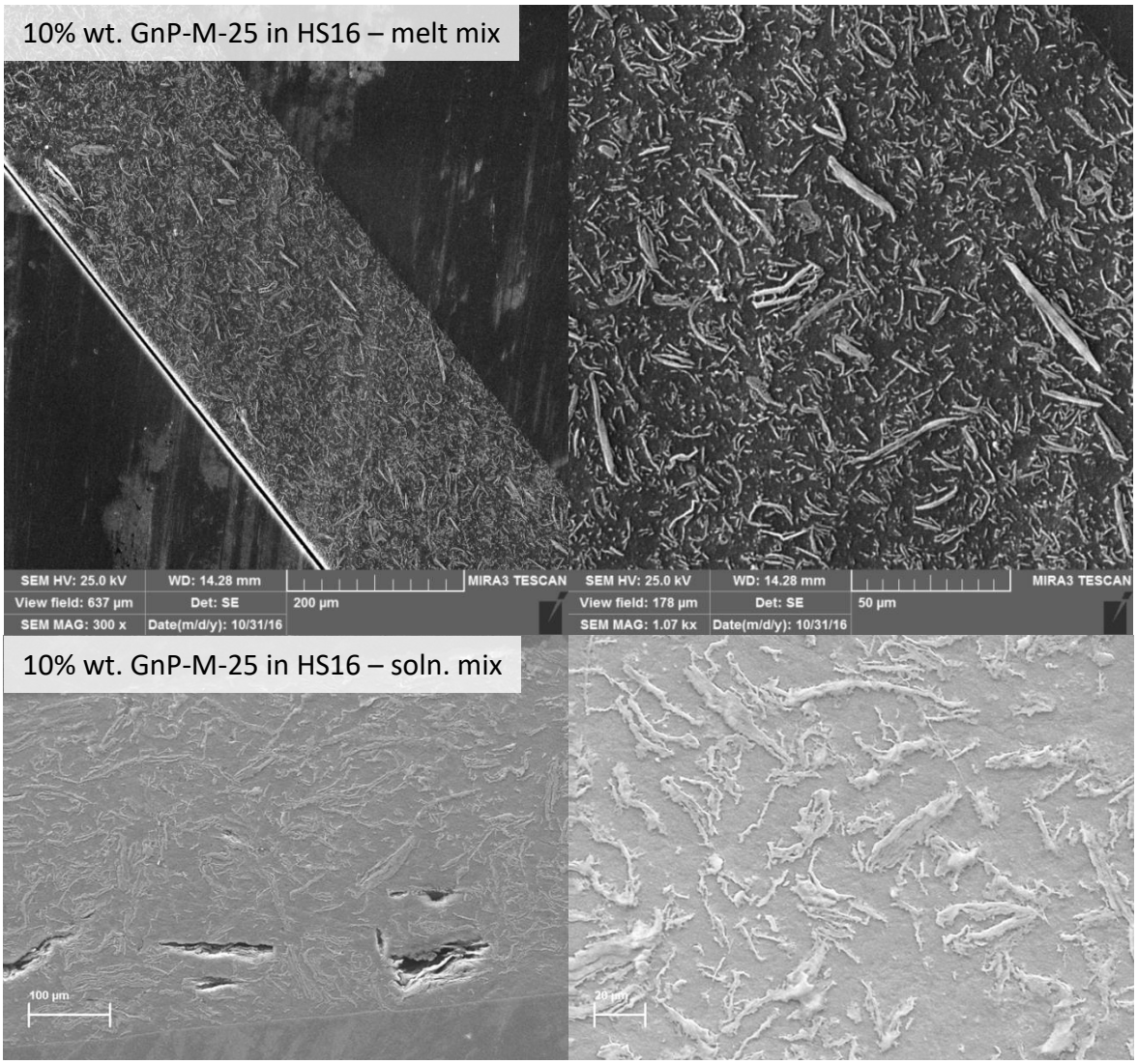

Figure 6.10. SEM comparison between solution mixed and melt mixed composites.

6.4 Conclusions

This chapter sought to take advantage of the combination of properties of both one and two dimensional nanofillers to form multifunctional nanocomposites with biobased polyamide 610. The two dimensional, cost effective GnP has been shown to improve the mechanical properties, thermal stability, and barrier properties of the biobased polyamides, but dispersion difficulties and the tendency of the large aspect ratio platelets to align with the flow of the polymer results in the percolation threshold of the composites to be much higher than theory would dictate. One dimensional nanofillers tend to entangle and orient less in a viscous melt, so if used in conjunction with GnP, have the potential to greatly increase the conductivity, while maintaining barrier properties provided by GnP. Both CNT and CNF were investigated as additives. The flexural properties remained largely the same when substituting a portion of the GnP for one of the other nanofillers. When 2 wt. percent CNF are added to the matrix, the conductivity of the composite was found to have doubled. When 2 wt. percent CNT were added, there was an order of magnitude increase over the composites with only GnP. It was also found that using a plasma treatment to etch away a surface layer of polymer resulted in another order of magnitude increase in the four point probe conductivity. With a 20 wt. percent GnP, 5 wt. percent CNT composite, the conductivity was found to be 1.02 $S.m^{-1}$, which is nearly ten orders of magnitude higher than the neat polymer matrix conductivity. The theory that the one dimensional nanoparticles interconnected the two dimension GnP platelets was confirmed through SEM analysis. The barrier properties of the system were found to be proportional to GnP weight content added. This is due to the fact that the one dimensional nanoparticle does not add any additional tortuosity to the path created by the GnP in the polymer matrix, even when 5 wt. percent of CNT or CNF were added. Solution mixing of the GnP and polyamide also yielded a better conductivity than

melt mixing. A 10 wt. percent GnP composite that was solution mixed had a conductivity 3 orders of magnitude higher than a melt mixed composite of the same composition. Optimizing the technique and adding a small amount of CNT to the solution mixing process may yield an even better conductivity at lower nanofiller loadings.

REFERENCES

REFERENCES

[1] V. K. S. Shante and S. Kirkpatrick, *Advances in Physics An introduction to percolation theory*, no. October 2012. 2006.

[2] M. Moniruzzaman and K. I. Winey, "Polymer nanocomposites containing carbon nanotubes," *Macromolecules*, vol. 39, no. 16, pp. 5194–5205, 2006.

[3] Y. Li, J. Zhu, S. Wei, J. Ryu, Q. Wang, L. Sun, and Z. Guo, "Poly(propylene) Nanocomposites Containing Various Carbon Nanostructures," *Macromol. Chem. Phys.*, vol. 212, no. 22, pp. 2429–2438, 2011.

[4] K. Kalaitzidou, H. Fukushima, and L. T. Drzal, "Multifunctional polypropylene composites produced by incorporation of exfoliated graphite nanoplatelets," *Carbon N. Y.*, vol. 45, no. 7, pp. 1446–1452, 2007.

[5] W. E. Van Zyl, M. Garcia, B. a. G. Schrauwen, B. J. Kooi, and J. T. M. de Hosson, "Hybrid polyamide silica nanocomposite synthesis and mechanical testing," *Macromol. Mater. Eng.*, p. 106, 2002.

[6] F. C. Chiu and I. N. Huang, "Phase morphology and enhanced thermal/mechanical properties of polyamide 46/graphene oxide nanocomposites," *Polym. Test.*, vol. 31, no. 7, pp. 953–962, 2012.

[7] F. M. Smits, "MEASUREMENT OF SHEET RESISTIVITIES WITH THE 4-POINT PROBE," *Bell Syst. Tech. J.*, vol. 37, no. 3, pp. 711–718, 1958.

[8] Y. SINGH, "ELECTRICAL RESISTIVITY MEASUREMENTS: A REVIEW," *Int. J. Mod. Phys. Conf. Ser.*, vol. 22, pp. 745–756, Jan. 2013.

[9] J. N. Coleman, U. Khan, and Y. K. Gun'ko, "Mechanical Reinforcement of Polymers Using Carbon Nanotubes," *Adv. Mater.*, vol. 18, no. 6, pp. 689–706, 2006.

[10] J. N. Coleman, U. Khan, W. J. Blau, and Y. K. Gun'ko, "Small but strong: A review of the mechanical properties of carbon nanotube–polymer composites," *Carbon N. Y.*, vol. 44, no. 9, pp. 1624–1652, 2006.

[11] Y. Zou, Y. Feng, L. Wang, and X. Liu, "Processing and properties of MWNT/HDPE composites," *Carbon N. Y.*, vol. 42, no. 2, pp. 271–277, 2004.

CHAPTER 7 - SUMMARY AND FUTURE WORK

7.1 Summary

The research presented in this dissertation focused on investigating nanocomposites for their potential uses in automotive fuel tank and line systems. In order to accomplish this, it was theorized that combining a polymer with graphene nanoplatelets (GnP) would yield a multifunctional nanocomposite that is mechanically sound, thermally stable, electrically conductive, and has excellent barrier properties against permeating oxygen and fuel. Multiple synthesis techniques and polymers were explored.

In the second chapter, melt mixing was used to combine high density polyethylene (HDPE) with three different grades of GnP and the crystallinity, mechanical, thermal, electrical, and barrier properties were characterized. The concentration range of the GnP was 0 to 40 wt. percent. All three grades of GnP improved the flexural modulus and strength with increase GnP concentration. However, impact resistance was greatly decreased even with only 0.2 wt. percent GnP added into the polymer matrix. The thermal stability of the composites was greatly improved, due to the excellent thermal conductivity of GnP. The crystallinity of the composites increased at concentrations lower than 2 wt. percent, due to GnP acting as a nucleating site, but larger concentrations did not yield an increase in crystallinity. Electrical conductivity of the composites was found to be largely unaffected until concentrations above 30 wt. percent GnP were reached. The barrier properties of the matrix were found to be greatly enhanced, due to the GnP creating a tortuous path for permeating gases to follow. A 20 wt. % GnP-M-15 composite yielded a 77% reduction in oxygen permeation. Similar trends were observed with fuel

permeation as a 15 wt. % GnP-M-15 composite yielded a 74% reduction in fuel permeation (compared to a 73% reduction in oxygen permeation at the same loading). Scanning electron microscopy (SEM) analysis of the nanocomposites revealed that the dispersion and alignment of the GnP was not ideal, and it was determined that there were additional processing techniques that could yield an optimized nanocomposite.

Chapter 3 focused on various processing techniques to improve the properties of the HDPE-GnP composites. These techniques included microlayer co-extrusion, solution dispersion, cryomilled base polymer, and coating the GnP surface with a material to improve the compatibility with the polymer matrix. Microlayer co-extrusion yielded highly aligned GnP structures in HDPE, which improved the relative barrier properties, however dispersion issues were still present and did not yield absolute improvements over the simple melt mixing process. The solution dispersion approach yielded improve barrier properties when the HDPE-GnP mixture was directly compressed into a film, but if processed through a melt mixing process again, those advantages were lost. Cryo-milling the HDPE into a particle size that was more similar to the GnP resulted in a small improvement to the barrier properties, but the mechanical properties were lessened as some polymer chains had been broken. A wax coating of the GnP resulted in a recovery of a portion of the lost impact resistance, but had little benefit for the barrier properties. Additionally, the flexural reinforcement properties of the GnP were decreased due to a low modulus interface between the polymer matrix and the GnP. Similar results were obtained with an HDPE compatible elastomeric coating.

In Chapter 4, a layer by layer deposition approach was taken to see if the barrier properties of a polymer could be improved using only a small amount of material. In the first method, ionic charges were used to deposit a cationic polymer, either polyethylenimine (PEI) or

Poly(diallyldimethylammonium chloride) (PDAC), and then a layer of sulfonated polystyrene (SPS) coated GnP. With a 40 bilayer deposition, there was a 60% reduction in the oxygen transmission rate compared to the base substrate. Another method was to deposit monolayers of GnP that were formed by taking advantage of the surface energy differences between chloroform and water. Depositing 15 layers of GnP again resulted in a 60% reduction in oxygen permeation, and the weight content of GnP was estimated to only be 0.9 wt. percent. This method exceeded the barrier properties of the 2 wt. percent melt mixed composite with less than half of the GnP.

In Chapter 5, adding GnP to a biobased polyamide was investigated to determine if an electrically conductive polymer with great barrier and mechanical properties could be synthesized. Using a 5 minute mixing time in the extrusion process, a 10 wt. percent GnP composite yielded a 100% improvement in flexural modulus and a 25% improvement in flexural strength. However, the impact resistance was again reduced by up to 50%. The thermal stability of the composites was greatly improved through the addition of GnP, due to the excellent thermal properties of the nanofiller. The electrical properties of the composites were largely unaffected up to 15 wt. percent GnP, at which point there was a three order of magnitude increase. This was attributed to poor dispersion and the fact that the large aspect ratio causes many of the platelets to align with the flow of the polymer, meaning there could be many points where platelets are not touching, breaking up the percolated network. With a 5 minute mix time, the barrier properties of the composite were improved by up to 50%. Increasing the mixing time resulted in a better dispersion of the platelets, as evidenced through SEM analysis, and resulted in an overall 75% reduction in oxygen transmission through the composites. Clearly dispersion is playing a large factor in the composite properties. With larger scale melt mixing, there may not

be a need for such a long mix time since specific screw mixing elements could be optimized compared to a simple co-rotating screw design.

The final chapter investigated an enhancement of the conductivity of the biobased polyamides and GnP nanocomposites through the synergistic combination with a one dimensional nanofiller. Both carbon nanotubes (CNT) and carbon nanofibers (CNF) were investigated. With the addition of either CNT or CNF, the mechanical properties largely remained constant. The barrier properties also only depended on the GnP concentration, as the CNT and CNF do not add any tortuosity to the path for permeating gas particles. However, the electrical conductivity was doubled through the addition of 2 wt. percent CNF, and it was increased by an order of magnitude with CNT. It was also found that a plasma treatment of the composite surface resulted in an additional order of magnitude increase in the conductivity due to the removal of a polymer rich layer from the surface. With a 20 wt. percent GnP, 5 wt. percent CNT composite, there was over ten orders of magnitude increase compared to the neat polymer. SEM analysis confirmed that the one dimensional nanofillers helped improve the conductivity by connecting the large amounts of GnP dispersed in the polymer. Additionally, solution dispersing the GnP in the polyamides was shown to be a potential route to lowering the total weight content needed for conductivity.

The overall results of this work helped to demonstrate that GnP can greatly improve the flexural properties, thermal stability, and barrier properties of a polymer matrix. Through synergistic effects of adding a small amount of a one dimensional nanofiller, excellent conductivity can also be achieved.

7.2 Future Work

7.2.1 Solution Mixing with the Biobased Polyamide Composites

The conductivity and barrier property improvements of the biobased polyamides with GnP are very promising, especially with the addition of a one dimensional nanoparticle to help connect the platelets. The greatest conductivity increases required high loadings of the nanofillers. Initial investigations into a solution based mixing method of GnP and the polyamides have shown promising results. The polyamides can be dissolved in formic acid to create a less viscous mixing environment. With a 10 wt. percent GnP composite, the barrier properties were unable to be measured with the commercially available Mocon OX-TRAN 2/20 because the transmission rate was too low to be monitored. SEM analysis of the cross-section showed that the dispersion of the platelets were greatly improved, with less agglomerates and much longer platelets that were not reduced in size due to the mixing environment of melt extrusion. It was also found to have higher conductivity than the 20 wt. percent GnP composite, also demonstrating an improved dispersion. Optimizing this solution based approach may yield a composite with great barrier and conductivity properties at lower loadings than required with melt mixing.

7.2.2 Large Scale Production of Biobased Polyamide Composites

Melt mixing the GnP with the biobased polyamides required a long residence time in the micro extruder used to achieve a good dispersion. With a large scale extruder, this residence time may not be necessary. Using kneading and mixing elements within the screws, compared to simple co-rotating screws, may yield a much better dispersion in a shorter mixing time. This would potential allow for a lower loading of GnP to achieve the same properties. Additional processing,

such as micro-layer co-extrusion, may also yield interesting results if the dispersion of the platelets could be improved. Scaling up the production of nanocomposites is an important aspect to understand and investigate. While the masterbatch approach with the HDPE prior to microlayer co-extrusion did not yield additional improvements due to breakdown of the platelets, a masterbatch approach could still be investigated more thoroughly. Once the masterbatch was compounded, the secondary processing with HDPE to the desired concentrations could be done with mostly conveying elements that would ensure the platelets do not undergo too much size reduction.

7.2.3 Optimizing Plasma Treatment Time

Plasma treating the nanocomposite films resulted in large improvements in the conductivity of the nanocomposites. This was theorized due to the removal of a thin layer of polymer on the surface that acts as insulation, preventing good contact with the polymer. Using a plasma treatment of 15 minutes resulted in an order of magnitude increase of the conductivity. This amount of time was chosen because it was known that that long would reveal the carbon nanofillers well for SEM analysis, however it may be that shorter times would yield similar results. Investigating the etching rate, plasma treatment gas, as well as other effects could yield insightful results into the conductivity enhancement due to the treatment.

7.2.4 Functionalization of the GnP

Dispersion plays a key role in the properties of a nanocomposite when the filler is added. If there is poor dispersion, then the surface area of the nanofillers is not being taken advantage of, and the resulting properties will not be optimal. SEM analysis of the HDPE and polyamide composites revealed that GnP tends to agglomerate with itself, restacking into larger platelet stacks. If the GnP was functionalized so that the interaction between the GnP and the polymer was increased, the degree of this agglomeration may be greatly reduced. This functionalization could be either through covalent or non-covalent functionalization. Non-covalent functionalization was demonstrated in Chapter 3 with the wax and elastomeric coatings of the GnP which showed improved dispersion. Also the sue of pi-pi coupling agents designed to interact with the GnP basal plane might prove useful if they also were selected to interact with the polymer. Finding a compatible coating with the polyamides may yield interesting results, especially if covalent functionalization could also be achieved. Covalent functionalization would tend to occur at the edges of the platelets since the basal planes of GnP are relatively defect free. If a short chain polyamide could be grafted to the edges of the platelets, then the GnP would more easily disperse into the polymer matrix, resulting in better property enhancement at lower loadings.